GROUND PENETRATING RADAR

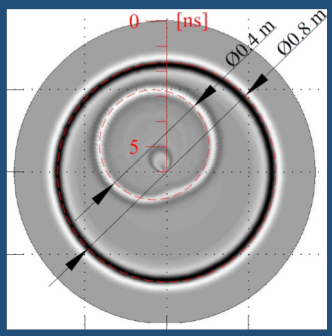

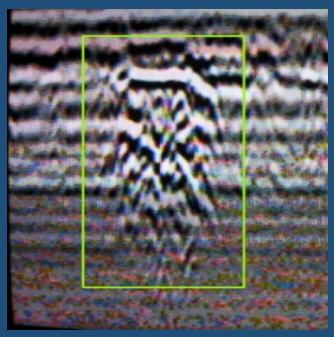

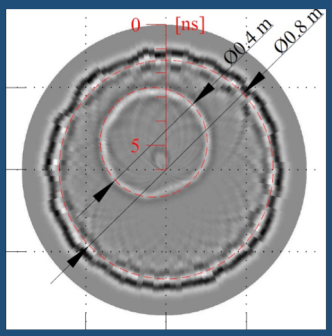

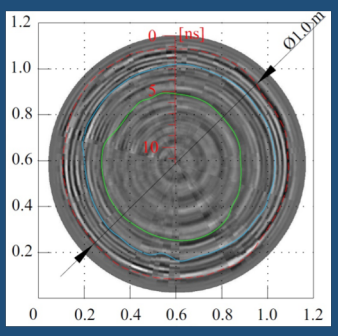

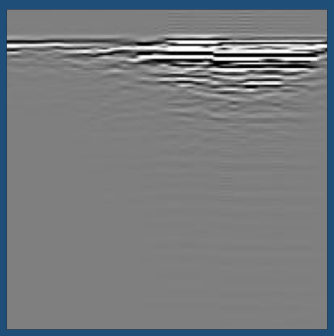

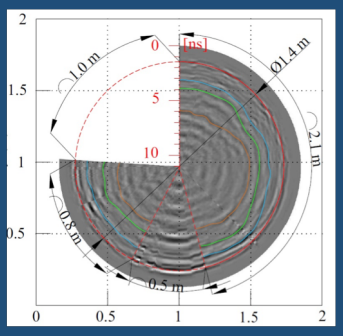

Issue 1, Volume 2

March 2019

www.GPRadar.eu/journal

Ground Penetrating Radar is an open access peer-reviewed journal published quarterly by TU1208 GPR Association. TU1208 GPR Association was founded in September 2017 as a follow up of the COST Action TU1208 "Civil engineering applications of Ground Penetrating Radar," to further support cooperation between Universities, research centres, private companies and public agencies active in the Ground Penetrating Radar field. Responsibility for the contents of the manuscripts published on *Ground Penetrating Radar* rests upon the Authors and not upon TU1208 GPR Association or its Members.

All Manuscripts should be submitted at:
http://gpradar.eu/journal/submission.html

All correspondence and communication should be directed to:
Ground Penetrating Radar c/o TU1208 GPR Association
Via Flaminio Ponzio 14, 00153 Rome, Italy
journal@GPRadar.eu

This is **Issue 1**, **Volume 2**, published in **March 2019**. All papers are available in open access at http://gpradar.eu/journal
This issue includes: Editorial, Preface, four papers, a retraction note, Table of Contents, News & Announcements.

ISSN 2533-3100

Ground Penetrating Radar
Volume 2, Issue 1, March 2019

EDITORIAL & PREFACE

Ground Penetrating Radar
Volume 2, Issue 1, March 2019 doi: 10.26376/GPR2019EP1

EDITORIAL

Welcome to Issue 1, Volume 2 of *Ground Penetrating Radar*, the first peer-refereed, open-access, international academic journal designed to advance scientific knowledge and foster innovative engineering solutions in the field of Ground Penetrating Radar (GPR).

This issue includes four papers (see the Preface for an introduction to the papers), a Retraction Note, and a 'News & Announcements' section.

We are delighted to inform our Readers and Authors that we have recently joined Crossref, this will guarantee higher discoverability and visibility of *Ground Penetrating Radar* papers to the research community. Crossref was founded in 2000 by a group of publishers who needed an efficient method to connect their journal articles, and so they started using DOIs to link references between articles. When an article is registered with Crossref, the bibliographic metadata of that article are submitted, such as the title, authors, publication dates, online location, the DOI, and the references, to name a few. This makes it easier, e.g., for a Reader to locate all items registered in Crossref citing a certain article. Not only new *Ground Penetrating Radar* papers, but also papers published on *Ground Penetrating Radar* in 2018 are going to be registered in CrossRef! Moreover, we have updated the journal website and each published paper now has a dedicated webpage.

We are also pleased to inform you that two Special Issues are being launched:

- The last issue of Volume 2 (to be published in December 2019) will be a collection of scientific papers resuming contributions presented during Session GI4.1 "Ground Penetrating Radar: Technology, Methodology, Applications and Case Studies" of the 2019 European Geosciences Union General Assembly (7-12 April 2019, Vienna, Austria). This Special Issue will be edited by Alessandro Fedeli (University of Genoa, Italy), Aleksandar Ristic (University of Novi Sad, Serbia), Milan Vrtunski (University of Novi Sad, Serbia), and myself. Papers can be submitted by Authors of GI4.1 abstracts and session Attendees.
- Submissions are open for a Special Issues entitled "New perspectives for the study and preservation of cultural heritage with the aid of noninvasive prospecting." This Special Issue will be edited by Raffaele Persico (CNR – National Research Council, Italy), Mercedes Solla (University of Vigo, Spain), and Xavier Dérobert (IFSTTAR – Institut Français des Sciences et Technologies des Transports, de l'Aménagement et des Réseaux, Nantes, France).

 doi: 10.26376/GPR2019EP1

More information on these Special Issues and the calls for papers are found in the News & Announcements section.

Another piece of news is that we have set up a Twitter profile dedicated to *Ground Penetrating Radar*, where scientific insights into papers published on our journal are being twitted: GPR_OpenAccess.

All *Ground Penetrating Radar* papers are processed and published in true open access, free to both Authors and Readers, thanks to the generous support of TU1208 GPR Association and to the voluntary efforts of the journal Editorial Board. The present issue is also supported by IDS Georadar s.r.l. (idsgeoradar.com).

Do you have suggestions to improve the journal? Would you like to join the Editorial Board or propose a Special Issue? You are most welcome to send us a message at journal@gpradar.eu.

The Editor-in-Chief
Lara Pajewski

Ground Penetrating Radar
Volume 2, Issue 1, March 2019 doi: 10.26376/GPR2019EP1

PREFACE

The first issue of the second volume of *Ground Penetrating Radar* includes four papers authored by scientists from 11 institutes in 9 countries (Belgium, Canada, Czech Republic, Estonia, Greece, Italy, Portugal, Serbia, Turkey).

The issue is opened with a paper entitled "**Influence of bark surface roughness on tree trunk radar inspection**," authored by Jana Jezova and Sébastien Lambot [1]. The paper deals with microwave radar testing of tree trunks for the evaluation of their internal structure, with a main focus on investigating how the surface roughness of a trunk influences radar data. Several numerical simulations and laboratory measurements were carried out, to compare radargrams obtained by testing a cylinder with a smooth surface and a cylinder having an irregular surface. Then, real trees with different surfaces and internal structures were tested, to validate the simulation and laboratory findings. The results presented in this paper indicate that the presence of a rough and irregular bark can significantly inhibit the ability to study the internal structure of a tree with a radar. On the other hand, if the bark is smooth, the internal composition of a tree can be successfully estimated even for highly heterogeneous specimens.

The second paper is entitled "**Discrimination of dispersive materials from radar signals using Q***" and is authored by Chun An Tsai, Rebecca Ghent, Alexander Boivin, and Dylan Hickson [2]. Via a combination of laboratory measurements and simulation results, the Authors demonstrate the potential of distinguishing two dispersive materials by estimating the quality factor using radar signals at two different frequencies. Complex dielectric permittivity measurements were carried out on a pulp sample mainly composed of pyrite and quartz, from a massive sulphide mine, as well as on a calcium-rich montmorillonite sample, for comparison. For the montmorillonite sample, a dispersive behaviour caused by water was observed, consistent with previous studies. For the pulp sample, a dispersive behaviour independent of water was observed, which could be distinguished from the behaviour of moist clays by estimating the quality factor at two different frequencies. Simulations with the inverted parameters were implemented with gprMax, to further verify the idea.

The third paper is entitled "**Real-time visualization of the data gathered by a reconfigurable stepped-frequency GPR system**;" it is authored by Filippo Brigatti [3]. Recent improvements made to the acquisition software of a reconfigurable stepped-frequency ground penetrating radar (GPR) prototype are presented in this work, which was carried out during the Master thesis in Electronic Engineering of the Author. In particular, real-time data visualization was not yet implemented in the

 doi: 10.26376/GPR2019EP1

previous version of the acquisition software, although this is a common feature available in all commercial systems. By developing suitable procedures for a more efficient data handling, the Author upgraded the software and enabled real-time visualization of the radargrams measured by the prototype. The most significant parts of the code are available for download as 'Supplementary materials.'

The last paper of this issue stems from COST (European Cooperation in Science and Technology) Action TU1208 "Civil engineering applications of Ground Penetrating Radar." The paper is entitled "**TU1208 GPR Roadshow: Educational and promotional activities carried out by members of COST Action TU1208 to increase public awareness on the potential and capabilities of the GPR technique**" and is authored by myself, Hannes Tonisson, Kaarel Orviku, Miro Govedarica, Aleksandar Ristic, Vladislav Borecky, Salih Serkan Artagan, Simona Fontul, and Klisthenis Dimitriadis [*4*]. The purpose of this paper is to present descriptions, principles, and impact of a successful series of science communication initiatives about the GPR technique, overall denominated "TU1208 GPR Roadshow." Part of the Roadshow consisted of a series of six non-scientific workshops and practical demonstrations held in Portugal, Italy, Greece, Croatia, Serbia, and the Czech Republic, from March 2016 to May 2017. Audiences went well beyond the GPR scientific community and primarily included representatives from public agencies and private companies, as well as interested citizens. The workshops were attended by almost 500 participants in total: we were able to raise considerable interest in various countries and our events were catalysts for a series of new activities. Another significant part of the Roadshow consisted of a series of promotional and educational initiatives carried out in Estonia. Before these initiatives, very few people in Estonia knew what GPR was and how it could be used in different application fields. Several lectures were delivered in schools, practical workshops were held during the Researchers' Nights as well as during other large communication events, and short lectures were given on TV.

Many thanks to the Authors of these four papers for choosing *Ground Penetrating Radar*. Thank you very much to all researchers and experts involved into the revision process of the papers, for their voluntary efforts. I am grateful to TU1208 GPR Association (gpradar.eu/tu1208) and IDS Georadar s.r.l. (idsgeoradar.com), for supporting the publication of this issue, and as always to COST (cost.eu) for having funded and supported the Action TU1208 (gpradar.eu).

The Editor-in-Chief
Lara Pajewski

 doi: 10.26376/GPR2019EP1

References

[1] Jana Jezova and Sébastien Lambot, "Influence of bark surface roughness on tree trunk radar inspection," Ground Penetrating Radar, Volume 2, Issue 1, March 2019, pp. 1-25, https://doi.org/10.26376/GPR2019001.

[2] Chun An Tsai, Rebecca Ghent, Alexander Boivin, and Dylan Hickson, "Discrimination of dispersive materials from radar signals using Q*," Ground Penetrating Radar, Volume 2, Issue 1, March 2019, pp. 26-50, https://doi.org/10.26376/GPR2019002.

[3] Filippo Brigatti, Real-time visualization of the data gathered by a reconfigurable stepped-frequency GPR system, Ground Penetrating Radar 2019, Volume 2, Issue 1, March 2019, pp. 51-66, https://doi.org/10.26376/GPR2019003.

[4] Lara Pajewski, Hannes Tonisson, Kaarel Orviku, Miro Govedarica, Aleksandar Ristic, Vladislav Borecky, Salih Serkan Artagan, Simona Fontul, and Klisthenis Dimitriadis, "TU1208 GPR Roadshow: Educational and promotional activities carried out by members of COST Action TU1208 to increase public awareness on the potential and capabilities of the GPR technique," Ground Penetrating Radar, Volume 2, Issue 1, March 2019, pp. 67-109, https://doi.org/10.26376/GPR2019004.

Ground Penetrating Radar
Volume 2, Issue 1, March 2019

SCIENTIFIC PAPERS

Ground Penetrating Radar
Volume 2, Issue 1, March 2019
https://doi.org/10.26376/GPR2019001

Influence of Bark Surface Roughness on Tree Trunk Radar Inspection

J. Ježová and S. Lambot

Université catholique de Louvain, Louvain-la-Neuve, Belgium –
jana.sebestov@gmail.com, sebastien.lambot@uclouvain.be
(J. Ježová is the Corresponding Author)

Ground penetrating radar; tree trunk inspection; non-destructive testing; roughness influence.

Abstract

Microwave radar testing of tree trunks is one of the ways for the trunk interior evaluation. The interpretation of the radar images can be a very complex task - among others due to the roughness of the tree bark. This paper studies the influence of a surface roughness on radar data of observed cylindrical objects, trees in particular. During our study, we did numerical simulations and laboratory measurements to compare radar data obtained by testing a cylinder with a smooth and an irregular surface. Then, several real trees with different surfaces and internal structures were tested to validate our findings. Those experiments indicate that the presence of a rough and irregular bark can significantly inhibit our ability to study the internal structure of the tree with the radar. On the other hand, if the bark is smooth, it is possible to infer the internal composition of the tree even for highly heterogeneous specimens.

Keywords: Ground penetrating radar; tree trunk inspection; non-destructive testing; roughness influence.

1 Introduction

Trees are a very important part of humans' lives. They are crucial for oxygen production, they are a necessary source of construction material, they have an indisputable effect on the climate and they have a significant influence on well-being in urban areas. Then, it is inevitable to pay attention to their condition. As a result of a natural degradation of wood and a human intervention to trees and their habitats, the stability of tree trunks is constantly decreasing which leads to endangering

https://doi.org/10.26376/GPR2019001

people and infrastructures. In order to prevent collapses of trees, it is highly important to investigate their internal structure [1]. From the macroscopic point of view, tree trunks are composed of bark, sapwood and heartwood with different mechanical properties. Within them, we can observe natural defects (knots, reaction wood, cross grain, etc.) or biological degradation (caused by fungi, insects etc.).

There are several destructive and non-destructive methods for tree trunk evaluation [2]. Core drilling, knife test or penetrometer testing are examples of the destructive ways for tree trunk inspection [3]. Gilbert et al. [4], Lin et al. [5] or Brancheriau et al. [6] used ultrasonic tomography to detect decayed wood in living tree trunks. This method is based on emitting sonic waves into the trunk and evaluating its mechanical state by the sonic waves responses. Guyot et al. [7] and Elliott et al. [8] used electrical resistance tomography (ERT) for evaluating the internal structure of tree trunks. ERT measures the subsurface distribution of electrical resistance (which is a function of humidity, density, etc.) with several electrodes following a specific geometric pattern along an investigated object. Van den Bulcke et al. [9] used X-ray tomography for analysing tree rings to measure the age of trees. Ground-penetrating radar (GPR) is being increasingly used as a non-invasive device for tree trunk interior inspection. It is based on emitting electromagnetic waves into media and capturing them after scattering on the internal structures of the studied object.

Nicolotti et al. [10] compared three non-destructive methods for the tree trunk investigation, namely, electric, ultrasonic and georadar tomography. Al Hagrey [11] also tested the same techniques for tree trunks and the root zone in order to evaluate their moisture. Butnor et al. [12] used the GPR in order to detect decays in tree trunks and provided a comparison between data obtained from gymnosperms and angiosperms. Lorenzo et al. [13] used the GPR to test a root zone of trees and tree trunks. They observed advantages of using a metal sheet to increase reflections from the other side of the tree. Fu et al. [14] provided a living tree trunk ray-based tomography using the GPR in a reflection and transmission mode. Mazurek and Łyskowki [15] tested two shielded antennas (1.6 GHz and 0.8 GHz) for a tree trunk inspection in both reflection and transmission mode in a longitudinal direction to the tree. Li et al. [16] proposed a ray-based tomography of a living tree trunk and

https://doi.org/10.26376/GPR2019001

compared a polar and real cross-section shape of a data visualisation. Takahashi and Aoike [17] combined the reflection and transmission mode of the GPR to distinguish heartwood and decay in logs and living tree trunks.

Tree trunk inspection using GPR is a very complex discipline for several reasons. First, living wood is a humid material with a very variable water content (which can range from about 30% to more than 200% of the weight of wood substance [18]) which is the cause of the electromagnetic waves attenuation. Second, significant heterogeneity and anisotropy of wood further complicate the interpretation of the radar data as the relative permittivity of wood depends also on a grain direction [19, 20]. Third, an irregular shape of a tree trunk does not allow for a good contact or at least a constant distance between a radar antenna and the tree trunk surface. Having various distances between the surface and the antenna leads to irregular surface reflections in radar images which are not straightforward to filter out. And last, but not least, in order to inspect tree trunks, it is essential to keep a good contact of the antenna with bark for better impedance matching. This is not always possible due to the bark roughness.

The influence of the surface roughness on radar data was already very well described by Pinel et al. [21] who studied wave scattering from multilayered random rough surfaces for road applications. Tosti et al. [22] dealt with the roughness of a railway ballast during evaluation of its dielectric properties with the GPR. Ardekani et al. [23] studied scattering and attenuation of radar signal due to a vegetation cover. Lambot et al. [24] and Jonard et al. [25] observed the soil roughness influence on the monostatic GPR signal inversion to retrieve surface moisture.

The objective of this paper is to see the influence of the tree trunks rough surface on GPR images. In that respect, we simulated two cylindrical configurations with a smooth and rough surface using a finite difference time domain simulator, namely, gprMax2D [26, 27]. To check the validity of the numerical simulations, two laboratory measurements on a corresponding cylindrical model were done. The laboratory model contained also a smooth and a rough surface. Finally, four radar acquisitions on real trees with various surfaces and internal structures were carried out. Two trees with a rough bark and two trees with a smooth bark were chosen. Both pairs of trees consisted of a relatively

https://doi.org/10.26376/GPR2019001

healthy tree and a tree with a visible cavity. Data were processed using two filtering methods: free-space response subtraction and the average background removal. For more intuitive readability of the GPR images, the cartesian radargrams were projected to the polar coordinates.

2 Numerical simulations

The first step in understanding the effect of the surface roughness on our measurements was to simulate a cylindrical structure with a smooth and with a rough surface. In our previous experiments [28, 29], we studied reflections curves occurring in simulated and measured radargrams of a cylindrical laboratory model. All those experiments were done for a smooth surface. To see the influence of a rough surface, the same configuration with a rough surface was simulated. The configuration had a similar shape as a laboratory cylindrical model which is filled with sand. The rough surface was designed to have a random thickness (up to 70 mm) while the internal parts of the model remained the same (dry sand with air). The rough surface was created by generating 1000 random points in a known annular area with outer radius 4 cm larger than the current model. The generated points were used as centres of a series of filled circles (with a radius of 3 cm). The circles randomly overlapped each other and created a filled area with a rough edge. Figure 1 shows a configuration with a smooth surface (a) and with a stochastic rough surface (b). The relative permittivity of the sand was set to 3 and the relative permittivity of the generated surface was set to 2 to be slightly different than sand. The numerical simulations were done using the open source software gprMax2D [26, 27] using the Finite-Difference Time-Domain (FDTD) method [30] and which is specifically dedicated to GPR applications. The operating source was a Ricker wavelet with a centre frequency of $f_c = 900$ MHz. The spatial resolution of the numerical model geometry in the x and y directions was 2,5 mm.

Figure 2 shows the simulated radargrams of the smooth configuration (left) and the configuration with the random rough surface (right) for both choices of data filtering (free-space response subtraction and average background removal). In all images, we can see the surface reflection (at about 1.5 ns), the reflection from the opposite side of the model (at about 10 ns), the reflection curves originating from internal inhomogeneities

https://doi.org/10.26376/GPR2019001

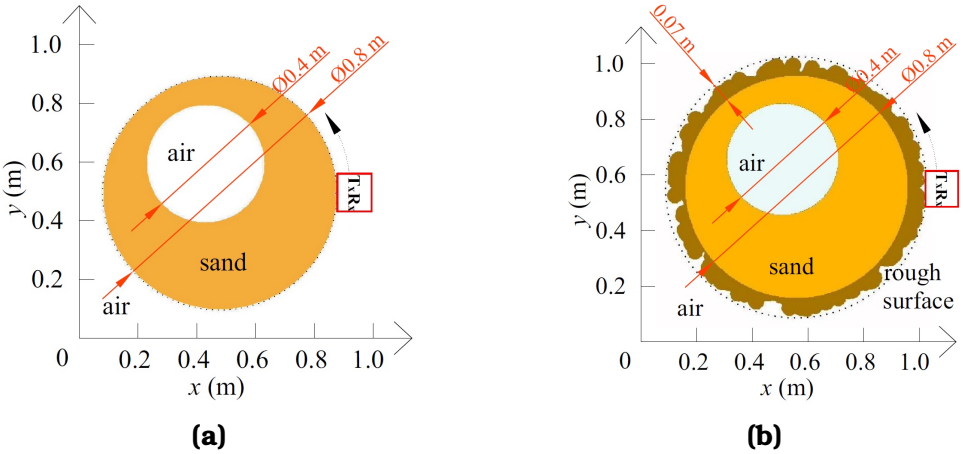

Figure 1: Configurations of the tree trunk model for numerical simulations in gprMax2D: a) With a smooth surface, b) with a rough surface with the tickness up to 7 cm.

(two sinusoidal shapes at about 3-7 ns corresponding to the closest and the furthest point on the void to the receiver) and the total internal reflection (TIR) at about 14 ns (explained by Ježová et al. [28, 29]).

Figure 2a (smooth surface, free-space response subtraction) provides very clear reflection curves described above without any particular noise (other minor reflections). The reflections of the opposite side of the model (at 10 ns) and the TIR are stronger at the positions of 0.5-1.2 m when the antenna is close to the internal void. Then, at the propagation time of 7-14 ns we can see cross-shaped reflections at the positions of 1.7-2.5 m when the antenna is far from the internal void. Both cases occur due to the symmetrical geometry regarding the antenna position and the internal void which can cause additional reflections. We already described this phenomenon in our previous study [31].

In Figure 2b (rough surface, free-space response subtraction), many reflections in the background are present. This fact, however, does not prevent the visibility of the internal void reflections and the TIR, but it makes other reflections less visible (e.g., the opposite side reflection at 10 ns). Just below the surface reflection, we can observe a reflection originating from the interface between the rough surface and the cylinder. In the image, the opposite side of the observed model is not represented by a line, but we can see it through a series of irregular reflections

https://doi.org/10.26376/GPR2019001

at about 10 ns. It is worth mentioning that we cannot see any additional reflections caused by the symmetry of the model-hole-antenna configuration because this phenomenon was significantly suppressed by the rough surface.

In Figure 2c (smooth surface, average background subtraction), the reflections pointing at the internal inhomogeneities, opposite side reflection and TIR are well visible. Nevertheless, the surface reflection was almost fully eliminated by the average background removal as it is constant. Furthermore, a constant line at about 3 ns now appeared in the radargram as a result of the filter. In the radar data, we can see a strong reflection at 3 ns in positions of 0.9-1 m as a part of the sinusoidal reflection of the internal void. Its values affected the average value which was subtracted from the whole image at this time. This may cause problems during a tomography of the medium as it displays a non-existing external contour of the model. Also in this case, we can observe a stronger opposite side reflection curve and the TIR as well as the cross-shaped reflections caused by the symmetrical geometry.

In Figure 2d (rough surface, average background subtraction), we can again observe many minor reflections caused by the rough surface, especially at the closer edge of the configuration (at about 1-2 ns) and its opposite side (at about 10 ns). The strong constant reflections appearing in Figure 2b (surface reflection and TIR) were weakened but generally, the images are very similar for both choices of the filtering. Also in this case, a constant line at 3 ns appeared as a result of the use of the average background removal.

To better visualize of the GPR images, a polar representation of them was made. To keep the surface reflection of the configurations, the images processed with the free-space response subtraction were chosen. To project into the polar representation of the radargram, the GPR image was cut in the middle part corresponding to approximately 4.6 ns (according to its ε_r = 3 and the geometric radius r = 0.4 m) from the source reflection (1.5 ns). Therefore, the image was split at the propagation time of 6.1 ns. Figure 3a shows the polar representation of the simulated radargram of the smooth case. We can see very well the external and internal contours of the configuration without any additional reflection. The image is very clear and corresponds to the simulated cylinder also with its size. Figure 3b shows the polar representation of the

https://doi.org/10.26376/GPR2019001

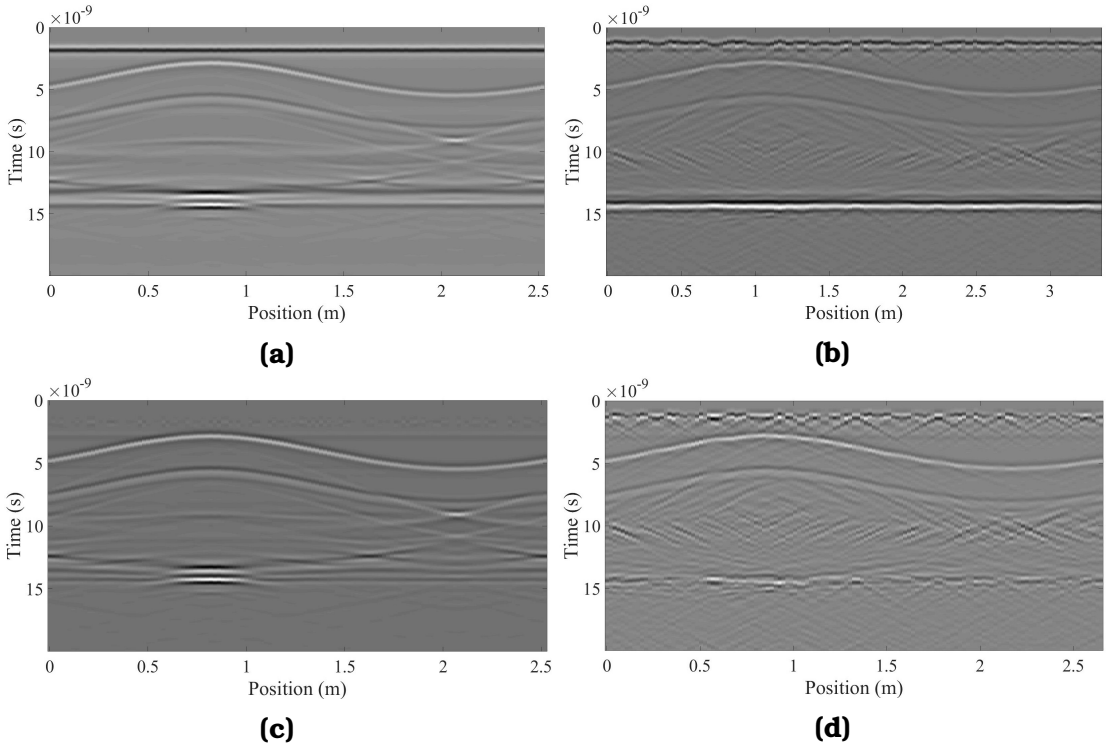

Figure 2: Numerical simulations using gprMax2D of a laboratory tree model with a smooth surface (left) and with a rough surface (right). The radar data were processed: a-b) with a free-space response subtraction, c-d) with an average background subtraction.

configuration containing the random rough surface. We can observe the very rough surface of the model edge and the slightly smoother surface of the circle which follows. The internal void is very well displayed despite the rough surface. In both images, a small reflection (coordinates [0.6, 0.6] in Figures 3a and 3b) appeared as an artifact of the projection. This indicates, that such a visualization is only illustrative, as we calculated the model centre assuming homogeneous permittivity of ε_r = 3, which is violated by the presence of the internal void.

3 Laboratory measurements

The next step of the rough surfaces evaluation was done in laboratory conditions. In particular, we performed two radar measurements of a laboratory cylindrical model made from two tubes (paper and PVC) and

https://doi.org/10.26376/GPR2019001

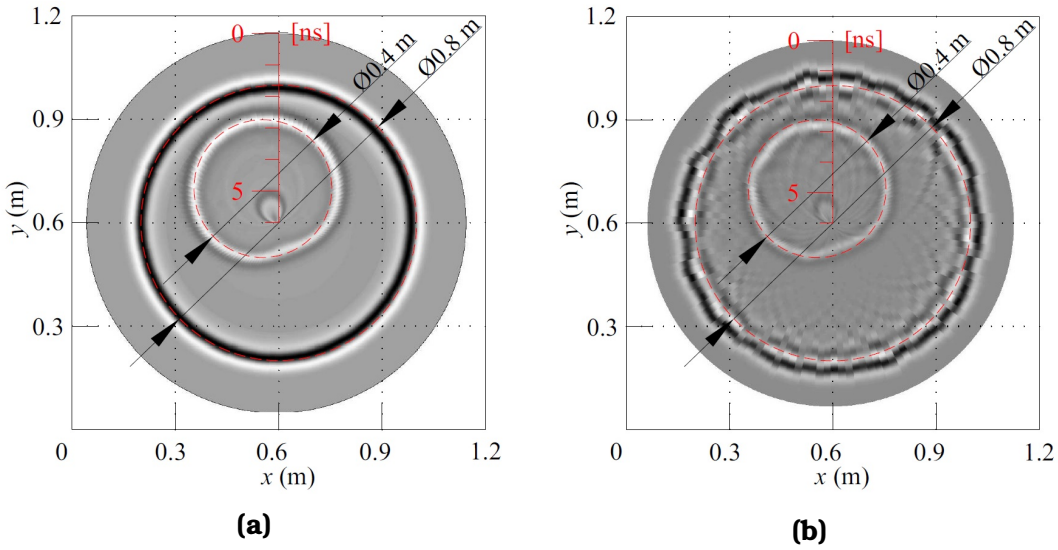

Figure 3: Polar representations of the numerical simulations with gprMax2d of the configuration with: a) Smooth surface, b) rough surface. The simulated data were processed with the free-space response subtraction.

sand (as a filling material). Analogically to the numerical simulations, the cylindrical model had a smooth surface for the first measurement while for the second, an irregular inhomogeneous structure made of paper and polystyrene was installed on the external surface of the larger tube to emulate the shape of the tree bark (see Figure 4). Both measurements were carried out with a lightweight radar system including a dielectric-coupled TEM horn antenna, a micro vector network analyser (Planar R54, Copper Mountain Technologies, Indianapolis, USA, [32]), an Intel computer Stick, a battery and a webcam for remote positioning. The antenna was filled with paraffin wax (ε_r = 2.2) in order to better couple the antenna impedance with the investigated medium (dry sand with ε_r = 3). This radar system (see Figure 5) was described in detail in [32]. In order to get the return loss of the antenna H_i, it was calibrated against a copper sheet (3×3 m) using the antenna model of Lambot et al. ([33]). For the calibration, a VNA (ZNB8, Rohde & Schwarz, Munich, Germany) was used to feed the antenna. The VNA was calibrated following Open-Short-Match reference calibration kit standards. The operating frequency was set to 0.5-3.5 GHz with a frequency step of 2 MHz.

In order to validate the observations made about different approaches

https://doi.org/10.26376/GPR2019001

(a) (b)

Figure 4: Laboratory tree trunk model: a) with a smooth surface, b) with a bark.

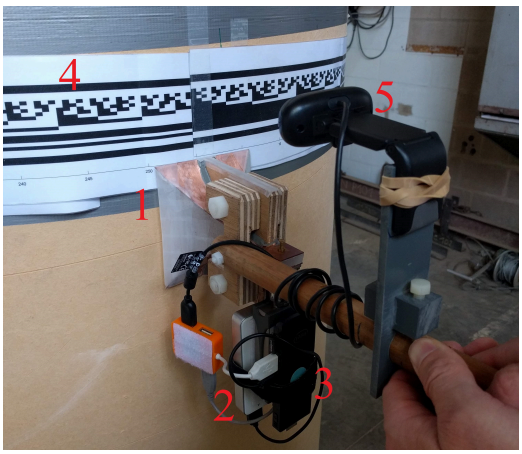

Figure 5: The mini radar system set up for the measurement of the laboratory cylindrical model with a smooth surface. 1) dielectric TEM horn antenna, 2) battery with VNA, 3) Intel computer, 4) barcode ruler, 5) webcam for remote positioning.

to background removal in the previous section, two different types of filtering was used again, namely, the free-space response subtraction (Figures 6a and 6b) and the average background subtraction (Figures 6c and 6d). Unsurprisingly, the laboratory images have different appearance than the simulated ones, especially those treated with free-space response subtraction where the antenna effects were removed. Both images with this filter contain periodically repeating multiple reflections between the antenna and the medium. In the simulated images, we used a point source dipole for emitting the signal, however, in the

https://doi.org/10.26376/GPR2019001

laboratory conditions a real antenna was used. By free-space response subtraction, we eliminated the internal reflections in the antenna, but not the reflections originating from its contact with the medium.

Both cases (smooth and rough) have very similar appearance and we can observe the surface reflection (at about 1.2 ns) and the internal void reflection (sinusoidal shape at about 2-5 ns). We can also see the strongest parts of the TIR (14 ns, 0.5-1.2 m) and the cross-shaped reflection (0.7-14 ns, 1.7-2.5 m) which we were able to see much better in the simulation. The remaining reflections are not recognizable very well as they have been obfuscated by the multiple reflections from various surfaces that have not been included in the simulation.

The second set of GPR images (using the average background subtraction) are, compared to free-space response subtraction, very well readable. We can immediately see that they describe a cylinder with the same internal structure but different surfaces. Figure 6c shows the GPR image of the smooth laboratory cylinder. As for the simulated case, the surface reflection was practically eliminated by the average background subtraction because the antenna was in contact with the surface and, therefore, the distance was constant and so, easily eliminated by this filter. Nevertheless, we can see very well the sinusoidal reflection from the internal void closest point (at about 2-5 ns) and the furthest point (about 2.6 ns further) as two parallel curves. We can also see a relatively constant reflection curve at about 10 ns which points at the opposite side of the cylinder. At 14 ns, we can see the TIR which is not visible so well as in the simulated images, but it is recognizable. Same as during the simulations, the curves are thicker at the positions 0.5-1.2 m. The cross-shaped reflection (0.7-14 ns, 1.7-2.5 m) is again well visible. At the position of 1.3 m and the time of about 1.2 ns, we can see a very strong hyperbolic reflection corresponding to a metallic structural wire hidden in the laboratory cylinder.

Figure 6d shows the GPR image of the laboratory cylinder with the rough surface. We can see more or less the same reflections as in the previous case with the smooth surface (Figure 6c). Also here we can see the opposite side reflection curve which is bolder at the positions 0.5-1.2 m and the cross-shaped reflection (0.7-14 ns, 1.7-2.5 m). This illustrates the fact, that the bark laboratory emulation is less rough than the one used in the numerical simulations. Nevertheless, we can

https://doi.org/10.26376/GPR2019001

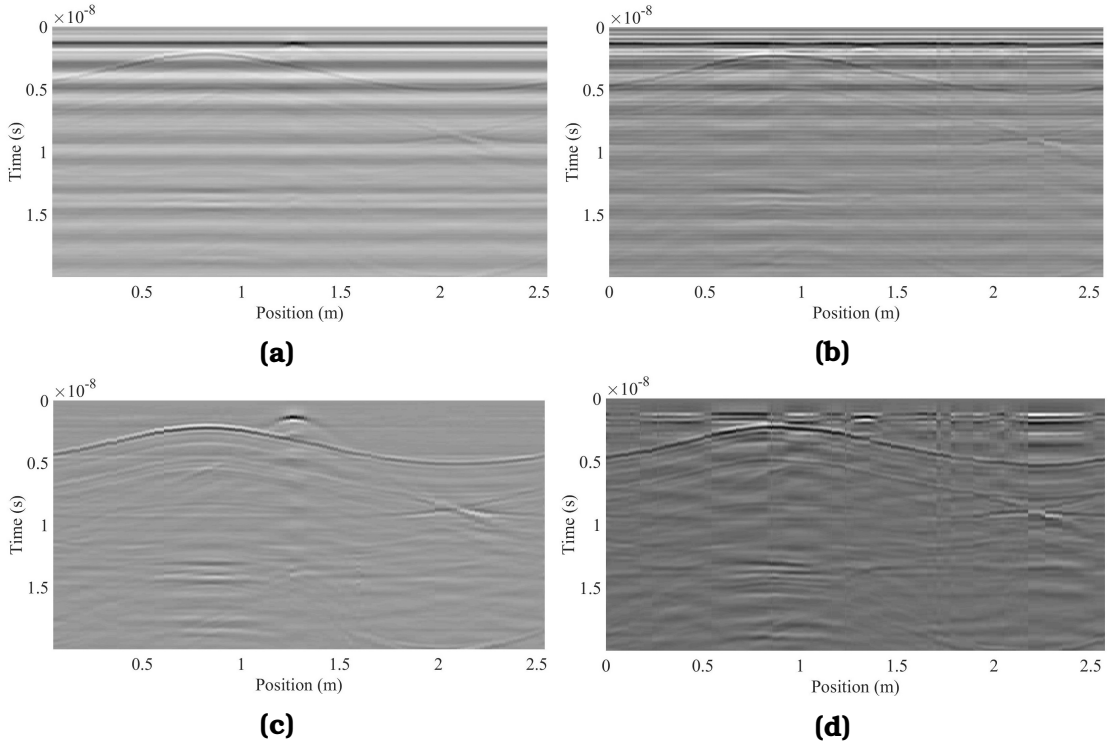

Figure 6: A laboratory tree trunk model measuremen with a smooth surface (left) and with a bark (right). The radar data were processed: a-b) with a free-space response subtraction, c-d) with an average background subtraction.

observe certain differences. First, the reflection corresponding to the surface of the cylinder was not eliminated by the average background removal, because the distance between the antenna and the surface was not constant due to the irregular (rough) artificial surface. We cannot, however, see the direct reflections corresponding to the artificial bark created on the laboratory model surface as paper and polystyrene have similar ε_r to the air. Second, the surface-antenna interaction caused the same multiples as we could see in Figures 6a and 6b, but because of the rough surface, it is not distributed constantly in direction x (position change). Hence, the average background subtraction could not eliminate it. Therefore, there is a lot of noise which makes the image more difficult to interpret. Finally, we can see only hints of the metallic wire reflection due to the noise in the radargram.

We represented the laboratory radargrams in the polar coordinates in the same way as we did for the simulated radar images. In

https://doi.org/10.26376/GPR2019001

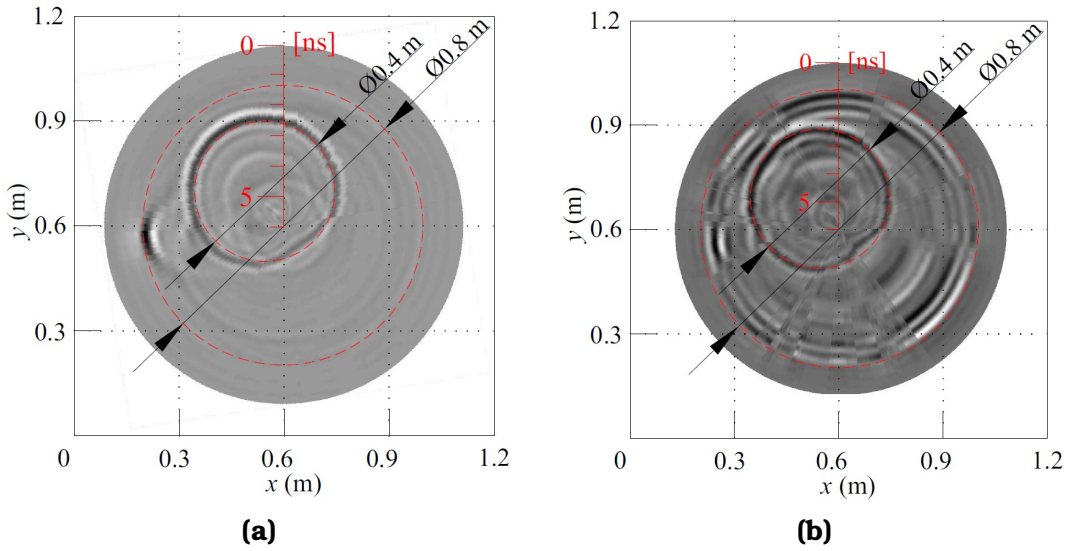

Figure 7: Polar representations of the simulated data of the configuration with: a) Smooth surface, b) rough surface. The simulated data were processed by the average background removal.

contrast to the previous section, the second filtering method (average background removal) exhibited better readability of the radargrams than the free-space response subtraction due to missing multiple reflections. Figure 7a displays the smooth cylindrical model radargram with two outstanding reflections pointing at the internal void at the position (0.5, 0.7) and the metallic wire at the position (0.2, 0.6). Due to the average background subtraction, the contour of the model surface is not so well visible which makes it difficult to read comfortably the image without the red contour. Figure 7b shows the polar representation of the radargram of the cylinder with the rough surface emulation. In this case, the model external border is well visible as well as the internal void. The image is, nevertheless, quite noisy.

4 Real tree trunk measurements

To see the real influence of a bark and of an internal structure on the radar data acquisition, we performed several measurements on real tree trunks. For the experiments, we chose four trees with different external and internal properties. All measurements were performed

https://doi.org/10.26376/GPR2019001

Figure 8: A living sweet chestnut with a rough bark in Waterloo (Belgium).

using the same lightweight radar system with a dielectric-coupled TEM horn antenna as for the laboratory measurements. The frequency range was set again to 0.5-3.5 GHz. All measurements were done in near-field conditions where the antenna was in contact with the bark. For all radar images, we applied the average background removal, as it showed better performance during the laboratory tests and an exponential gain function.

4.1 Living tree with a rough bark (Waterloo - Chestnut)

The first case study was a living tree (sweet chestnut, *Castanea Sativa*) in the Castle-Farm of Hougoumont, Waterloo, Belgium, with a very rough bark (see Figure 8). The tree is very old as it was present during the Battle of Waterloo in 1815 (the tree is situated in the battle site). This tree had about 6 m in circumference (almost 2 m in diameter). The radar data acquisition was not very easy due to the exceptional roughness of the bark and also the very irregular shape of the tree trunk cross-section. Hence, the antenna was never fully in contact with the surface of the tree trunk. Furthermore, only 5 m of its circumference was inspected because of poor accessibility (bushes around the trunk).

Figure 9 displays a radar image of that tree. The polar representation shows the part of the tree trunk which was investigated. For the polar representation, the ε_r of the medium was estimated to be 9 (as a living old tree) leading to 20 ns as the centre of the trunk because the diameter of the tree was about 2 m. We can observe very clearly the surface reflection (red curve at about 1.2 ns) which is very irregular. Another reflection (green curve) is visible at about 2.5 ns, and it has the same shape as the

https://doi.org/10.26376/GPR2019001

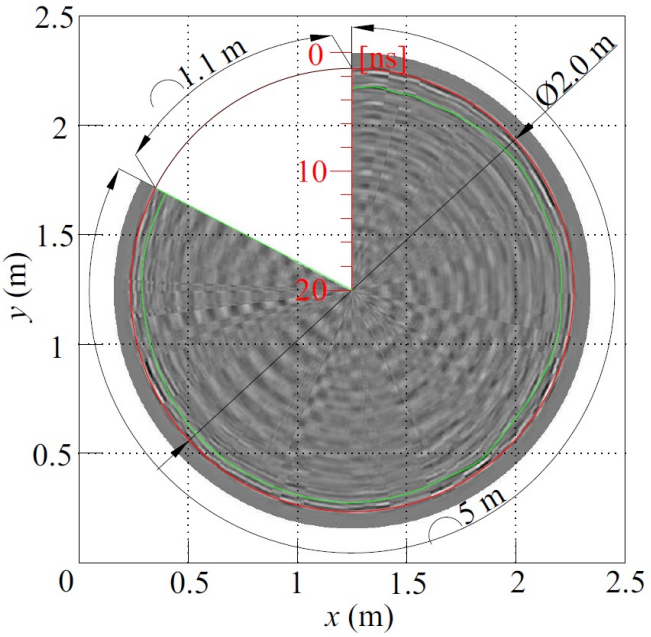

Figure 9: A polar representation of the radar image of a living chestnut with a bark (in Waterloo) up to 20 ns which is the estimated centre of the trunk (for ε_r = 9). Surface reflection is highlighted with a red curve, its first multiple reflection is highlighted with a green curve.

surface reflection. This means, that the reflection at 2.5 ns is a multiple reflection of the surface which repeats again, but much more feebly also at about 4 ns in the radargram (and the next ones would be more visible if we used higher gain function). The rest of the image is very noisy despite the applied filter. Therefore, we can assume, that nearly all waves were reflected from the bark or absorbed in the relatively humid sapwood.

4.2 Living tree with a rough bark and a cavity (Sohier - Oak)

Another case study was the inspection of a living oak (*Quercus robur*) with a rough bark and with a significant cavity in the trunk (see Figure 10). This tree was situated in the countryside in Sohier, Belgium. The tree trunk cross-section was more regular than the one of the previous tree and the texture bark was slightly finer. The circumference of the tree was about 4 m (giving the diameter of about 1.3 m). Its bark was partly missing and through one side we could see an open internal cavity of a very irregular shape (20-40 cm in diameter).

https://doi.org/10.26376/GPR2019001

Figure 10: A living oak with an internal cavity in Sohier (Belgium). Missing bark and the opening to the internal cavity.

Figure 11 shows a radar image in polar coordinates obtained by the radar inspection of the oak. We present only the part of the radargram with outstanding reflection curves (about 43% of the circumference) because the radar data were affected by very strong reflections at the positions corresponding to a cavity or a missing bark. Same as for the previous tree, we evaluated the ε_r to 9 and so, we determined the centre of the trunk to be at the propagation time of 13 ns (for a diameter of about 1.3 m). We can see the surface reflection at about 1.2 ns (red curve) and also its multiple at about 2.5 ns (blue curve). This radar image is very noisy due to the rough surface and very heterogeneous medium, but we can observe certain reflection curves at 5-6 ns (green curve). This reflection points at the internal irregularity (probably the cavity) in the trunk. In this example, we can see an importance of the electromagnetic properties evaluation. We set the ε_r as a homogeneous value for the whole tree trunk, nevertheless, the ε_r in the cavity was 1. Therefore, the size of the cavity appears larger in the polar representation ($\approx$ 0.9 m) than in reality ($\approx$ 0.4 m).

4.3 Living tree with a smooth bark (Louvain-la-Neuve - Beech)

The third case study was a radar inspection of a living European beech (*Fagus sulvatica*) in a forest in Louvain-la-Neuve, Belgium, with

https://doi.org/10.26376/GPR2019001

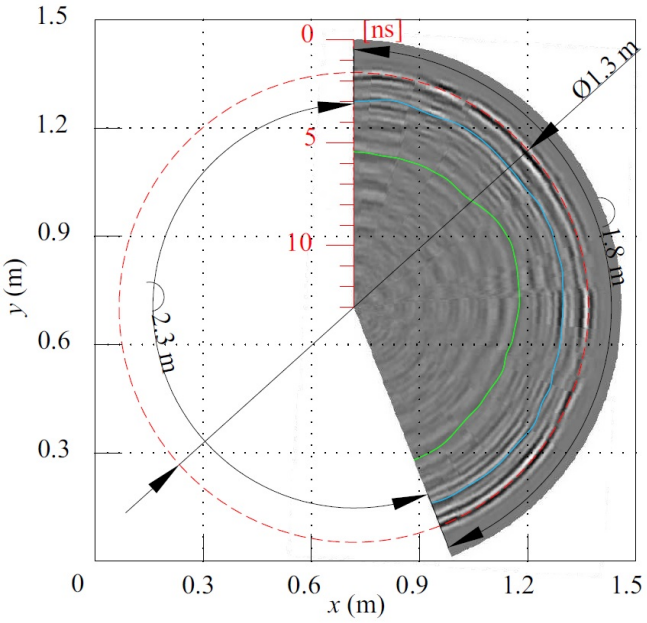

Figure 11: A polar representation of a radar image of a living oak with an internal cavity (in Sohier) until 13 ns which is the estimated centre of the trunk (for ε_r = 9). Red curve points at the surface reflection, blue curve shows its multiple and green cruve highlights the internal cavity.

a relatively smooth bark (see Figure 12). This tree had a circumference of about 3 m (almost 1 m in diameter), and it had a relatively regular cross-section (circular shape). It was therefore relatively easy to keep the contact between the antenna and the tree trunk surface without almost any air gaps.

In Figure 13, the radar image of the living beech tree is displayed in polar coordinates. We estimated the centre of the trunk at about 11 ns (for a relatively healthy living tree trunk, ε_r = 12), knowing the tree trunk circumference 3 m and so, it diameter almost 1 m. Because the distance between the antenna and the surface was almost constant, it was easy to reduce multiple reflections which were constant too. The image then appears less noisy than the previous cases. In Figure 13, the surface reflection at 1.2 ns is highlighted by a red curve. The curve is very clear and quite smooth. Afterwards, closer to the centre, we can observe other reflections with a different shape than the surface contour (blue and green curves). Those reflections correspond to certain interfaces inside the tree trunk. Changes of electromagnetic properties may correspond to

https://doi.org/10.26376/GPR2019001

Figure 12: A living beech tree in Louvain-la-Neuve (Belgium).

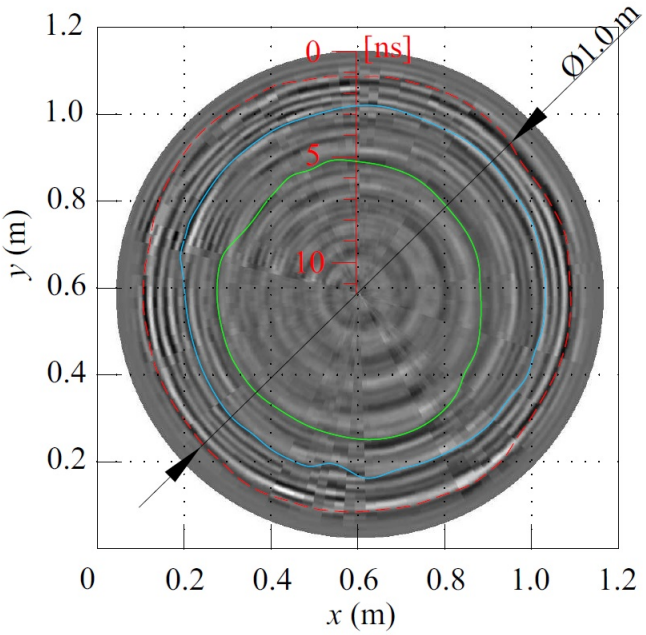

Figure 13: A polar representation of the living beech (in Louvain-la-Neuve) radar image until 11.5 ns which is the estimated centre of the trunk (for ε_r = 12).

changes of humidity or density of wood. It will then point at heartwood or decayed wood. Because we can see two layers in the trunk, we assume to have detected decayed wood in different stages of rot.

https://doi.org/10.26376/GPR2019001

Figure 14: A dead sweet chestnut in Waterloo (Belgium).

4.4 Dead tree without bark (Waterloo - Chestnut)

The last case study was a radar inspection of a dead sweet chestnut (*Castanea Sativa*) in the Castle-Farm of Hougoumont, Waterloo, Belgium (see Figure 14). This tree was visibly dead. It was already without its bark and inside the tree trunk. We could see a large irregular cavity. The cross-section of the trunk was relatively regular and the trunk surface was very smooth. The circumference of the tree trunk was about 4.5 m which gave us its diameter of about 1.4 m. The inspection was not done around the whole trunk because of a difficult accessibility (bushes).

In Figure 15, we can see a radar image in polar coordinates obtained by the radar inspection of the dead sweet chestnut. We estimated ε_r for this tree to 5, as the tree was dead and dry, and moreover, it contained a large cavity. Then, the centre of the trunk was calculated to approximately 11 ns (knowing the diameter about 1.4 m). The image shows the part of the trunk which was investigated. The wedge in the lower part of the image corresponds to the opening to the cavity in the tree trunk. In this part, only multiple reflections are visible, as the antenna was in free space. Nevertheless, the rest of the image shows the data obtained by the radar measurement when the antenna was in contact with the bark. The surface reflection is, again, highlighted by a red curve. It is quite regular and by its shapes, it corresponds to the real trunk surface shape. Then, we can see several reflections (blue, green

https://doi.org/10.26376/GPR2019001

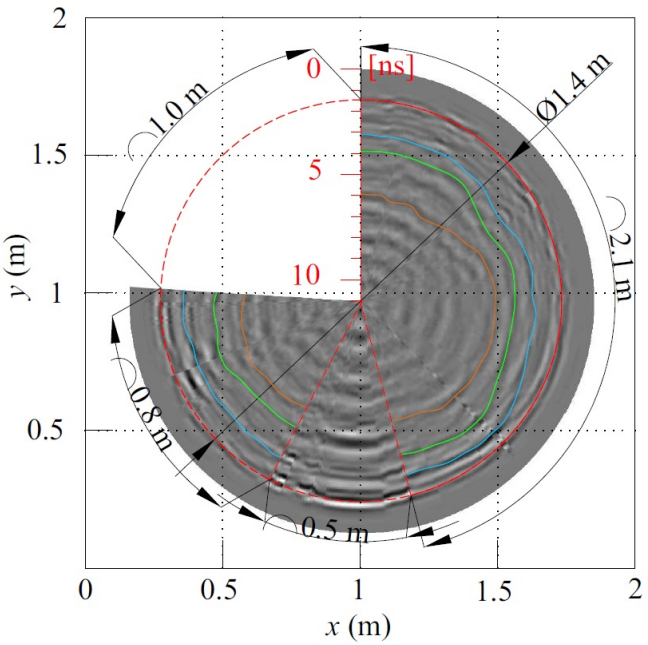

Figure 15: Polar representation of the dead sweet chestnut (in Waterloo) radar image until 11 ns which is the estimated centre of the trunk (for ε_r = 5).

and orange) pointing at the very complex internal structure of the tree trunk.

5 Summary and Conclusions

In this paper, we studied the influence of the surface roughness on the appearance of radar images, specifically for tree trunk radar inspection. We performed simulations comparing a cylindrical model with a smooth and a rough surface. To check the correctness of the simulation, we performed measurements on a laboratory cylindrical model with a smooth and a rough surface corresponding to the simulated configuration. The radar data were treated using two different filters, namely, free-space response subtraction and average background subtraction.

In both cases, the rough surface made the GPR images noisy and less readable. It did not prevent detection of the large inhomogeneities in the observed model, but it made observation of the small objects (e.g, the metal wire hidden in the laboratory cylinder) very complicated.

https://doi.org/10.26376/GPR2019001

Furthermore, the presence of the irregular surface practically eliminated the phenomenon originating from a symmetrical antenna-cylinder geometry.

For the two cases (numerical simulations and laboratory measurements), a different type of filtering turned out to be more suitable. The free-space response subtraction, which worked perfectly for the simulated images, did not provide a good filtering for the real measurements, as it did not eliminate the reflections originating from the interaction between the antenna and surfaces. Therefore, the average background subtraction was used for the measurements with the real antenna even though it removed the constant surface reflection which was important for expressing the radar image in a realistic way.

Despite the fact that the mini-radar system provided very good radar images of the laboratory cylindrical model, we can observe certain limitations for a tree trunk inspection. We performed radar measurements of four types of trees, specifically, two trees with a rough bark, two trees with a smooth bark. Both pairs consisting of a relatively healthy tree and a tree with a cavity. The radar data show the difficulty of a satisfactory data acquisition of trees with a rough bark. The signal was significantly reflected which prevented detecting internal interfaces in living wood, which is very humid and causes signal attenuation. On the other hand, the radar data obtained by the measurement of the trees with a smooth bark showed relatively clearly the internal structure of the trunks despite the living wood humidity.

We demonstrated that the major limitation of the tree trunk inspection with the GPR is most likely the high degree of irregularity of the bark. Additionally, to improve the tree radar data, we suggest a usage of dielectric antennas with similar electromagnetic properties of wood. To avoid having air gaps between the antenna and the tree trunk surface, a flexible material may be considered as a dielectric for future antennas.

Acknowledgment

The authors would like to acknowledge the support of the Fonds de la Recherche Scientifique (FNRS), Belgium, through the SENSWOOD project (Convention n° 19526260). We would like to thank the staff of the Castle-Farm of Hougoumont, Waterloo, Belgium, who allowed us to

https://doi.org/10.26376/GPR2019001

perform the measurements. This research was also carried out within the framework of EU funded COST Action TU1208 "Civil Engineering Applications of Ground Penetrating Radar".

References

[1] F. Kollmann and W. Cote, Jr., *Principles of Wood Science and Technology I, Solid Wood*. Berlin Heidelberg New York: Library of Congress Springer-Verlag, 1968, vol. Catalog Card Number 67-29 614.

[2] P. Niemz and D. Mannes, "Non-destructive testing of wood and wood-based materials," *Journal of Cultural Heritage*, vol. 13, no. 3 SUPPL., pp. S26–S34, September 2012.

[3] M. Larjavaara and H. C. Muller-Landau, "Comparison of decay classification, knife test, and two penetrometers for estimating wood density of coarse woody debris," *Canadian Journal of Forest Research*, vol. 40, no. 12, pp. 2313–2321, November 2010.

[4] G. S. Gilbert, J. O. Ballesteros, C. A. Barrios-Rodriguez, E. F. Bonadies, M. L. Cedeño Sánchez, N. J. Fossatti-Caballero, M. M. Trejos-Rodríguez, J. M. Pérez-Suñiga, K. S. Holub-Young, L. A. W. Henn, J. B. Thompson, C. G. García-López, A. C. Romo, D. C. Johnston, P. P. Barrick, F. A. Jordan, S. Hershcovich, N. Russo, J. D. Sánchez, J. P. Fábrega, R. Lumpkin, H. A. McWilliams, K. N. Chester, A. C. Burgos, E. B. Wong, J. H. Diab, S. A. Renteria, J. T. Harrower, D. A. Hooton, T. C. Glenn, B. C. Faircloth, and S. P. Hubbell, "Use of sonic tomography to detect and quantify wood decay in living trees," *Applications in Plant Sciences*, vol. 4, no. 12, p. 1600060, December 2016.

[5] C.-J. Lin, Y.-C. Kao, T.-T. Lin, M.-J. Tsai, S.-Y. Wang, L.-D. Lin, Y.-N. Wang, and M.-H. Chan, "Application of an ultrasonic tomographic technique for detecting defects in standing trees," *International Biodeterioration & Biodegradation*, vol. 62, no. 4, pp. 434 – 441, December 2008.

https://doi.org/10.26376/GPR2019001

[6] L. Brancheriau, A. Ghodrati, P. Gallet, P. Thaunay, and P. Lasaygues, "Application of ultrasonic tomography to characterize the mechanical state of standing trees (picea abies)," *Journal of Physics: Conference Series*, vol. 353, no. 1, p. 012007, March 2012.

[7] A. Guyot, K. T. Ostergaard, M. Lenkopane, J. Fan, and D. A. Lockington, "Using electrical resistivity tomography to differentiate sapwood from heartwood: application to conifers," *Tree Physiology*, vol. 33, no. 2, pp. 187–194, February 2013.

[8] M. L. Elliott, T. K. Broschat, and L. Göcke, "Preliminary evaluation of electrical resistance tomography for imaging palm trunks," *Arboriculture & Urban Forestry*, vol. 42, no. 2, pp. 111–119, March 2016.

[9] J. V. den Bulcke, E. L. Wernersson, M. Dierick, D. V. Loo, B. Masschaele, L. Brabant, M. N. Boone, L. V. Hoorebeke, K. Haneca, A. Brun, C. L. L. Hendriks, and J. V. Acker, "3d tree-ring analysis using helical x-ray tomography," *Dendrochronologia*, vol. 32, no. 1, pp. 39 – 46, January 2013.

[10] G. Nicolotti, L. V. Socco, R. Martinis, A. Godio, and L. Sambuelli, "Application and comparison of three tomographic techiques for detection decay in trees," *Journal of Arboriculture*, vol. 29, no. 2, pp. 66–78, March 2003.

[11] S. A. Al Hagrey, "Geophysical imaging of root-zone, trunk, and moisture heterogeneity," *Journal of Experimental Botany*, vol. 58, no. 4, pp. 839–854, January 2007.

[12] J. R. Butnor, M. L. Pruyn, D. C. Shaw, M. E. Harmon, A. N. Mucciardi, and M. G. Ryan, "Detecting defects in conifers with ground penetrating radar: Applications and challenges," *Forest Pathology*, vol. 39, no. 5, pp. 309–322, October 2009.

[13] H. Lorenzo, V. Pérez-Gracia, A. Novo, and J. Armesto, "Forestry applications of ground-penetrating radar," *Forest Systems*, vol. 19, no. 1, pp. 5–17, April 2010.

[14] L. Fu, S. Liu, and L. Liu, "Internal structure characterization of living tree trunk cross-section using GPR: Numerical examples and field

https://doi.org/10.26376/GPR2019001

data analysis," in *Proceedings of the 15th International Conference on Ground Penetrating Radar, GPR 2014*, June 2014, pp. 155–160.

[15] E. Mazurek and M. Łyskowski, "Evaluation of gpr surveys for assessment of trees condition in urbanized areas," *Geology, Geophysics and Environment*, vol. 40, no. 3, pp. 291–296, January 2015.

[16] W. Li, J. Wen, Z. Xiao, and S. Xu, "Application of ground-penetrating radar for detecting internal anomalies in tree trunks with irregular contours," *Sensors (Switzerland)*, vol. 18, no. 2, February 2018.

[17] K. Takahashi and K. Aoike, "Gpr measurements for diagnosing tree trunk," in *2018 17th International Conference on Ground Penetrating Radar (GPR)*, June 2018, pp. 1–4.

[18] R. J. Ross and F. P. L. USDA Forest Service., "Wood handbook : wood as an engineering material," Tech. Rep., April 2010.

[19] I. Rodríguez-Abad, R. Martínez-Sala, R. Capuz Lladró, R. Díez Barra, and F. García-García, "Assessment of the variation of the moisture content in the pinus pinaster ait using the non destructive gpr technique," *Materiales de Construccion*, vol. 61, no. 301, pp. 143–156, March 2011.

[20] I. Rodríguez-Abad, R. Martínez-Sala, F. García-García, and R. Capuz-Lladro, "Nondestructive methodologies for the evaluation of moisture content in sawn timber structures: ground-penetrating radar and ultrasound techniques," *Near Surface Geophysics*, vol. 8, pp. 475–482, December 2010.

[21] N. Pinel, C. Le Bastard, C. Bourlier, and M. Sun, "Asymptotic modeling of coherent scattering from random rough layers: Application to road survey by GPR at nadir," *International Journal of Antennas and Propagation*, vol. 2012, 2012.

[22] F. Tosti, L. Bianchini Ciampoli, A. Calvi, A. M. Alani, and A. Benedetto, "An investigation into the railway ballast dielectric properties using different GPR antennas and frequency systems," *NDT and E International*, vol. 93, pp. 131–140, January 2018.

https://doi.org/10.26376/GPR2019001

[23] M. R. M. Ardekani, D. C. Jacques, and S. Lambot, "A layered vegetation model for gpr full-wave inversion," *IEEE Journal of Selected Topics in Applied Earth Observations and Remote Sensing*, vol. 9, no. 1, pp. 18–28, January 2016.

[24] S. Lambot, M. Antoine, M. Vanclooster, and E. C. Slob, "Effect of soil roughness on the inversion of off-ground monostatic GPR signal for noninvasive quantification of soil properties," *Water Resources Research*, vol. 42, no. 3, March 2006.

[25] F. Jonard, L. Weihermüller, H. Vereecken, and S. Lambot, "Accounting for soil surface roughness in the inversion of ultrawideband off-ground GPR signal for soil moisture retrieval," *GEOPHYSICS*, vol. 77, no. 1, pp. H1–H7, January 2012.

[26] A. Giannopoulos, "Modelling ground penetrating radar by gprmax," *Construction and Building Materials*, vol. 19, no. 10, pp. 755–762, December 2005.

[27] C. Warren, A. Giannopoulos, and I. Giannakis, "gprmax: Open source software to simulate electromagnetic wave propagation for ground penetrating radar," *Computer Physics Communications*, vol. 209, pp. 163 – 170, December 2016.

[28] J. Ježová, L. Mertens, and S. Lambot, "Ground-penetrating radar for observing tree trunks and other cylindrical objects," *Construction and Building Materials*, vol. 123, pp. 214–225, October 2016.

[29] J. Ježová, J. Harou, and S. Lambot, "Reflection waveforms occurring in bistatic radar testing of columns and tree trunks," *Construction and Building Materials*, vol. 174, pp. 388 – 400, June 2018.

[30] A. Taflove, S. C. Hagness, and M. Piket-May, "9 - computational electromagnetics: The finite-difference time-domain method," in *The Electrical Engineering Handbook*, W.-K. CHEN, Ed. Burlington: Academic Press, 2005, pp. 629 – 670.

[31] J. Ježová and S. Lambot, "Reflection waveforms occurring in gpr tree trunk testing," *2016 16th International Conference on Ground Penetrating Radar (GPR)*, pp. 1–5, June 2016.

https://doi.org/10.26376/GPR2019001

[32] ——, "A dielectric horn antenna and lightweight radar for material inspection," *Under Review in Journal of Applied Geophysics*, 2018.

[33] S. Lambot, E. C. Slob, I. D. Van Bosch, B. Stockbroeckx, and M. Vanclooster, "Modeling of ground-penetrating radar for accurate characterization of subsurface electric properties," *IEEE Transactions on Geoscience and Remote Sensing*, vol. 42, no. 11, pp. 2555–2568, November 2004.

Ground Penetrating Radar
Volume 2, Issue 1, March 2019
https://doi.org/10.26376/GPR2019002

Discrimination of Dispersive Materials from Radar Signals Using Q*

Chun an Tsai[1], Rebecca Ghent [1,2],
Alexander Boivin[2], and Dylan Hickson[3]

[1]Department of Physics, University of Toronto, Toronto, Canada –
ctsai@physics.utoronto.ca, ghentr@es.utoronto.ca
(C. Tsai is the Corresponding Author)

[2] Department of Earth Sciences, University of Toronto, Toronto, Canada –
alex.boivin@mail.utoronto.ca

[3] Centre for Research in Earth and Space Science, York University,
Toronto, Canada – dylan.hickson@gmail.com

Abstract

Using a combination of laboratory measurements and modeling results, we demonstrate the potential of distinguishing two dispersive materials by estimating quality factor (Q) using radar signals at two different frequencies. Here, we report on new complex dielectric permittivity measurements of a pulp sample mainly composed of pyrite (25%) and quartz (55%) from a massive sulphide mine, which shows frequency-dependent permittivity, and of a calcium-rich montmorillonite sample (STx-1b) for comparison. We made these measurements using the coaxial transmission line technique. To understand the dispersion observed in both samples, we fitted the measured complex permittivities using the Cole-Cole model to obtain the relaxation times that best represent the dielectric losses. We chose montmorillonite as the "control" material because it readily absorbs water, which has well-known dielectric relaxation mechanisms, thus providing a means of testing whether the pulp sample relaxations could be distinguished from those caused by adsorbed water. Our inverted montmorillonite relaxation times show one interlayer-water relaxation and one free water relaxation, as expected for this clay structure. By contrast, the pyrite-quartz sample shows intrinsic dispersion that is independent of the influence of water. The measurements show that the two materials have opposite concavity in the attenuation v.s. frequency plot, which can be detected using Q* in principle. Using these results, we conducted a series of 3D Finite-Difference-Time-Domain (FDTD) simulations in a cross-hole setup to*

https://doi.org/10.26376/GPR2019002

explore the effects of the observed dispersion on material detectability. We show that it is possible to distinguish intrinsically dispersive materials from those that are simply wet.

Keywords: Ground penetrating radar; Dispersion; Complex permittivity measurement; Spectral decomposition; Quality factor.

1 Introduction

Ground penetrating radar (GPR) is a nondestructive measurement technique which uses the transmission or reflection of electromagnetic (EM) waves to locate targets, anomalies or interfaces beneath or within natural or artificial surfaces. One basic assumption of GPR surveys is that subsurface features return reflections that are replicas of the transmitted signal with lower amplitudes. This implies that electrical properties of materials are independent of frequency within the frequency range of GPR, which is often referred to as the "GPR plateau" [1]. While this assumption holds true for most materials in the frequency band of GPR operation, some materials, especially materials that contain water, have frequency-dependent dielectric permittivities. As the complex permittivity varies with frequency, both the velocity and attenuation of the EM waves also change. This type of dispersion is categorized as physical property dispersion [2]. Scattering from heterogeneities in the subsurface can cause frequency-dependent attenuation as well. The attenuation measured in the field is mainly the combination of intrinsic dispersion and scattering dispersion, and it is difficult to isolate the two. There are several parameters used to characterize frequency-dependent attenuation. Turner and Siggins [3] show that, similar to seismic wave analysis [4], we can use a constant Q^* parameter to characterize materials with frequency-dependent attenuation in GPR surveys. Bradford [5] defines a more general dispersion parameter D that includes all frequency-dependent attenuation. One of the methods to extract Q^* from radar signals is the spectral shift method [6]. As the signal propagates, the peak frequency shifts lower from the original source value, and the difference can be used to estimate Q^* of the material.

In previous studies, water content was reported to be the major cause of dispersion. Therefore materials containing variable amounts of water,

 https://doi.org/10.26376/GPR2019002

such as clay [7–10] and concrete [11–13] are of major interest in the study of frequency-dependent attenuation of radar waves. Our goal for this project was to identify a dispersion behaviour that is independent of the influence of water and determine whether the difference can be identified from radar signals [14]. Since clay is a typical soil material that can absorb a large amount of water, we chose a montmorillonite sample as a reference material to characterize the influence of water on its dielectric properties. We measured the complex permittivity of the montmorillonite at varying moisture levels, then fitted the data with a multi-pole Cole-Cole model to obtain the dielectric relaxations responsible for the dispersion. We also fitted the measurements of a pulp sample that is mainly composed of pyrite and quartz from the LaRonde massive sulphide mine that shows a different dispersive behaviour from the montmorillonite sample. Then, we show with numerical simulations that it is possible to distinguish between these two types of dispersive behaviours by comparing the Q* values at two frequencies. We believe that this technique expands the potential application of radar signals in material characterization.

2 Theory

2.1 Electromagnetic wave propagation in dielectrics

A GPR system generates EM waves that are either pulsed or continuous, in the frequency range of 10 MHz to a few GHz. The EM waves penetrate and propagate in the dielectric, then are transmitted or reflected to the receiving antenna, depending on the setup of the survey. The propagation of EM waves in dielectrics is controlled by many factors, such as antenna characteristics, scattering, attenuation, etc. Here we focus on the study of complex relative permittivity, which characterizes the speed and attenuation of EM waves during propagation. Complex relative permittivity consists of a real and an imaginary part:

$$\epsilon^*(\omega) = \epsilon'(\omega) - j\epsilon''(\omega) \tag{1}$$

where ϵ^*, ϵ' and ϵ'' are the complex, real, and imaginary components of relative permittivity, respectively. For most materials, the complex permittivity is dependent on frequency f, and $\omega = 2\pi f$. In this study, we

https://doi.org/10.26376/GPR2019002

assume that the relative magnetic permeability is 1 for all materials. This is quite accurate for most materials and a common assumption made in many studies. The electric field of a plane wave at position $\vec{r}$ and time t is given by

$$\vec{E}(\vec{r},t) = \vec{E_0} e^{j(\vec{k}\cdot\vec{r}-\omega t)} \tag{2}$$

where $\vec{E_0}$ is the constant amplitude vector and $\vec{k}$ is the complex wave vector. The complex wave vector is given by

$$\vec{k} = (\beta - j\alpha)\hat{k} \tag{3}$$

where the unit vector $\hat{k}$ denotes the direction of propagation of the wave. The phase constant β and attenuation constant α are defined as

$$\beta = \frac{\omega}{c_0}\sqrt{\frac{\epsilon'}{2}\left[\sqrt{1+\left(\frac{\epsilon''}{\epsilon'}\right)^2}+1\right]} \tag{4}$$

$$\alpha = \frac{\omega}{c_0}\sqrt{\frac{\epsilon'}{2}\left[\sqrt{1+\left(\frac{\epsilon''}{\epsilon'}\right)^2}-1\right]} \tag{5}$$

where c_0 is the speed of EM waves in free space ($\sim 3\times10^8$ m/s). We can multiply α by 8.686 to convert to the more commonly used units of dB/m. The phase velocity of the wave can is given by $v = \omega/\beta$. Note that when the imaginary part of the relative permittivity is small compared to the real part, the phase velocity can be approximated as $v = c_0/\sqrt{\epsilon'}$.

In general, attenuation and phase velocity of EM waves are frequency dependent in real materials. One way to characterize frequency-dependent attenuation is using quality factor Q, which is defined as

$$Q = \frac{\omega}{2v\alpha} \tag{6}$$

This parameter describes the ratio of energy stored to energy dissipated in one cycle. For most materials encountered in GPR surveys, the frequency-dependent attenuation is linear in the relevant frequency bandwidth [3]. Thus we can approximate the linear region with the best fit line described by

https://doi.org/10.26376/GPR2019002

$$\alpha = \alpha_0 + \frac{\omega - \omega_0}{2vQ^*} \tag{7}$$

where α_0 is the attenuation at a reference frequency ω_0. As radar signals propagate in dispersive materials, the peak of the amplitude spectrum shifts due to frequency-dependent attenuation, and we can measure $Q*$ from the amount of frequency shift. The relation between $Q*$ and the corresponding spectral shift of a Ricker wavelet is given by [5, 6]

$$\frac{1}{Q^*} = \frac{4}{t}\frac{(\omega_m^2 - \omega_t^2)}{\omega_m^2 \omega_t} \tag{8}$$

where ω_m is the spectral maximum of the source and ω_t is the spectral maximum at time t.

2.2 Models of dielectric dispersion

In this paper we study the frequency-dependent complex permittivity with the Debye model [15] and the Cole-Cole [16] model. The Debye model describes how pure polar molecules (dipoles) behave in the presence of an electric field. Instead of reacting instantaneously, the dipoles need a period of time, called the relaxation time, to reorient themselves along the direction of the applied electric field. To be more specific, relaxation time τ is defined as the time required to reach $1/e$ (e being Euler's number) of the original polarization when the field is removed; and the frequency dependence of the permittivity is given as:

$$\epsilon^*(\omega) = \epsilon_\infty + \sum_{n=1}^{N} \frac{\epsilon_{s,n} - \epsilon_\infty}{1 + j\omega\tau_n} - j\frac{\sigma_{dc}}{\omega\epsilon_0} \tag{9}$$

where ϵ_∞ is the relative permittivity at infinite-frequency limit, ϵ_s is the relative permittivity at static limit, τ is the relaxation time, and σ_{dc} is the Direct Current (DC) electrical conductivity. The summation symbol indicates that there may be more than one type of polar molecule involved. It is often useful to write out the real and the imaginary parts of (9) explicitly:

$$\epsilon^* = \epsilon' - j\epsilon'' \tag{10}$$

https://doi.org/10.26376/GPR2019002

$$\epsilon' = \epsilon_\infty + \frac{\epsilon_s - \epsilon_\infty}{1 + \omega^2\tau^2} \qquad \epsilon'' = -\frac{\omega\tau(\epsilon_s - \epsilon_\infty)}{1 + \omega^2\tau^2} + \frac{\sigma_{dc}}{\omega\epsilon_0} \tag{11}$$

The Debye model has also been modified into various forms to describe experimental results. The most general form is the Havriliak-Negami (HN) relaxation, which has two additional parameters compared to Debye's model. It was first used to describe dielectric relaxation in polymers [17]. The one-pole HN relaxation is:

$$\epsilon^* = \epsilon_\infty + \frac{\epsilon_s - \epsilon_\infty}{[1 + (j\omega\tau)^\gamma]^\nu} \qquad 0 \leq \gamma, \nu \leq 1 \tag{12}$$

If $\beta = 1$, HN relaxation reduces to a Cole-Cole relaxation. If $\gamma = 1$, HN relation reduces to a Cole-Davidson relaxation. The Debye relaxation is a special case of HN relaxation where $\gamma = \nu = 1$. The parameter γ controls the "broadness" of the relaxation peak. The smaller γ is, the broader the relaxation peak would be on the frequency axis. On the other hand, ν describes the "asymmetry" of the relaxation peak. When $\nu = 1$, the relaxation peak is symmetrical.

3 Methodology

In order to quantitatively describe the dispersion caused by water, we measured the complex permittivity of a clay sample under various moisture levels. We chose the calcium-rich montmorillonite as our reference sample because its structure is well-understood. We also measured the complex permittivity of pulp prepared from drilling core samples that is mostly composed of quartz and pyrite. We then fitted the permittivity data to the Cole-Cole model for interpretation of the relaxation mechanisms.

3.1 Laboratory measurements

We measured the permittivity of two powdered samples: calcium-rich montmorillonite (STx-1b) from the Clay Minerals Society and a pulp sample (pyrite and quartz) provided by Agnico Eagle Mines Ltd. There is about 25% pyrite (FeS_2) and 55% quartz in the sample from X-ray

https://doi.org/10.26376/GPR2019002

fluorescence results. The samples were measured using the coaxial transmission line technique. We used the Keysight E5071C ENA series vector network analyzer (VNA) that measures from 300 kHz to 14 GHz in combination with METAS VNA Tools II software. Due to the length of the sample holder and the large uncertainty in the low-frequency range, we only used measurements from 50 MHz to 8.5 GHz. The software automatically calculates the uncertainty in measurements [18]. Two Maury Microwave SC-35 cables were connected to the two ports of the VNA, and each cable was connected to a 3.5 mm/14 mm adapter. The 14 mm side was then connected to the sample holder, which has a length of 15 cm. The GR-900LZ sample holder is a cylindrical tube that has two parts: the outer conductor and the inner conductor. The inner diameter of the outer conductor is 14 mm, and the outer diameter of the inner conductor is 6 mm. Prior to each measurement, the VNA and the corresponding setup were calibrated using the full two-port Through-Reflection-Match (TRM) method [19]. The input and output signals from both ports are measured to determine the real and imaginary parts of the S-parameters. The complex permittivity can be calculated from the S-parameters using the non-iterative stable transmission/reflection method for low-loss material [20–22] The magnetic permeability μ_r is assumed to be 1.

To observe the effect of water on permittivity more clearly, we first baked the clay sample at 115 °C for 48 hours [23] in order to remove the surface (free) water and to keep the interlayer water [24, 25]. We also prepared a "moisture chamber" to achieve various moisture content. The moisture chamber is a sealable box with water covering the bottom. The samples were placed in a aluminum pan that was raised above the water surface. The sealable box ensures that water vapour can diffuse into the sample evenly. We varied the time the samples spend in the box to control the moisture content. We measured the baked sample first, then placed it into the moisture chamber for 3, 5, 7, 15, and 24 hours. We baked the samples for at least 24 hours between each measurement to ensure that the water content is entirely controlled by the time the samples spend in the moisture chamber. We calculated the water content by weight percentage. Instead of performing the same series of moisture measurements, we measured the pyrite-quartz sample under ambient and baked conditions only.

 https://doi.org/10.26376/GPR2019002

Since dielectric permittivity varies as a function of density, the data were normalized to a bulk density of 1.60 g/cm^3 as shown in (13) [26–28]:

$$\epsilon^*_{norm} = \epsilon^*(1.92)^{d_n - d} \tag{13}$$

where ϵ^* is the complex permittivity, d_n = 1.60 g/cm^3, and d is the bulk density of the measured sample.

3.2 Decomposition of relaxation poles

We inverted the complex permittivity measurements to fit the Cole-Cole model with a DC conductivity term:

$$\epsilon^* = \epsilon_\infty + \frac{\epsilon_{s1} - \epsilon_\infty}{1 + (j\omega\tau_1)^{\alpha_1}} + \frac{\epsilon_{s2} - \epsilon_\infty}{1 + (j\omega\tau_2)^{\alpha_2}} - j\frac{\sigma_{dc}}{\omega\epsilon_0}. \tag{14}$$

The best fit to the baked clay sample was achieved using a 1-pole model while the moist sample was best fit using a 2-pole model, suggesting one and two relaxation mechanisms, respectively. The number of relaxation poles we found to best fit the measured data is also consistent with the structure of montmorillonite. The interlayer bound water should be retained at our drying temperature, which was shown in previous studies to possess a different relaxation time from free water [10, 29]. To invert for the parameters, we used a Levenberg-Marquardt scheme to perform least-squares fitting using the Lmfit module in Python [30].

3.3 Numerical simulation

In order to investigate the possibility of using dispersive properties to enhance GPR surveys, we performed numerical simulations based on the inversion of results calculated using the software gprMax [31]. GprMax is an open source software that simulates electromagnetic wave propagation by solving Maxwell's equations in a three-dimensional (3D) spatial domain using a Yee-grid scheme [32] and the finite-difference time-domain (FDTD) method. To handle dispersive materials, the software provides built-in Debye, Drude, and Lorentz models, for which arbitrary numbers of relaxation poles can be added to the simulation. The Cole-Cole model cannot be directly implemented into FDTD code.

https://doi.org/10.26376/GPR2019002

Therefore, we use multi-Debye relaxations to approximate the inversion using the Cole-Cole model [33]. The number of Debye poles was chosen so that the Debye inversion produces the closest residual with our original Cole-Cole inversion.

The 3D simulation space we used is 1.4 m $\times$ 0.4 m $\times$ 0.4 m, with a spatial discretization of 4 mm in all three coordinates. The time-step (7.7 ps) used was derived from the 3D Courant-Friedrichs-Lewy condition:

$$\Delta t \leq \frac{1}{c\sqrt{\frac{1}{(\Delta x)^2}+\frac{1}{(\Delta y)^2}+\frac{1}{(\Delta z)^2}}} \tag{15}$$

where Δx, Δy and Δz represent the spatial discretization in the x, y, and z directions, respectively. We used a simplified cross-hole setup with two Hertzian dipoles as the antennas. A schematic section of the simulation domain is shown in Figure 1. The transmitting antenna is located at (x, y, z) = (0.1 m, 0.2 m, 0.2 m) and the receiving antenna is located at (x, y, z) = (0.8 m, 0.2 m, 0.2 m). The source waveform is a Ricker wavelet with a center frequency of 400 MHz and 1200 MHz, polarized in the z-direction. A 10-cell perfectly-matched-layer (PML) is implemented on all faces of the simulation domain to prevent reflections back into the dielectric.

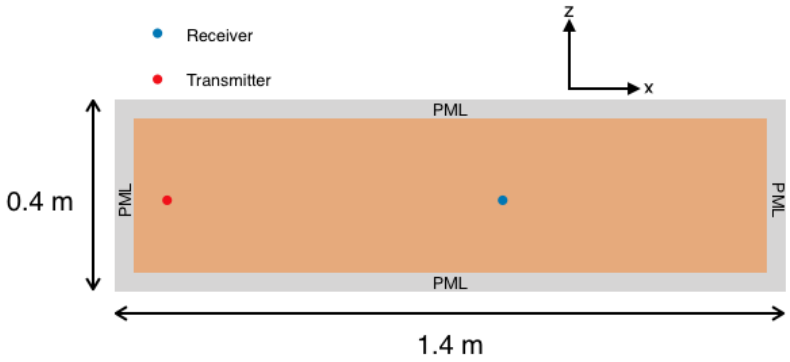

Figure 1: An x-z plane illustration of the simulation setup, in $y = 0.2$. The transmitting antenna is located at (x, y, z) = (0.1 m, 0.2 m, 0.2 m) and the receiving antenna is located at (x, y, z) = (0.8 m, 0.2 m, 0.2 m). The grey area represents the PML that prevent reflections back into the simulation space.

https://doi.org/10.26376/GPR2019002

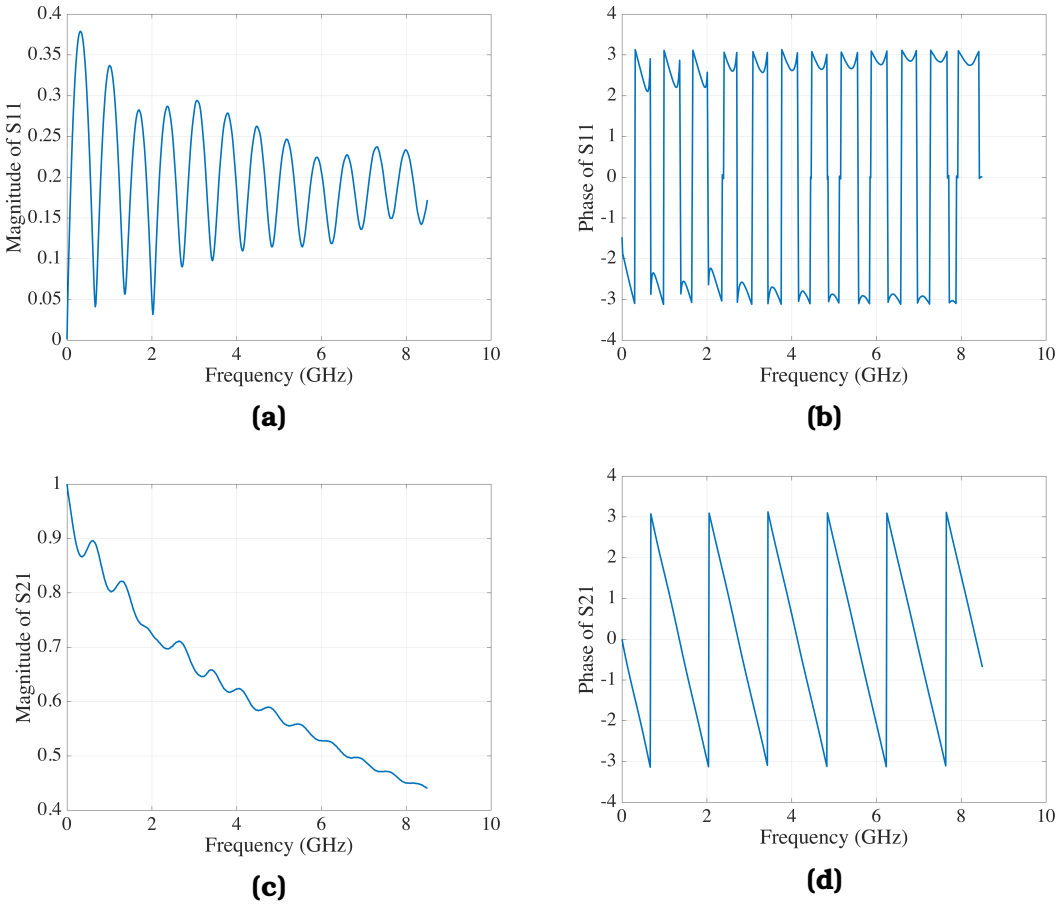

Figure 2: The magnitude and phase measurements of S_{11} and S_{21} from the baked montmorillonite sample. (a) S_{11} magnitude spectrum. (b) S_{11} phase spectrum. (c) S_{21} magnitude spectrum. (d) S_{21} phase spectrum.

4 Results and discussion

4.1 Measurements and inversions

The complex permittivities were computed from the measured S-parameters using the aforementioned method. An example of the S-parameter measurement is shown in Figure 2. We used a 1-pole Cole-Cole model to fit the baked sample and a 2-pole Cole-Cole model to fit the samples containing moisture. The results are shown in Table 1. Knowing the possible relaxation mechanisms in a material is helpful

https://doi.org/10.26376/GPR2019002

for determining the number of poles to use for inversion. In our clay experiment, free and bound water are the two most likely causes of relaxation [8, 10], consistent with our two-pole fit.

Table 1: Inversion results of montmorillonite sample STx-1b under various moisture levels. The moisture content by wt% corresponds to 3-hour, 5-hour, 7-hour, 15-hour and 24-hour period in the moisture chamber.

Moisture by wt%	Baked	3.06	4.48	5.88	7.29	9.89
ϵ_∞	3.20	3.30	3.48	3.47	3.64	3.80
$\epsilon_{s1} - \epsilon_\infty$	1.88	7.15	7.29	9.36	10.6	12.5
τ_1 (ns)	1.79	14.0	1.78	1.48	1.63	1.57
α_1	0.389	0.488	0.647	0.660	0.681	0.682
$\epsilon_{s2} - \epsilon_\infty$		0.264	0.412	0.643	0.825	1.13
τ_2 (ps)		10.3	10.0	6.96	10.0	8.88
α_2		0.850	1.00	1.00	1.00	1.00
σ_{dc} (mS/m)	0.618	0.220	1.38	2.11	2.68	4.57
bulk density (g/cm^3)	0.816	0.833	0.833	0.853	0.871	0.874
rms error	0.0122	0.00160	0.00632	0.00909	0.00974	0.0135

We show the change in the residual from a 1 to a 3-pole model in Figure 3, as an additional evaluation of the number of poles required for inversion; the figure shows that the addition of relaxation poles to the baked sample inversion does not result in a better fit. The extra poles have extremely small amplitudes compared to the amplitude of the original 1-pole model. The residuals for the inversions of the moisturized samples decrease from 1- to 3- Cole-Cole fits, but the decrease is less significant from 2 to 3 poles than from 1 to 2 poles. This level-off in the residual curve is not as evident in the 7-hour and 15-hour experiment as in the 3- and 5-hour experiments. In the 24-hour case, however, we see the level-off in the misfit curve becomes more apparent again. We judge that our data are best fit by a Cole-Cole models with 2 poles, rather than 3.

https://doi.org/10.26376/GPR2019002

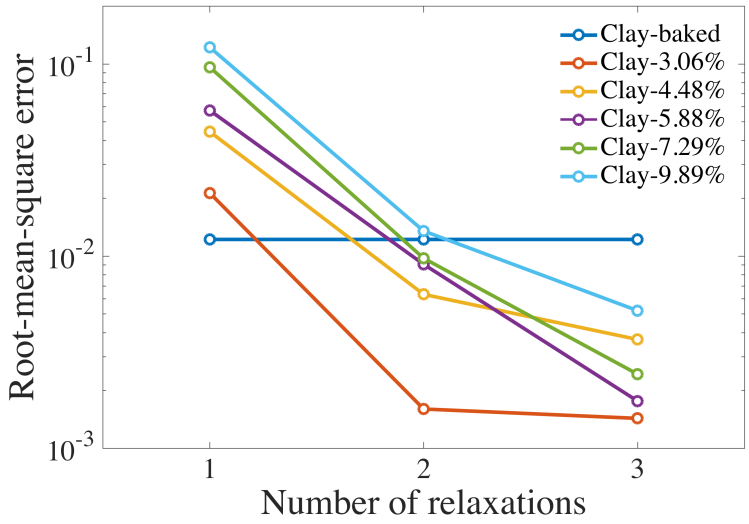

Figure 3: Root-mean-square error from inversion with 1-, 2-, and 3-pole Cole-Cole models.

Figure 4 shows the representative frequency spectra of the clay sample as well as the inverted curve (dark blue line) obtained from (14). The effect of each relaxation pole, and the DC conductivity, are also depicted as curves below the measured data. We can see that the DC conductivity only contributes to the lowest-frequency part of the spectra. The yellow curve contributes to the highest-frequency part of the spectra in the samples containing moisture. The corresponding relaxation time is around 9 ps, which agrees with the accepted value of the first relaxation pole of free water [10, 34]. The blue curve aligns with the data in most of the frequency range, which corresponds to a relaxation time around 1.65 ns. We attribute this to the relaxation caused by bound water in the interlayer between two 2:1 sheets. Each 2:1 sheet is composed of two tetrahedral sheets of silica sandwiching one central octahedral sheet of alumina [35]. Our value for this intermediate relaxation is lower than the previously reported values [10, 29], but is within the same order of magnitude. The inverted bound water relaxation time in the 3-hour case is much higher than the rest of the inversions. We believe that this is a numerical result rather than a physical one.

https://doi.org/10.26376/GPR2019002

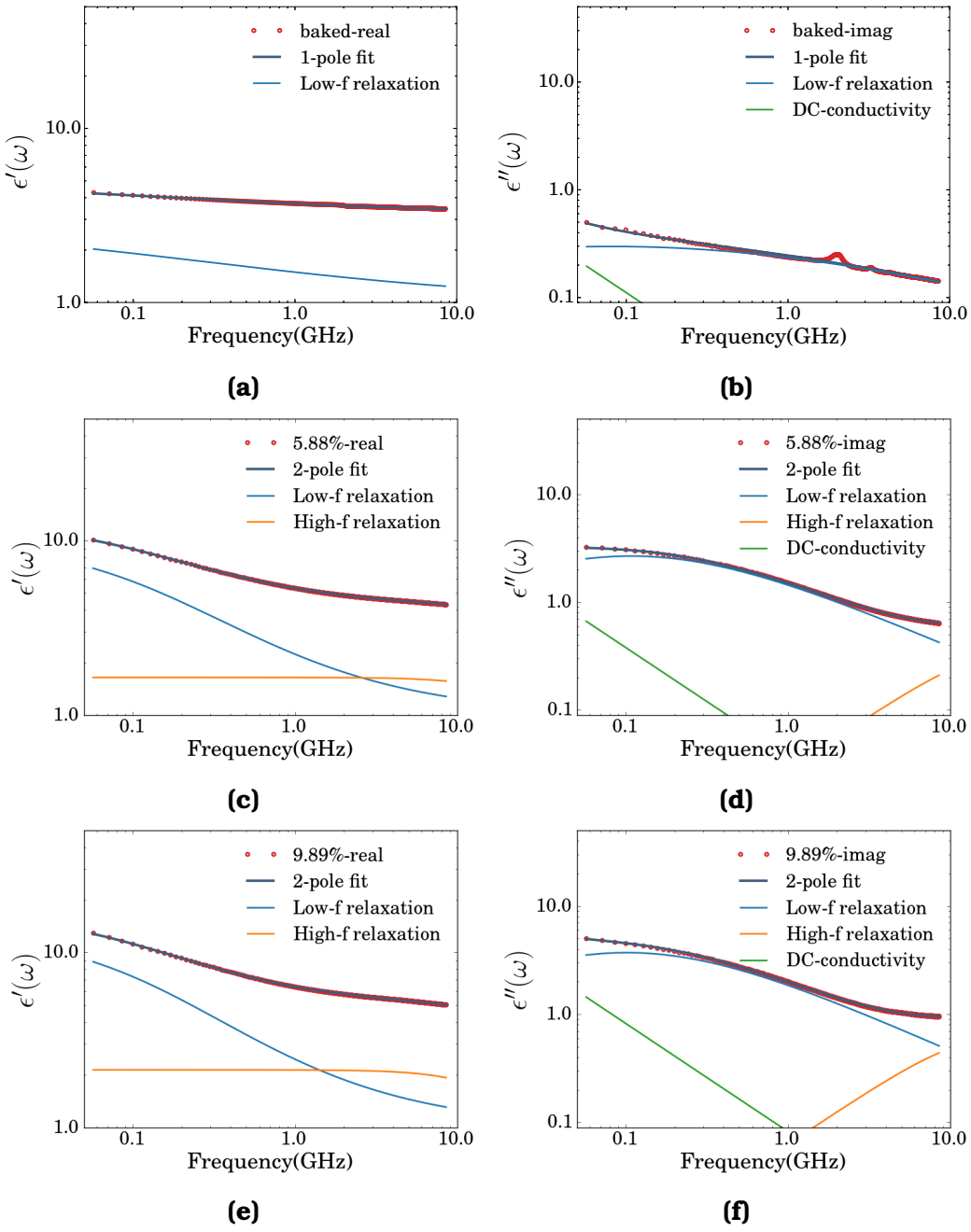

Figure 4: Complex permittivity and Cole-Cole model inversions of the montmorillonite sample under different moisture levels. The red dotted lines are the measurements and the dark blue lines are the inversion results using either 1-pole or 2-pole model. The orange and light blue lines represent high-frequency relaxation and low frequency relaxation, respectively. The green line represents the contribution from the DC conductivity. (a)-(b) baked clay. (c)-(d) 7-hr clay. (e)-(f) 24-hr clay. The measurement uncertainty above 800 MHz is less than 5%.

https://doi.org/10.26376/GPR2019002

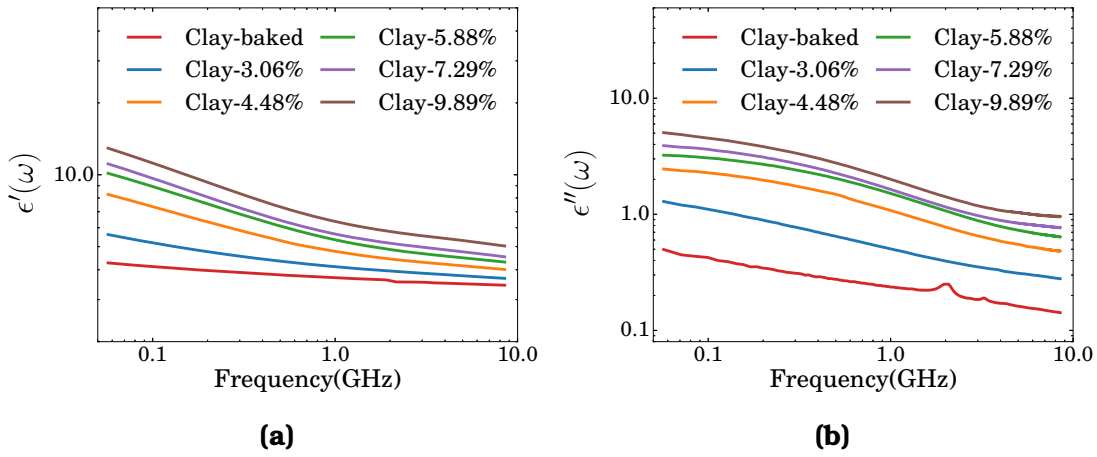

Figure 5: Comparison between the dielectric permittivity of the montmorillonite samples at various moisture levels shows a steady trend for both the real and the imaginary parts. (a) Real part of the permittivity measurement. (b) Imaginary part of the permittivity measurement.

Figure 5 shows the real and imaginary part of all the montmorillonite measurements. The trend from low to high moisture content is clear in both figures. As the moisture content increases, both the real and imaginary part increase gradually. The 3-hour curves do not show any sudden change from the rest of the measurements. Moreover, the shape of the imaginary part indicates that the 3-hour sample is in the "transition" from being better fitted with 1 pole to being better fitted with 2 poles. The inversion algorithm cannot fully capture this transition and produces a relaxation time that is not consistent with that of wetter samples as a result.

We measured/inverted the pyrite-quartz sample using the same procedure. However, the pyrite-quartz sample was baked at 250°C to ensure that all water was gone. The results for the baked sample are shown in Figure 6, where (a) is real part $\epsilon'(\omega)$, and (b) is the imaginary part $\epsilon''(\omega)$. The pyrite-quartz sample clearly shows a dispersive behaviour that is distinct from that caused by water. The imaginary part of the pyrite-quartz sample goes up steadily from about 0.2 GHz to the end of the spectrum, while the clays have a decreasing trend in the same frequency range.

https://doi.org/10.26376/GPR2019002

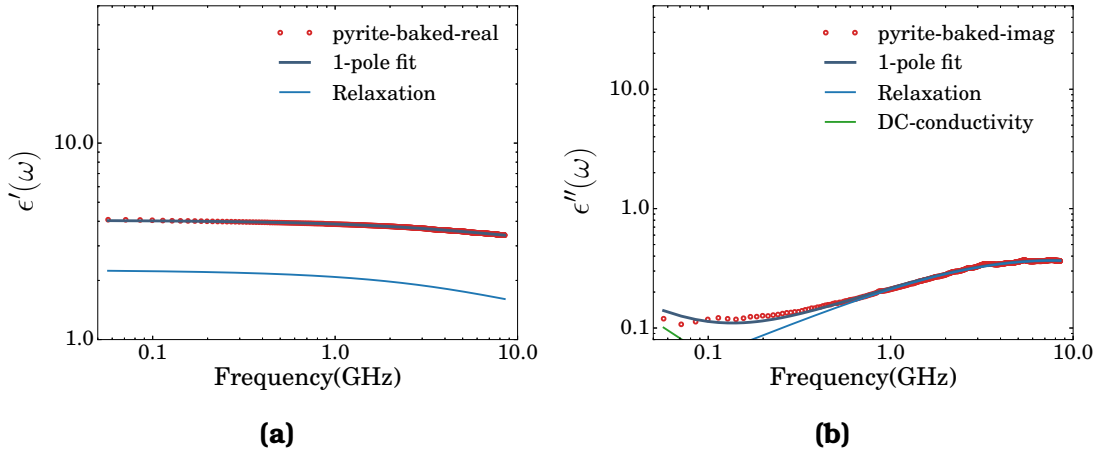

Figure 6: Complex permittivity and Cole-Cole model inversion of the baked pyrite-quartz sample. The red dotted lines are the measurements and the dark blue lines are the inversion results using 1-pole model. The light blue line represents relaxation peak determined from inversion. The green line represents the contribution from the DC conductivity. The measurement uncertainty above 800 MHz is less than 5%.

We plot the attenuation constant using the inverted parameters of the montmorillonite samples in Figure 7. The increasing moisture content not only increases the magnitude of attenuation in montmorillonite, but also the slope with respect to frequency. Therefore, Q^* also decreases with increasing moisture content according to (7). Notice the slope is greatest in the low-frequency region. This suggests that we should obtain a larger Q^* using a low-frequency source, and a smaller Q^* with a high-frequency source. By contrast, the attenuation constant of pyrite-quartz sample is shown in Figure 8. Because of the opposite concavity of the attenuation curve, the pyrite-quartz should give a higher Q^* when using a low-frequency source compared to a high-frequency source. We can therefore distinguish between the two dispersive behaviours, one caused by water and one intrinsic to the pyrite-quartz sample, by estimating Q^* at two frequencies. This method essentially takes the second derivative of attenuation with respect to frequency into consideration, in contrast to the traditional constant-Q^* approach.

https://doi.org/10.26376/GPR2019002

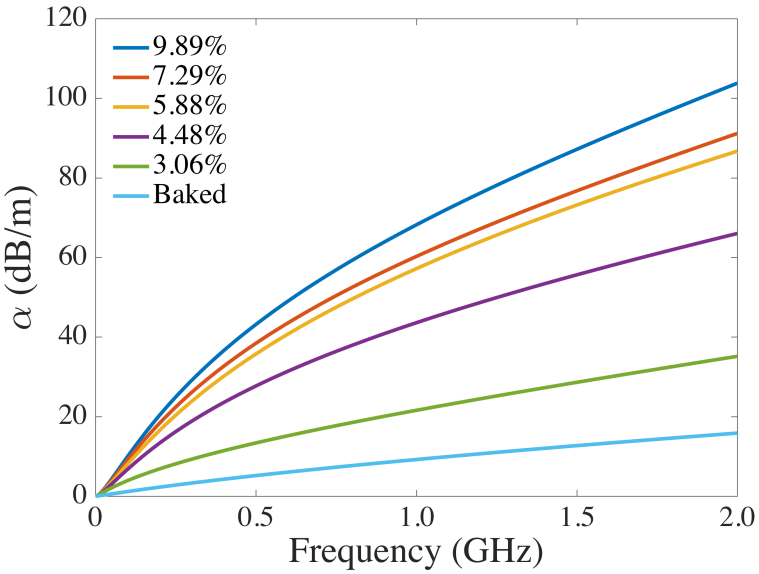

Figure 7: Attenuation α of the clay at varying moisture levels calculated from the Cole-Cole inversions.

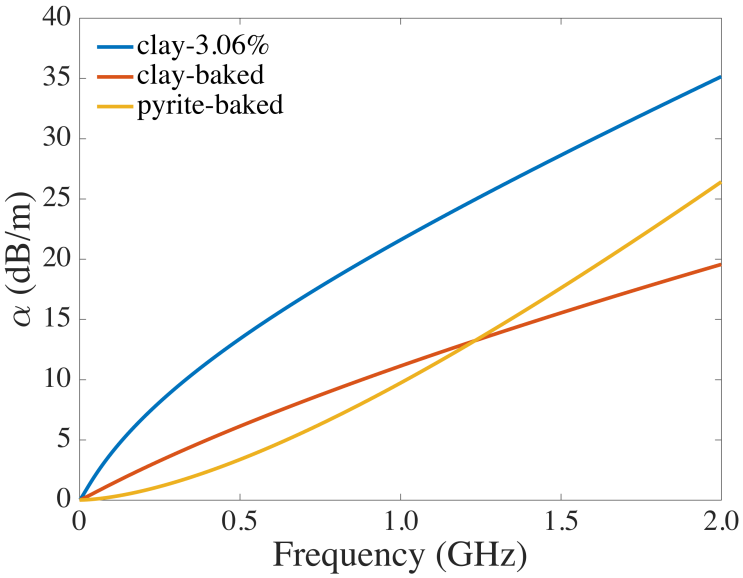

Figure 8: Attenuation α of clay at 3.06%, baked clay, baked pyrite-quartz sample.

https://doi.org/10.26376/GPR2019002

4.2 Simulation

We performed numerical simulations using the permittivity data from the samples. In each simulation, the space is filled with one single material of interest (filled-space). We use a 1200 MHz Ricker wavelet in one set of simulations and a 400 MHz Ricker wavelet in another. The results from the simulations are shown in Figure 9 and Figure 10. While we inverted the permittivity data with Cole-Cole model to give physical interpretation of the parameters, we inverted the same data with Debye model in order to implement the simulations in gprMax. The number of Debye relaxation poles was chosen to best approximate the residuals from the Cole-Cole model inversion. In Figure 9 (a) and Figure 10 (a), the amplitudes of the received signals are scaled to better illustrate the difference in shape. We use the time difference between the positive peak of the received signal and the positive peak of the input signal to calculate the travel time. The spectral shifts of the signals are shown in Figure 9 (b) and Figure 10 (b). The peak frequency shifts more in samples with higher water content due to increase attenuation, as expected. With the travel time and spectral shift information, we can calculate Q^* for the materials at 1200 MHz and 400 MHz using (8).

We calculated Q^* using both the spectral shift method and the attenuation data from inverted parameters. The results are given in Table 2 and Table 3. All the clay samples have a lower Q^* value obtained from attenuation at 400 MHz compared to 1200 MHz. In contrast, the baked pyrite-quartz sample has a higher Q^* at 400 MHz compared to 1200 MHz. This difference essentially gives information about the second derivative of attenuation with respect to frequency, which is the key to distinguish two different dispersive behaviours. We can observe a similar pattern in the calculation using the spectral shift method. This suggests the possibility of applying the concept in field data. However, there are several differences between the spectral shift calculation and the direct calculation from attenuation. Firstly, the spectral shift method overestimates Q^* for low-attenuation materials (baked clay and baked pyrite-quartz), and underestimates Q^* for the rest of the samples. Secondly, the Q^* values obtained from these two methods differ more at 1200 MHz than at 400 MHz, especially for the high-attenuation materials.

https://doi.org/10.26376/GPR2019002

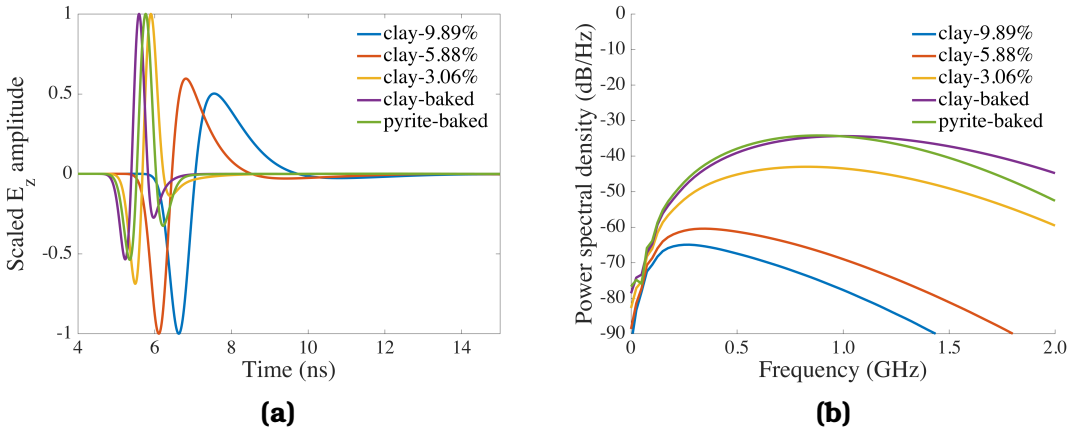

Figure 9: (a) Received signals in time domain and (b) corresponding power spectral density from a Ricker waveform centred at 1200 MHz. The materials are clays at 9.89%, 5.88%, 3.06% water content, baked clay, and baked pyrite.

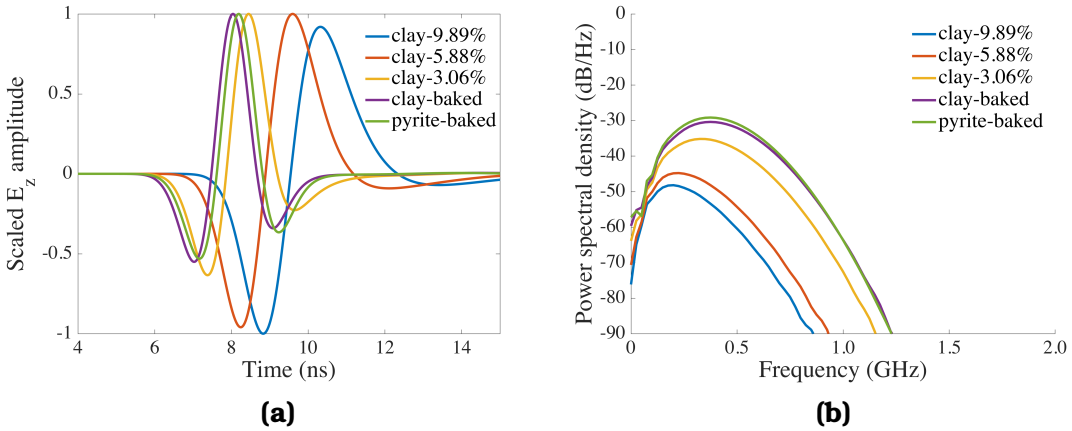

Figure 10: (a) Received signals in time domain and (b) corresponding power spectral density from a Ricker waveform centred at 400 MHz. The materials are clays at 9.89%, 5.88%, 3.06% water content, baked clay, and baked pyrite-quartz.

There are two factors controlling the spectral shift calculation: the travel time and the shift in spectral maximum. We compare the phase velocity calculated from travel time and the theoretical phase velocity for the 1200 MHz case in Figure 11. The travel time estimated from peak-to-peak has to be larger than the actual value to produce a larger Q*. However, Figure 11 shows that the estimated phase velocities should

https://doi.org/10.26376/GPR2019002

Table 2: Comparison of Q* calculated directly from attenuation curves and Q* calculated from spectral shifts for the clay samples with different water contents.

Moisture by wt%	Baked	3.06	4.48	5.88	7.29	9.89
1200 MHz from α	19.6	12.8	8.1	6.3	6.4	6.0
400 MHz from α	15.8	9.3	4.9	3.9	3.9	3.7
1200 MHz from spectral shift	22.7	11.7	5.1	3.2	3.2	2.9
400 MHz from spectral shift	19.8	8.9	3.8	3.1	2.6	2.8

Table 3: Comparison of Q* calculated directly from attenuation curves and Q* calculated from spectral shifts for the pyrite-quartz sample.

Pyrite-quartz	Baked
1200 MHz from α	11.5
400 MHz from α	19.3
1200 MHz from spectral shift	14.0
400 MHz from spectral shift	22.1

give larger Q* than that shown in Table 2. The estimated phase velocities are lower than the actual values except for the baked clay sample. This means we already use longer travel times in the spectral shift method for high-attenuation materials. The problem therefore is caused by frequency estimation.

Although spectral maximum is used to calculate Q* in [5], centroid frequency is used in [6] instead. The amplitude spectrum of the clay sample with 9.89% is shown in Figure 12. Clearly the spectral maximum is lower than the centroid frequency of the spectrum. As a result, the frequency shift appears to be larger, and causes the spectral shift method to produce a lower Q*. In addition, the spectral maximum of the 400 MHz spectrum is closer to its centroid frequency than the 1200 MHz spectrum. Therefore the 400 MHz estimation of Q* is closer to the Q* obtained directly from α. Calculating the centroid frequency requires knowing the source spectrum; however, measuring source spectrum can be difficult in the field due to noise. Using the spectral maximum avoids this problem.

https://doi.org/10.26376/GPR2019002

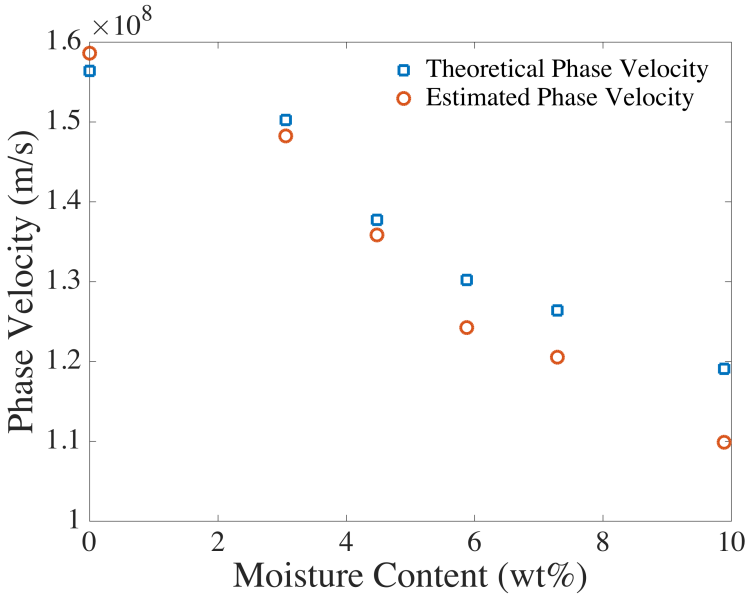

Figure 11: The theoretical and estimated phase velocities of the clay for different moisture levels using a1200 MHz Ricker wavelet source.

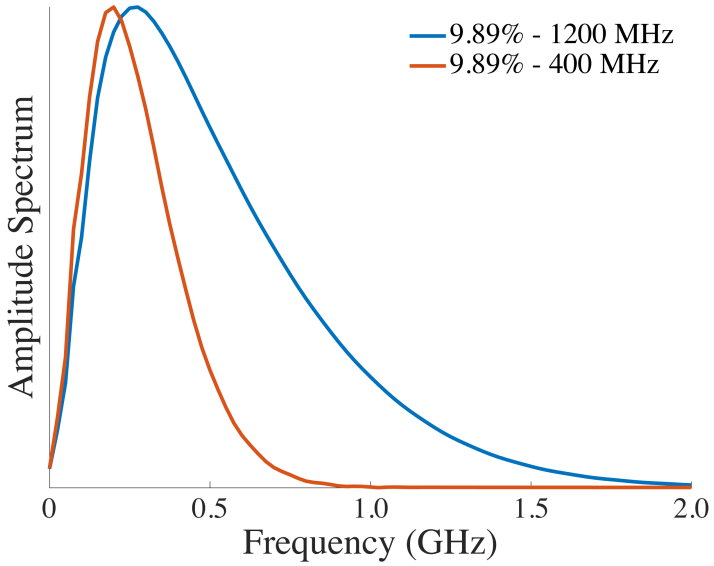

Figure 12: Amplitude spectra of the received signals from simulations using 1200 MHz and 400 MHz source. The centroid frequency is higher than spectral maximum for the frequencies since the spectra are not symmetric.

https://doi.org/10.26376/GPR2019002

We have shown that although the estimation from the spectral shift method is not very accurate, the idea of distinguishing two dispersive materials by measuring the difference between Q^* at two frequencies is verified numerically. There are several potential limitations to this technique. In practical applications, the subsurface environment is much more complex than a single homogeneous material. Moreover, heterogeneities within the material may give rise to scattering loss that does not correspond to the material properties. Most importantly, the materials need to have detectable change in Q^* at the chosen frequencies.

5 Conclusion

Through measurements of the STx-1b Ca-rich montmorillonite sample under various moisture levels, we have identified dispersive behaviours caused by water that are consistent with previous studies. The relaxation times were obtained by inverting the permittivity data using the Cole-Cole model. We also measured the complex permittivity of a pulp sample, mainly composed of pyrite and quartz, from a massive sulphide mine. The pyrite-quartz sample has dispersive behaviours that are independent of water, which can be distinguished from that of moist clays by estimating Q^* at two different frequencies. A suite of simulations with the inverted parameters was implemented using gprMax to verify this idea. Our results show that the spectral shift method correctly identifies the pattern of change in Q^* of these two samples at 400 MHz and 1200 MHz. Instead of a target-locating technique, we demonstrate how radar signals can also be used to distinguish two actual dispersive behaviours. Application of the concept to field data will be conducted in the future.

References

[1] J. L. Davis and A. P. Annan, "Ground-penetrating radar for high-resolution mapping of soil and rock stratigraphy," *Geophysical Prospecting*, vol. 37, no. 5, pp. 531–551, July 1989, doi: 10.1111/j.1365-2478.1989.tb02221.x.

https://doi.org/10.26376/GPR2019002

[2] A. P. Annan, "Transmission dispersion and GPR," *Journal of Environmental and Engineering Geophysics*, vol. 1, no. B, pp. 125–136, January 1996, doi: 10.4133/jeeg1.b.125.

[3] G. Turner and A. F. Siggins, "ConstantQattenuation of subsurface radar pulses," *Geophysics*, vol. 59, no. 8, pp. 1192–1200, August 1994, doi: 10.1190/1.1443677.

[4] K. Aki and B. Chouet, "Origin of coda waves: Source, attenuation, and scattering effects," *Journal of Geophysical Research*, vol. 80, no. 23, pp. 3322–3342, August 1975, doi: 10.1029/jb080i023p03322.

[5] J. H. Bradford, "Frequency-dependent attenuation analysis of ground-penetrating radar data," *Geophysics*, vol. 72, no. 3, pp. J7–J16, May 2007, doi: 10.1190/1.2710183.

[6] Y. Quan and J. M. Harris, "Seismic attenuation tomography using the frequency shift method," *Geophysics*, vol. 62, no. 3, pp. 895–905, May 1997, doi: 10.1190/1.1444197.

[7] R. Calvet, "Dielectric properties of montmorillonites saturated by bivalent cations," *Clays and Clay Minerals*, vol. 23, no. 4, pp. 257–265, September 1975, doi: 10.1346/ccmn.1975.0230401.

[8] G. Sposito and R. Prost, "Structure of water adsorbed on smectites," *Chemical Reviews*, vol. 82, no. 6, pp. 553–573, December 1982, doi: 10.1021/cr00052a001.

[9] G. R. Olhoeft, "Electrical properties from 10-3 to 10+9 HZ–physics and chemistry," in *AIP Conference Proceedings*. AIP, March 1987, doi: 10.1063/1.36399.

[10] T. Ishida, T. Makino, and C. Wang, "Dielectric-relaxation spectroscopy of kaolinite, montmorillonite, allophane, and imogolite under moist conditions," *Clays and Clay Minerals*, vol. 48, no. 1, pp. 75–84, January 2000, doi: 10.1346/ccmn.2000.0480110.

[11] A. Robert, "Dielectric permittivity of concrete between 50 mhz and 1 ghz and GPR measurements for building materials evaluation,"

https://doi.org/10.26376/GPR2019002

Journal of Applied Geophysics, vol. 40, no. 1-3, pp. 89–94, October 1998, doi: 10.1016/s0926-9851(98)00009-3.

[12] G. Klysz, J.-P. Balayssac, and S. Laurens, "Spectral analysis of radar surface waves for non-destructive evaluation of cover concrete," *NDT & E International*, vol. 37, no. 3, pp. 221–227, April 2004, doi: 10.1016/j.ndteint.2003.09.006.

[13] W. Lai, T. Kind, and H. Wiggenhauser, "Frequency-dependent dispersion of high-frequency ground penetrating radar wave in concrete," *NDT & E International*, vol. 44, no. 3, pp. 267–273, May 2011, doi: 10.1016/j.ndteint.2010.12.004.

[14] J. H. Bradford, "Frequency dependent attenuation of GPR data as a tool for material property characterization: A review and new developments," in *2011 6th International Workshop on Advanced Ground Penetrating Radar (IWAGPR)*. IEEE, June 2011, doi: 10.1109/iwagpr.2011.5963870.

[15] P. J. W. Debye, *Polar molecules*. Chemical Catalog Company, Incorporated, 1929.

[16] K. S. Cole and R. H. Cole, "Dispersion and absorption in dielectrics i. alternating current characteristics," *The Journal of Chemical Physics*, vol. 9, no. 4, pp. 341–351, April 1941, doi: 10.1063/1.1750906.

[17] S. Havriliak and S. Negami, "A complex plane representation of dielectric and mechanical relaxation processes in some polymers," *Polymer*, vol. 8, pp. 161–210, January 1967, doi: 10.1016/0032-3861(67)90021-3.

[18] M. Wollensack, J. Hoffmann, J. Ruefenacht, and M. Zeier, "VNA tools II: S-parameter uncertainty calculation," in *79th ARFTG Microwave Measurement Conference*. IEEE, June 2012, doi: 10.1109/arftg79.2012.6291183.

[19] D. K. Rytting, "Network analyzer accuracy overview," in *58th ARFTG Conference Digest*. IEEE, November 2001, doi: 10.1109/arftg.2001.327486.

https://doi.org/10.26376/GPR2019002

[20] A. M. Nicolson and G. F. Ross, "Measurement of the intrinsic properties of materials by time-domain techniques," *IEEE Transactions on Instrumentation and Measurement*, vol. 19, no. 4, pp. 377–382, November 1970, doi: 10.1109/tim.1970.4313932.

[21] W. Weir, "Automatic measurement of complex dielectric constant and permeability at microwave frequencies," *Proceedings of the IEEE*, vol. 62, no. 1, pp. 33–36, January 1974, doi: 10.1109/proc.1974.9382.

[22] A. H. Boughriet, C. Legrand, and A. Chapoton, "Noniterative stable transmission/reflection method for low-loss material complex permittivity determination," *IEEE Transactions on Microwave Theory and Techniques*, vol. 45, no. 1, pp. 52–57, February 1997, doi: 10.1109/22.552032.

[23] P. L. Hall and D. M. Astill, "Adsorption of water by homoionic exchange forms of wyoming montmorillonite (SWy-1)," *Clays and Clay Minerals*, vol. 37, no. 4, pp. 355–363, August 1989, doi: 10.1346/ccmn.1989.0370409.

[24] P. Bala, B. K. Samantaray, and S. K. Srivastava, "Dehydration transformation in ca-montmorillonite," *Bulletin of Materials Science*, vol. 23, no. 1, pp. 61–67, February 2000, doi: 10.1007/bf02708614. [Online]. Available: https://doi.org/10.1007/bf02708614

[25] A. Kuligiewicz and A. Derkowski, "Tightly bound water in smectites," *American Mineralogist*, vol. 102, no. 5, pp. 1073–1090, May 2017, doi: 10.2138/am-2017-5918.

[26] G. R. Olhoeft, "Low-frequency electrical properties," *Geophysics*, vol. 50, no. 12, pp. 2492–2503, December 1985, doi: 10.1190/1.1441880.

[27] D. E. Stillman, "Frequency and temperature dependence in electromagnetic properties of martian analog materials," Ph.D. dissertation, Colorado School of Mines, Golden, Colo., 2006.

[28] D. Stillman and G. Olhoeft, "Frequency and temperature dependence in electromagnetic properties of martian analog minerals," *Journal*

https://doi.org/10.26376/GPR2019002

of Geophysical Research, vol. 113, no. E9, September 2008, doi: 10.1029/2007je002977.

[29] A. Benedetto, "Water content evaluation in unsaturated soil using GPR signal analysis in the frequency domain," *Journal of Applied Geophysics*, vol. 71, no. 1, pp. 26–35, May 2010, doi: 10.1016/j.jappgeo.2010.03.001.

[30] M. Newville, T. Stensitzki, D. B. Allen, and A. Ingargiola, "Lmfit: Non-linear least-square minimization and curve-fitting for python," 2014, doi: 10.5281/zenodo.11813.

[31] C. Warren, A. Giannopoulos, and I. Giannakis, "gprMax: Open source software to simulate electromagnetic wave propagation for ground penetrating radar," *Computer Physics Communications*, vol. 209, pp. 163–170, December 2016, doi: 10.1016/j.cpc.2016.08.020.

[32] K. Yee, "Numerical solution of initial boundary value problems involving maxwell's equations in isotropic media," *IEEE Transactions on Antennas and Propagation*, vol. 14, no. 3, pp. 302–307, May 1966, doi: 10.1109/tap.1966.1138693.

[33] I. Giannakis, A. Giannopoulos, and N. Davidson, "Incorporating dispersive electrical properties in FDTD GPR models using a general cole-cole dispersion function," in *2012 14th International Conference on Ground Penetrating Radar (GPR)*. IEEE, June 2012, doi: 10.1109/icgpr.2012.6254866.

[34] M. Loewer, J. Igel, and N. Wagner, "Spectral decomposition of soil electrical and dielectric losses and prediction of in situ GPR performance," *IEEE Journal of Selected Topics in Applied Earth Observations and Remote Sensing*, vol. 9, no. 1, pp. 212–220, January 2016, doi: 10.1109/jstars.2015.2424152.

[35] F. Uddin, "Clays, nanoclays, and montmorillonite minerals," *Metallurgical and Materials Transactions A*, vol. 39, no. 12, pp. 2804–2814, September 2008, doi: 10.1007/s11661-008-9603-5.

Ground Penetrating Radar
Volume 2, Issue 1, March 2019
https://doi.org/10.26376/GPR2019003

REAL TIME VISUALIZATION OF THE DATA GATHERED BY A RECONFIGURABLE STEPPED FREQUENCY GPR SYSTEM

FILIPPO BRIGATTI

Marketz SpA, Milano, Italy – filippobrigatti@virgilio.it

ABSTRACT

This paper describes recent improvements made to the acquisition software of a reconfigurable stepped-frequency ground penetrating radar (GPR) prototype, to allow real-time data visualization. In particular, real-time data visualization was not yet implemented in the previous version of the acquisition software, although this is a common feature available in all commercial systems. This was a bad problem for the GPR prototype: the possibility to visualize data in real time is obviously of vital importance, because it makes it possible for the user to easily identify promising areas in the field, or to recognize an anomalous functioning of the system without wasting a day of work. So far, real-time data visualization was not yet possible because the prototype at hand is equipped with three equivalent couples of antennas that can transmit and receive data simultaneously, which implies a quite large amount of data recorded per second. Nonetheless, by implementing suitable procedures for a more efficient data handling, the problem has been successfully solved and now the prototype is not anymore "blind" in the field.

KEYWORDS: Ground penetrating radar; stepped-frequency reconfigurable systems; acquisition software; real-time data visualization.

1. INTRODUCTION

Pulsed and stepped-frequency systems are the two most widely used categories of ground penetrating radar (GPR) systems. They are based on ideas and principles dating back to the first half of the twentieth century [1]. According to [2], the first GPR technology patent was registered in 1910 and regarded a system working in the frequency domain, whereas the first pulsed system was patented in 1926, only. Nonetheless, the commercial development of GPR systems started after the Second World War (which gave a substantial input to the development of radar technology) and regarded pulsed systems, first; later, stepped-frequency systems were commercialised, too. In particular, while pulsed systems

https://doi.org/10.26376/GPR2019003

were already commercialised in the sixties [1], the first experiments with commercial stepped-frequency systems date back to the seventies [3].

The debate on which system is best is still going on today [4, 5]. Stepped frequency systems are claimed to be more performant in terms of dynamic range and signal-to-noise ratio [4]. On the other hand, they present the problem that the receiver needs to have the same dynamic range as the transmitted signal, in order not to saturate when receiving the direct wave. Consequently, stepped-frequency technology is more complex, and this easily drives towards more expensive systems. However, the realization costs of pulsed and stepped frequency systems become similar for GPR systems with antenna arrays [6]. Probably, this is one of the main reasons why most commercial stepped-frequency systems are nowadays equipped with an array of antennas [7].

Although the majority of GPR systems currently are pulsed systems, we do not know in an absolute sense what is the best one between the pulsed and the stepped frequency technology. Probably, the answer to such a question also depends on the application. For example, according to [8] stepped-frequency systems are more promising for some high frequency applications such as demining. The possibility to reconfigure some hardware and software parameters during prospecting has been lately introduced for stepped-frequency systems [9]. In particular, a reconfigurable stepped-frequency system [10, 11] has been implemented within a research project called Aitech [12]. To the best of my knowledge, analogous reconfigurable pulsed systems do not yet exist.

Until recently, this reconfigurable stepped-frequency prototype had the problem that data were not visible in real time in the field. They were recorded in the field and could be viewed only during the post-processing. Real time data visualization is obviously an essential feature, which allows, e.g., checking the correct functioning of the system in the field and immediately identifying the presence of anomalies of interest in the area under test, so that a localized excavation can be carried out or further geophysical measurements can be made.

This paper summarizes the work carried out during my Master thesis in Computer Engineering, at the International Telematic University Uninettuno (Rome, Italy), in 2018, under the supervision of Dr Raffaele Persico (National Research Council of Italy, CNR, Lecce, Italy). My thesis was focused on developing new procedures to be integrated in the acquisition software of the above-mentioned reconfigurable stepped-frequency prototype, in order to allow real-time data visualization. In

 https://doi.org/10.26376/GPR2019003

Section 2, the prototypal reconfigurable GPR system and its original acquisition software are shortly described. In Section 3, the implementation of an improved version of the software is described, with a main focus on the procedures that have made it possible real-time data visualization during prospecting. Conclusions are drawn in Section 4.

2. THE STEPPED-FREQUENCY GPR PROTOTYPE

The prototypal GPR considered in this work is a stepped-frequency reconfigurable system, and in particular a stepped-frequency GPR where the three following parameters are programmable versus the frequency:

1. Integration time: Unlike any commercial stepped-frequency GPR, the reconfigurable prototype allows to set a different integration time for each frequency. This option allows to reject interferences (due, e.g., to external electromagnetic sources) without prolonging too much the acquisition time [13, 14].
2. Power attenuation: The reconfigurable prototype permits to program the power supplied to the transmitting antenna for each frequency. This option allows to equalize the shape of the synthetic pulse, if needed, and might be also used to avoid the saturation of the receiver at some frequencies.
3. Antennas: The reconfigurable prototype is equipped with a couple of shielded bow-tie antennas with two switches along each arm, as sketched in Figure 1. The switches are constituted of PIN diodes. By switching on and off the diodes, three equivalent couples of antennas can be achieved (“short”, “medium,” and “long”); hence, it is possible to change dynamically the geometry of the antennas. The system is capable to record three B-Scans simultaneously; to the best of my knowledge, commercial systems with dual antennas also exist, but they allow gathering two simultaneous B-Scans, at most. Moreover, in the case of the reconfigurable prototype at hand, all the equivalent antennas share the same gap, which customarily does not happen in commercial dual-band systems. The reconfigurable prototype can span the frequency range 50-1000 MHz three times (one for each equivalent antenna) at any measurement point, with a frequency step optionally equal to 2.5 or 5 MHz. The central frequencies of the three equivalent antennas are about 120, 250 and 520 MHz, for “long”, “medium” and “short” antennas, respectively.

https://doi.org/10.26376/GPR2019003

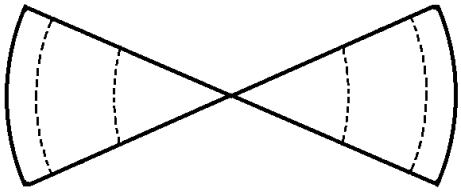

FIG. 1 – Scheme of the reconfigurable antenna. The antenna is "short" if all the switches (represented by dotted lines) are off, "medium" if the internal switches are on and the external switches are off, "long" if all the switches are on.

The original acquisition software of the reconfigurable prototype is called Eurydice. Eurydice configures the radar central unit according to settings defined by the user. In particular, according to the settings encoded by the user, the central unit will synchronize the aperture or closure of the antenna switches. Moreover, for each received signal the central unit will interrogate the odometer about the spatial position and save this information in the dedicated laptop computer along with the corresponding field data. Eurydice receives data packets at regular (uniform) time intervals; this, in general, does not correspond to regular spatial intervals because of the velocity variations of the human operator. Nonetheless, as the spatial positions are recorded with the data, the data can be suitably interpolated during post-processing to make the spatial step uniform. Data acquisition continues until Eurydice, following a command of the human operator, sends a stop request to the central unit.

3. UPGRADE OF THE ACQUISITION SOFTWARE

With the old version of Eurydice, the visualization of the data was possible only after collecting the data, i.e., in the post-processing stage. In particular, the visualization resulted from the execution of a homemade MATLAB script, which included the inverse fast Fourier transform for achieving time-domain data and an algorithm to perform spatial interpolation based on the information provided by the odometer.

As already mentioned in the Introduction, the lack of real-time data visualization was one of the main problems of the system, because the operator did not have an immediate picture of the investigated buried scenario and was not able to recognize in the field any possible incorrect functioning of the system.

https://doi.org/10.26376/GPR2019003

The main reason why no implementation of real-time data visualization had been devised when the system was realized, was the large amount of data received by the application. It was necessary to implement a software capable to efficiently manage those data; this task was postponed to later.

Each 'burst' of received data is composed by a header and a data section. The header contains information about the kind of sweep and spatial position, along with some "free Bytes" reserved for possible future developments. The size of the header is 16 Bytes; the length of the data section, instead, depends on the configuration settings. In particular, each received harmonic signal is encoded with 8 Bytes times a programmable factor, which depends on the integration time. The default integration time is about 100 μs, whereas the larger available multiplier for the default integration time is equal to 10; hence, the longest possible integration time is 1 ms and maximum 80 Bytes can be used to encode the received signal at each frequency.

In each 'burst' of data all the harmonic signals received within the chosen frequency sweep are present. If the human operator chooses the largest available band, the frequency sweep starts at 50 MHz and stops at 1 GHz. If a frequency step of 2.5 MHz is chosen, this means that overall 381 different frequencies are considered, codified with 381*80 + 16 = 30496 Bytes, for each antenna. If data are recorded for all of the three available couples of equivalent antennas, Eurydice receives 91488 Bytes for every measurement position.

From the documentation provided by the constructor of the system we know that, with this configuration, the GPR sends bursts of data at the speed of 10.4 A-Scans per second (the A-Scan refers to the data recorded over a single measurement position). Consequently, in one second the application receives about 300 KB referred to all of the three antennas.

The application saves continuously the data in a file; however, the dedicated laptop computer has a limited computational power. In particular, the GPR system is equipped with an Asus EEPC computer, with a dual core processor Intel-Atom 2600, 1.6 GHz clock, 1.98 GB RAM and 300 GB Hard Disk; the operating system Windows XP is installed on the laptop computer.

The software upgrade presented in this paper is essentially based on the idea of discarding as soon as possible all data not strictly needed for a satisfactory real-time visualization (all data are still recorded on the

https://doi.org/10.26376/GPR2019003

hard disk of the laptop computer and can be subsequently visualized, analysed, and processed). This introduces a small degradation of the real-time image, but the loss of quality is acceptable.

The upgraded software asks the human operator to choose the antennas they want to select for real-time visualization. Indeed, during prospecting, the human operator can visualize on the screen the raw data related to one couple of antennas, only; however, it is possible to switch in any moment from a radargram to another one, among those being simultaneously recorded (i.e., it is possible to modify the initial choice and select a different couple of equivalent antennas for real-time visualization).

The real-time visualization requires also the management of an interpolation problem. In fact, as already mentioned, the acquisition rate of the system is constant versus time, not versus the covered distance, because the velocity of the human operator (or even of a mechanical vehicle) is not uniform with time. In particular, when the GPR system moves faster along the observation line, a higher computational power is necessary for the real-time visualization of the data. On the other hand, if the system moves very slowly, the visualization software receives redundant data, which can be partially discarded in order to allow real-time visualization.

The strategy for dealing with this issue is illustrated in Figure 2, where different possible cases are depicted. First, let us specify that the user selects a-priori a uniform spatial step for the visualization, so that we have a sequence of prefixed point, equally spaced, where we wish to

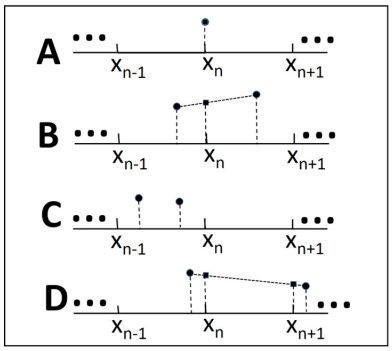

FIG. 2 – Sketch of the interpolation strategy implemented in the visualization software.

https://doi.org/10.26376/GPR2019003

calculate the data to be visualized by performing an interpolation of the actual data. The true data are, essentially, electric-field amplitudes measured over points that we do not know a-priori, but that we record sequentially together with the field amplitudes.

In Figure 2, the point x_n is the n_{th} position where we wish to calculate the data to be visualized. In particular, the first datum is by definition gathered at the abscissa zero, but for the subsequent points, some discrepancy arises between the "desired" point next to x_n and the position where the data are actually measured.

The situation A in Figure 2 represents the fortunate but possible case when the n^{th} datum is gathered exactly in the n^{th} desired position. In such case, the datum is just processed for the visualization (let us remind that the system receives data in frequency domain, and so an inverse Fourier transform has to be performed in order to achieve representable real data in the synthetic time domain).

The situation B in Figure 2 represents the case when the last two gathered data are one at the left-hand side of x_n (after x_{n-1}) and the other at the right-hand side of x_n (before x_{n+1}). In this case, the visualization software applies a linear interpolation between the last two gathered data (accounting for their position, too) and the datum in x_n is easily retrieved (linear interpolation is applied after the inverse Fourier transform, hence in the time domain).

A third possibility is depicted on the third scheme of Figure 2 and is labelled as situation C. In this case, the last two gathered data both fall within the same interval, i.e., between the last "already-interpolated" point x_{n-1} and the next "to-be-interpolated" point x_n. In this case, the visualization code just discards the penultimate gathered value and keeps the last one. The C case can of course occur several times in a row, especially when the GPR system is moved slowly. Indeed, in this case, situation C will occur several times in a raw, and at a certain point situation B or, more rarely, situation A will happen.

The computationally most demanding situation is of course the fourth illustrated case (situation D). In fact, in this case, the penultimate point falls between x_{n-1} and x_n, whereas the last point is between x_{n+1} and x_{n+2}. In this case, the system applies a linear interpolation, too, but the missed points to be retrieved are two instead of just one, which requires a longer computational time. Obviously, if the "skip" is even larger, the visualization code could be also compelled to calculate three, four or "k" interpolated values, requiring a progressively longer time for the

https://doi.org/10.26376/GPR2019003

interpolation. These larger interpolation calculations are needed when the system is moved too fast with respect to the spatial rate at which the data have to be interpolated. Of course, beyond a certain point, there is also a theoretical problem of underdamping of the field with consequent aliasing in the data, but at the typical velocity of a human operator this event customarily does not happen. The visualization code makes use of a buffer in order to compensate the difference of velocity between the acquisition rate and the elaboration rate, but if the system is moved too fast this buffer gets overcharged and the systems works not correctly, and eventually the acquisition process stops. On the other hand, if the velocity is very slow, the time needed for the prospecting increases and the files stored for the post processing are uselessly large.

Real-time data visualization is made further challenging for the system by the fact that the integration times of the harmonic components are not necessarily the same for each frequency. In fact, as explained in Section 2, the integration times are reconfigurable, and they can therefore have variegated lengths. Each integration tone, in particular, can be prolonged up to 10 times with respect to its default value [13]. However, in a real situation the multiplier parameter of the integration time will not be equal to 10 for all frequencies but only in the frequency intervals where noise or interferences are significant. For more details, the interested Reader is referred to [13]. Here, it is sufficient to say that an algorithm is able to program the ideal multiplication of the default integration time required for each harmonic tone, and then a threshold mechanism is applied to this calculation because for technological reasons the maximum value allowed for the extension of the prolongation factor is equal to 10, as already said.

The original Eurydice code was written in Vb.Net and made use of WinPcap libraries for internal communication [15]. For the software upgrade, the external ALGLIB [16] library was used too, in order to perform the inverse fast Fourier transform (IFFT) and deal more effectively with complex numbers.

The architecture of the upgraded code is schematixed in Figure 3. In particular, Figure 3 shows the data flow from the central unit of the GPR to the program, and in particular, the down pointing arrow indicates data packets rejected by the software for the real-time visualization. Then, the data useful for the visualization are collected in a ring buffer, where they are analysed; when necessary, they are sent to the graphical user interface (GUI).

https://doi.org/10.26376/GPR2019003

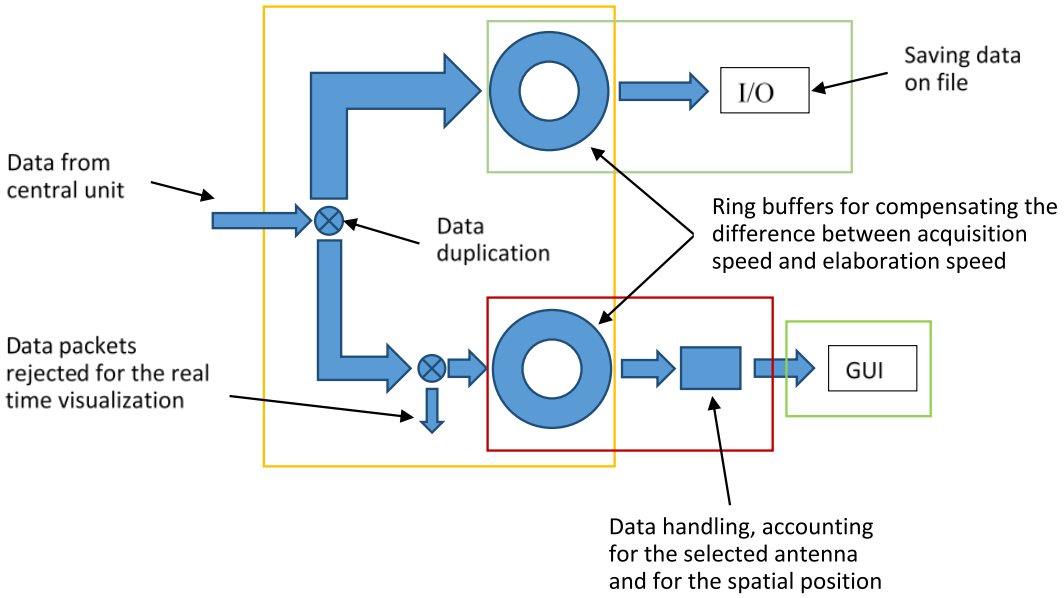

FIG. 3 – General scheme for the architecture of the upgraded Eurydice acquisition code. The upper branch was already implemented in the original software; the lower branch was added with the software upgrade.

Figure 4 is an alternative and expanded representation of the lower branch of Figure 3 (namely, the software upgrade). In particular, the various steps of the data-handling block are shown; these are:

- Recognition of useful data packets: The data packet is rejected if it comes from an equivalent antenna not selected for real-time visualization.
- Rejection of dead tone: This option was already present in the previous version of Eurydice. Not all of the measured harmonic data are saved, some of them are identified as “dead tones” and discarded. The dead tones are anomalous data not useful for the post processing and neither for the visualization.
- Management of integration times: Some averaging is done, to achieve the in-phase and quadrature components for each received harmonic tone.
- Spline interpolation: Possible edges in the received signal, due to commutations of the switches on the antennas, are smoothed.

https://doi.org/10.26376/GPR2019003

- Calibration and upgrade of the calibration vector: The calibration data are not considered for the visualization, but they are used to normalize the data in the frequency domain.
- First positional logic block: This block correlates the elaboration of each data packet to its spatial position. In particular, it attributes the right position to the last datum that has to be transformed in the time domain.
- Inverse Fourier transform: This block retrieves data in the synthetic time domain. Within this step an optional zero padding can be performed in order to interpolate data, in the time domain, for the graphical visualization.
- Second logical position block: This block commands the inverse Fourier transform of the second datum needed to perform the interpolation (the first was acquired within the previous two steps). Then, this block gives start to the interpolation needed for the graphical representation.
- Interpolation and plotting: This final block performs spatial interpolation and video visualization according to the options set by the user, such as the contrast level and the colour palette.

In the portion of the graph included between dashed lines, in Figure 4, all data packets are handled in the same way. After this point, the operations made on the data are still the same, but the outputs are stored in different memory areas. From the user point of view, the main two differences between real-time visualization and post-processing visualization are the following:

- Only a limited spatial length that can be visualized in real time. In particular, in Figure 5 there is written “Max: 80 m”: in fact, after 80 m the software stops plotting. The distance of 80 m refers by default to a choice of 2 cm for the spatial step. Please note that this does not mean that the user has to stop the measurement after 80 m. If the B-Scan is recorded over a line longer than 80 m, data will not be visualized anymore after 80 m, but they will continue to be regularly saved and stored in the computer. The limitation of 80 m has been chosen because in this way the needed amount of memory is allocated only at the beginning and is the same for all the pictures (i.e., no dynamical allocation of memory is needed).

https://doi.org/10.26376/GPR2019003

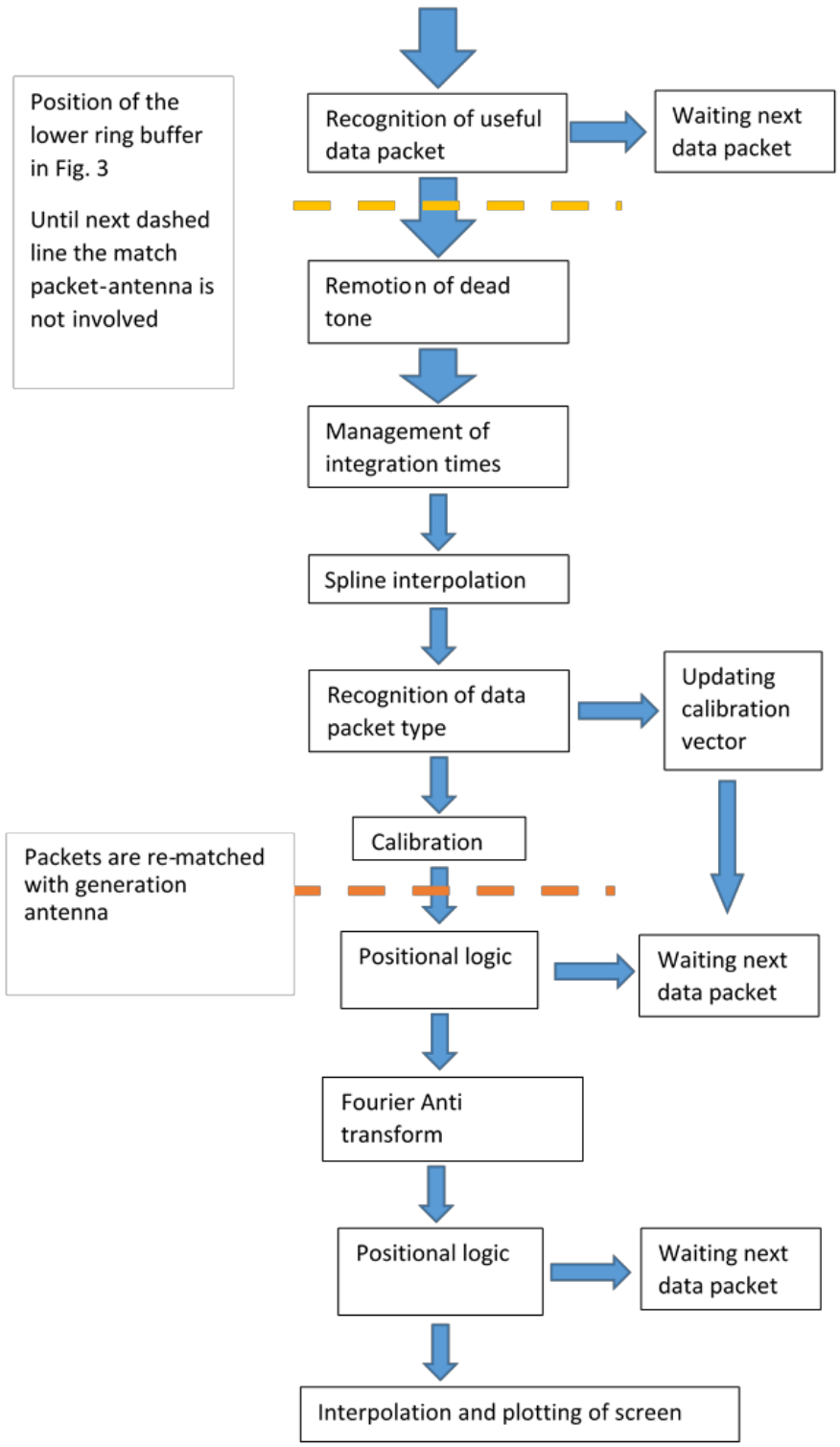

FIG. 4 – More detailled scheme of the lower branch of the diagram presented in Figure 3.

 https://doi.org/10.26376/GPR2019003

- The visualized time window has been chosen equal to 130 ns (without time interpolation), to guarantee a good readability of the graph. However, the bottom scale of the synthetic time domain data can be larger than this value, if the frequency step of the system is narrow enough to allow this. This means that the post-processed data can include also deeper time-depth levels.

The graphical user interface (GUI) of the new Eurydice software is shown in Figures 5 and 6. In particular, in Figure 5 two "panels" are presented; both these panels can be visualized by the user. The first panel is the interface for setting the parameters of the measurement; this panel was already present in the original version of the software. The second panel is available in the upgraded software, only; here, data are visualized in real time during the acquisition. In Figure 6, a screenshot of the second panel taken during a survey is shown.

For the interested Reader, the most interesting parts of the source code have been made available as 'Supplementary Materials' to this paper.

Download Supplementary Materials here:
http://gpradar.eu/onewebmedia/Supplementary_Materials_GPR-2-1-3_Brigatti.zip

4 CONCLUSIONS

In this paper, a reconfigurable stepped-frequency ground penetrating radar (GPR) prototype was briefly presented, emphasizing some special features not common in commercial systems, such as the possibility to set a suitable integration time at different frequencies, and the availability of three couples of equivalent shielded antennas in the system, sharing the same gap. The main objective of the present paper, though, was to describe the development of new dedicated software procedures, allowing real-time data visualization in the prototype at hand; this is obviously a common feature in commercial systems, but was not yet available in the prototype. In particular, before the upgrade of the acquisition software presented in this paper, the visualization of the recorded (raw) data was possible only during the post processing stage, by using some Matlab scripts. The user can now set a spatial interpolation step and choose one or more antennas for real-time visualization during the prospecting, with huge practical benefits.

Future work might regard the development of a new reconfigurable stepped-frequency GPR (and relevant software) for higher frequency applications, such as through-the-wall prospecting, where the use of such a system is expected to be especially effective in contrasting external interferences.

https://doi.org/10.26376/GPR2019003

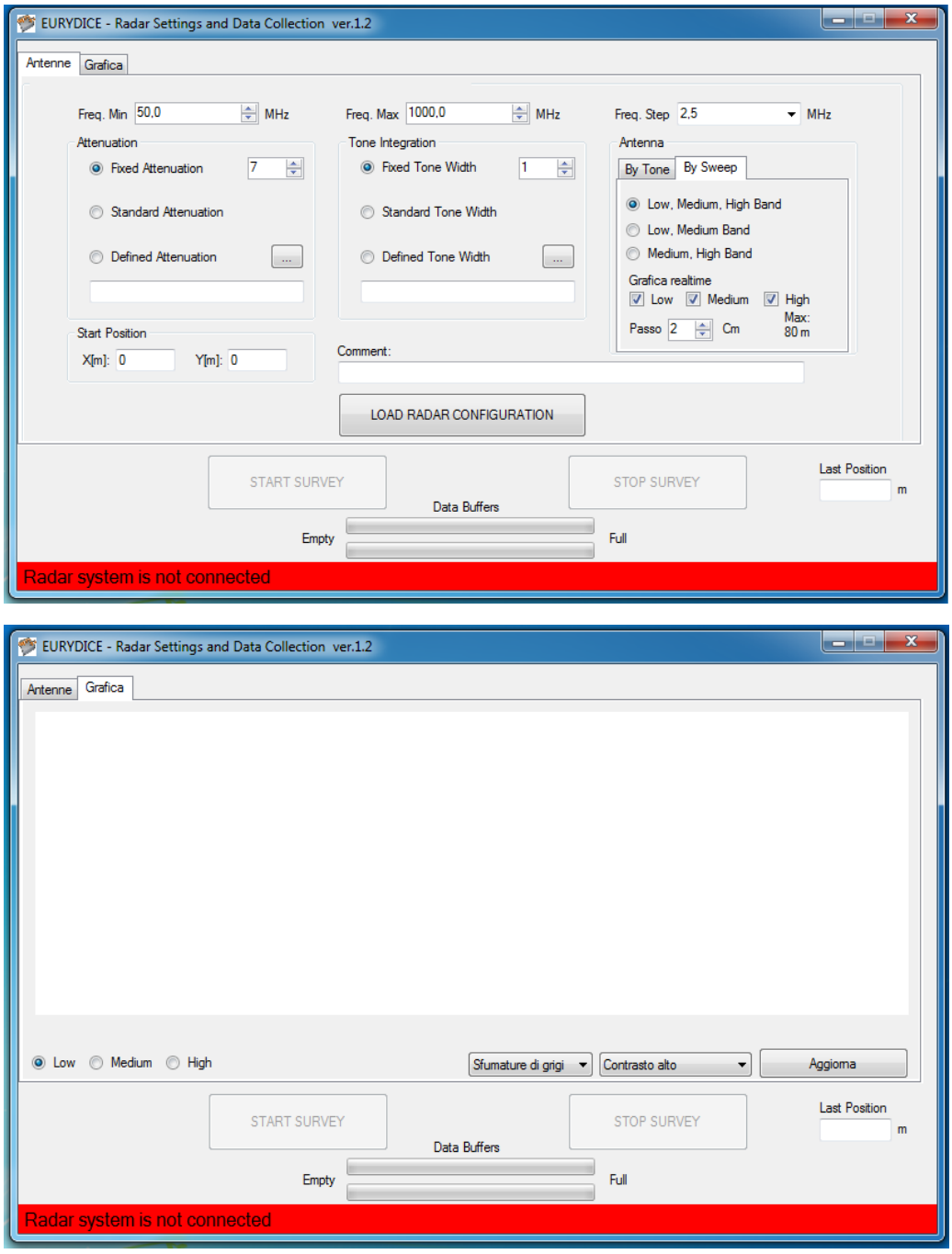

FIG. 5 – GUI of the upgraded software: data are visualized in real time on the panel shown in the lower part of the figure. Note that some terms are written in Italian: "Antenne" means "Antennas," "Grafica" means "Plot," "Sfumature di grigi" means "Greyscale," "Contrasto alto" means "High contrast," "Aggiorna" means "Refresh."

https://doi.org/10.26376/GPR2019003

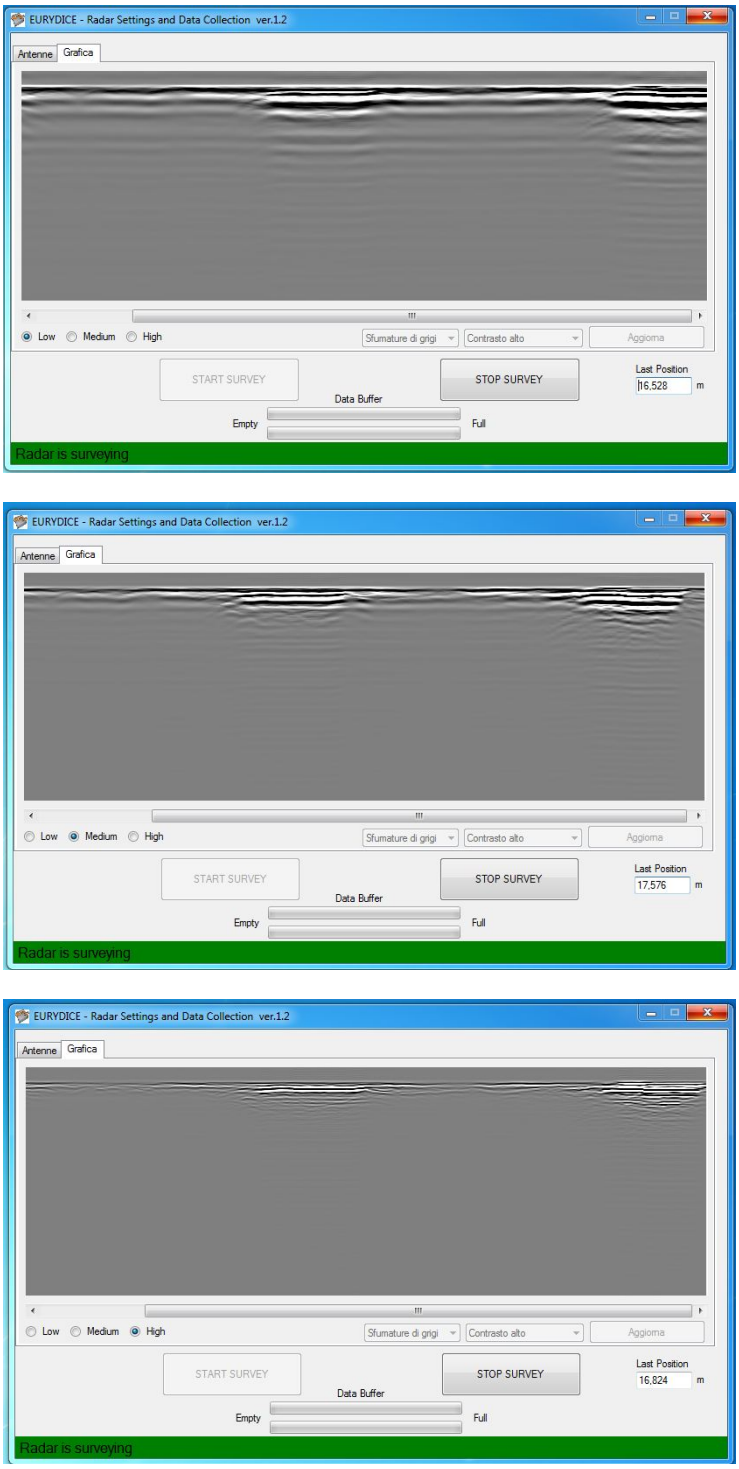

FIG. 6 – Screenshot of the software GUI during a real-field survey. Each picture shows a different B-Scan measured by a different equivalent couple of antennas.

https://doi.org/10.26376/GPR2019003

Further possible research advancements might regard the design of novel reconfigurable antennas with an optimized shape, and also the development of new processing algorithms for a more advanced exploitation of data recorded by different antennas. Compared to commercial systems equipped with dual antennas, such exploitation is expected to be easier when dealing with the prototype presented in this paper, due to the fact that the equivalent antennas share the same gap.

Download Supplementary Materials here:
http://gpradar.eu/onewebmedia/Supplementary_Materials_GPR-2-1-3_Brigatti.zip

REFERENCES

[1] D. Daniels, Ground Penetrating Radar, 2nd Edition, IET, 2004.

[2] History of Ground Penetrating Radar (GPR): www.obonic.de/article/ground-peentrating-radar-history/ [Last visited on January 23rd, 2019]

[3] L. Robinson, W. B. Weirand, and L. Yung, "Location and recognition of discontinuities in dielectric media using synthetic RF pulses," Proceedings of the IEEE, vol. 62(1), pp. 36-44, January 1974, doi: 10.1109/PROC.1974.9383

[4] D. A. Noon, "Stepped-Frequency Radar Design and Signal Processing Enhances Ground Penetrating Radar Performance," Ph.D. Thesis, Department of Electrical & Computer Engineering, University of Queensland, Australia, 1996.

[5] G. Tronca, I. Tsalicoglou, S. Lehner, and G. Catanzariti, "Comparison of pulsed and stepped frequency continuous wave (SFCW) GPR systems: Applications on reinforced concrete and brick/rock masonries," Proceedings of the 17th International Conference on Ground Penetrating Radar, pp. 819-822, Rapperswil, Switzerland, 18-21 June 2018, ISBN 978-1-5386-5777.

[6] M. Sato and R. Persico, "Ground Penetrating Radar: technologies and data processing issues for applications," within the volume "Sensing the Past" edited by Nicola Masini and Francesco Soldovieri, Springer, Louisville, USA, 2017, ISBN 978-3-319-50518-3, chapter 9, pp. 175-202.

[7] E. Eide, N. Linford, R. Persico, and J. Sala, "Advanced SFCW GPR systems," in Innovative Instrumentation and Data Processing Methods in Near Surface Geophysics, edited by R. Persico, S. Piro and N. Linford, Elsevier, Amsterdam, The Netherlands, 2018, chapter 8, pp. 253-286, ISBN 978-0-12-812429-1.

[8] M. Sato, J. Fujiwara, and K. Takahashi, "ALIS evaluation tests in Croatia," Proceedings of the SPIE, vol. 7303, Detection and Sensing of Mines, Explosive Objects, and Obscured Targets XIV; 73031B (2009), doi: 10.1117/12.818497.

https://doi.org/10.26376/GPR2019003

Event: SPIE Defense, Security, and Sensing, 2009, Orlando, Florida, United States.

[9] R. Persico and G. Prisco, "A Reconfigurative Approach for SF-GPR Prospecting," IEEE Transactions on Antennas and Propagation, vol. 56(8), pp. 2673-2680, August 2008, doi: 10.1109/TAP.2008.927516.

[10] R. Persico, M. Ciminale, and L. Matera, "A new reconfigurable stepped frequency GPR system, possibilities and issues; applications to two different Cultural Heritage Resources," Near Surface Geophysics, vol. 12(6), pp. 793-801, December 2014, doi: 10.3997/1873-0604.2014035.

[11] L. Matera, R. Persico, N. Bianco, G. Lepozzi, and G. Leopizzi, "Joined interpretation of Buried Anomalies from Ground Penetrating Radar data and endoscopic tests," Archaeological Prospection, vol. 23(4), pp. 301–309, September 2016, doi: 10.1002/arp.1545.

[12] Website of the A.I.Te.C.H. project: www.aitechnet.com [Last visited on January 23rd, 2019].

[13] R. Persico, D. Dei, F. Parrini, and L. Matera, "Mitigation of narrow band interferences by means of a reconfigurable stepped frequency GPR system," Radio Science, vol. 51(8), pp. 1322-1331, August 2016, doi: 10.1002/ 2016RS005986.

[14] R. Persico and G. Leucci, "Interference Mitigation achieved with a reconfigurable stepped frequency GPR System," Remote Sensing, vol. 8, pp. 1-11, Article ID 926, November 2016, doi: 10.3390/rs8110926.

[15] Website of the WinPcap library: www.winpcap.org [Last visited on January 23rd, 2019].

[16] Website of the ALGLIB project: www.alglib.net [Last visited on January 23rd, 2019].

Ground Penetrating Radar
Volume 2, Issue 1, March 2019
https://doi.org/10.26376/GPR2019004

TU1208 GPR Roadshow: educational and promotional activities carried out by members of COST Action TU1208 to increase public awareness on the potential and capabilities of the GPR technique

Lara Pajewski[1], Hannes Tõnisson[2], Kaarel Orviku[2], Miro Govedarica[3], Aleksandar Ristić[3], Vladislav Borecky[4], Salih Serkan Artagan[5], Simona Fontul[6], and Klisthenis Dimitriadis[7]

[1] Department of Information Engineering, Electronics and Telecommunications, Sapienza University of Rome, Rome, Italy – lara.pajewski@uniroma1.it
(L. Pajewski is the Corresponding Author)

[2] School of Natural Sciences and Health, Tallinn University, Tallinn, Estonia – hannes.tonisson@tlu.ee, kaarel.orviku@tlu.ee

[3] Faculty of Technical Sciences, University of Novi Sad, Novi Sad, Serbia – miro@uns.ac.rs, aristic@uns.ac.rs

[4] University of Pardubice, Pardubice, Czech Republic - vladislav.borecky@upce.cz

[5] Anadolu University, Eskişehir, Turkey – ssartagan@anadolu.edu.tr

[6] National Laboratory of Civil Engineering, Lisbon, Portugal – simona@lnec.pt

[7] Geoservice, Athens, Greece – klisthenis@geoservice.gr

Abstract

Our participation in the COST (European Cooperation in Science and Technology) programme gave us significant insights into the importance of explaining scientific findings to non-scientific audiences. In the framework of COST Action TU1208 "Civil engineering applications of Ground Penetrating Radar" we organised a series of dissemination activities to increase public awareness about ground penetrating radar (GPR) capabilities and applications, as well as to establish a dialogue with stakeholders and end-users of our research. Most of our educational and promotional activities were carried out in less-research intensive countries of the European continent, and we denominated the overall science communication initiative "TU1208 GPR Roadshow". The purpose of this paper is to present descriptions, principles, and results of our Roadshow. Part of

 https://doi.org/10.26376/GPR2019004

the Roadshow consisted of a series of non-scientific workshops and practical demonstrations held in Portugal, Italy, Greece, Croatia, Serbia, and the Czech Republic from March 2016 to May 2017. The primary objective of those events was to reach out to GPR stakeholders and potential new end users, at local, regional and national levels; a secondary goal was the education of interested students and citizens. Attendance was always free of charge; talks and explanations were mostly given in native language, with few exceptions. Overall, the Roadshow workshops and demonstrations had 483 participants. In parallel, an amazing series of activities with children and citizens were carried out in Estonia: several lectures were delivered in elementary and secondary schools, practical workshops were held during the Researchers' Nights, communication activities were organized in large events where enterprises were brought together with researchers, some lectures were given in summer schools, and short lectures were transmitted on public TV. All these initiatives have strongly increased public awareness of the potentialities of the GPR technique.

Keywords: Ground penetrating radar; science communication; public knowledge about science and technology; dissemination and outreach; scientific training.

1 Introduction

Researchers are rather confused about what science communication is, and they often underestimate its importance. Science communication mostly is about communicating with nonexperts, whereas many researchers stay in their 'ivory tower' and talk to colleagues within their specialist area, only. The communication strategy of researchers normally includes the presentation of activities and results in scientific conferences, publication of scientific papers in peer-reviewed scientific journals, and publication of scientific books and book chapters; the youngest researchers spread information about their studies on academic social networking sites, as well. If scientists wish to maximize the impact of their activities and receive more funding, it is imperative that they step out of their usual arenas and start communicating science to a broader audience; they need to establish a dialogue with stakeholders and end users of their research, and also with citizens of different ages and education levels. Nowadays there is a huge amount of research going on, on really important topics, that actually never really gets to policymakers, professional groups or commercialization; at the same time, too many citizens do not understand how important science

https://doi.org/10.26376/GPR2019004

is for society, how research is crucial for finding concrete solutions to global challenges, and how creating new knowledge and improving education is essential for increasing the quality of our lives.

A contemporary definition of science communication is given by Burns et al. [1] as the employment of proper abilities, actions, media, and dialogue to provide at least one of the following individual reactions to science (with the AEIOU vowel analogy): Awareness, Enjoyment, Interest, Opinion-forming, and Understanding. Science communication is a multifaceted subject which covers a range of issues from dissemination of scientific research to new models of public involvement where lay persons are supported to take part in science discussions and policy; and it attracts increasing consideration from research institutions, policy makers, practitioners and academicians [2].

To encourage science communication initiatives, the European Union (EU) is requiring that a comprehensive communication plan be included in all Horizon 2020 project proposals (as is well known, Horizon 2020 is the EU Framework Programme for Research and Innovation for 2014-2020) [3, 4]. Moreover, Horizon 2020 is launching dedicated calls for communication projects. The EU has recently prepared a "Guide to Science Communication" consisting of a series of short videos about science communication in general, with several tips on 'how to improve your communication efforts,' and a 60-minutes video on 'how to increase the communication impact of your research project' (all those videos are available on the European Commission "Innovation Union" YouTube channel). Further useful documents published at European level are the "Social media guide for EU funded R&I projects" [5] and the Intellectual Property Rights (IPR) HelpDesk brochure "Making the Most of Your H2020 Project" [6].

Ground Penetrating Radar (GPR) researchers are not different from researchers working in other scientific areas when it comes to science communication behaviour; and yet, given the vast application potential of the GPR technique, there is so much that can be shared with multiple interlocutors and at different levels. Our participation in Horizon 2020 via the COST (European Cooperation in Science and Technology) Action TU1208 "Civil engineering applications of Ground Penetrating Radar" gave us significant insights into the importance of explaining scientific findings to non-scientific audiences. We decided to put efforts into increasing public awareness about GPR capabilities and applications, as well as into establishing a dialogue with stakeholders

 https://doi.org/10.26376/GPR2019004

and end-users of our research. We therefore organized a heterogeneous series of educational and promotional activities that were mostly carried out in less-research intensive countries of the European continent (Inclusiveness Target Countries [7]); the overall science communication initiative was denominated "TU1208 GPR Roadshow".

This paper aims to present some descriptions, principles, and results of our Roadshow. It has to be noted that the Roadshow activities were entirely organized by researchers, sometimes in cooperation with private GPR service providers. When we started, we were totally unaware about science communication methods and strategies, most of us did not even know the meaning of the word 'stakeholder' and had never made a serious thought on who the 'end users' of their research were [8]. Therefore, the Roadshow activities represented our first steps in the 'world of science communication.' Nonetheless, the initiative was undoubtedly a big success; it raised considerable interest in various countries and was a catalyst for a series of new activities.

Part of the Roadshow consisted in a series of communication events held in Portugal, Italy, Greece, Croatia, Serbia, and the Czech Republic from March 2016 to May 2017 [9, 10]; the route of the Roadshow events is illustrated in Figure 1(a). The primary purpose of these events was to reach out to GPR stakeholders and potential new end users, at local, regional and national levels; a secondary goal was the education of interested students and citizens. The events organized in the various countries are presented as separate case studies in Sections 2-7 of this paper. Attendance was always free of charge, for all participants; the talks and explanations were mostly given in native language, with few exceptions. Overall, 483 participants attended the events and had the opportunity to learn what is GPR, how this technique can be used for 'seeing the unseen,' and what is the role of GPR in civil engineering works, archaeological investigations, and cultural heritage management (we mainly focused on these fields of application because the COST Action TU1208 project dealt with the use of GPR in civil-engineering). In our events, we also stressed how GPR profiling is a safe, environment-friendly, and non-destructive method of investigation. Feedback was collected after the events; participants expressed strong satisfaction, most often they asked us to organize further dissemination activities if not to establish a regular series of events, to be held annually or every few months, in order to keep the dialogue active and receive regular updates on the GPR research.

https://doi.org/10.26376/GPR2019004

(a)

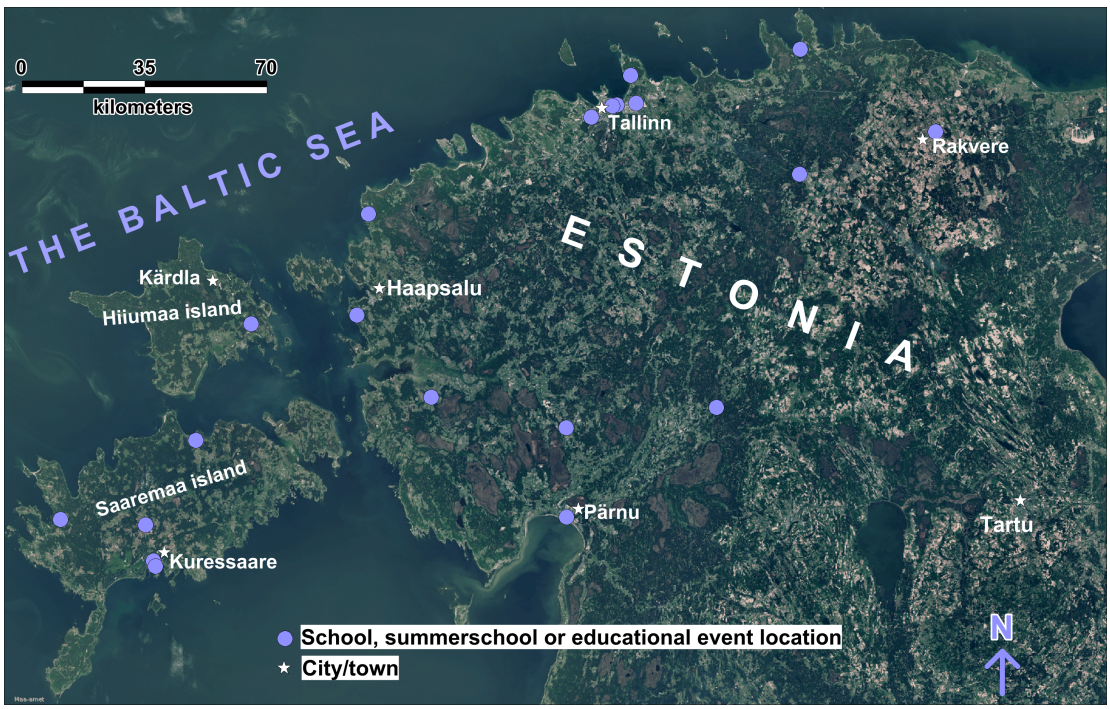

(b)

Figure 1: (a) Route of TU1208 GPR Roadshow communication events. **(b)** Map of Estonia, with blue dots indicating the locations of our numerous educational activities and events (the base satellite map is taken from the website of the Republic of Estonia Land Board).

 https://doi.org/10.26376/GPR2019004

In parallel, a series of promotional and educational activities were carried out in Estonia, which brought especially positive and tangible results; these activities are resumed in Section 8 and their numerous locations are shown in Figure 1(b). Estonia is a small and relatively young independent country, where many fields of research are making the first steps; moreover, the profession of the scientific researcher is not much acknowledged and popular among the students. GPR is not very commonly used in Estonia and was an almost unknown tool among Estonian people, until a few years ago. To the best of our knowledge, there were only two GPR systems in Estonia when COST Action TU1208 started, both of them owned by research groups working in the university; those groups were mostly employing GPR in the fields of geology, ecology, and archaeology. Now things are changing: there is an increasing interest in the use of GPR, not only for research but also for practical works in private and public sectors; indeed, the research groups owning GPR systems have reported that they have been recently involved in a growing number of projects ordered by private enterprises or public authorities. We are delighted to say that this phenomenon is most probably the result of the communication efforts made by the researchers from the Institute of Ecology at Tallinn University. A number of lectures delivered in elementary and secondary schools, practical workshops held during the Researchers' Nights, communication activities in large events where enterprises were brought together with researchers, lectures delivered in summer schools, and even short lectures transmitted on public television channels have all increased public awareness on the potentialities of the GPR technique.

2 Roadshow in Portugal

The pilot communication event of COST Action TU1208 was held on 2 March 2016 at the Laboratório Nacional de Engenharia in Lisbon (LNEC), Portugal; the local organiser was Dr Simona Fontul. A full-day non-scientific workshop on GPR basic principles and civil-engineering applications was offered to stakeholders and potential new end-users (namely, representatives from public agencies and private companies providing civil engineering services). The workshop was meant to be a "preliminary experiment" conducted by TU1208 to evaluate the feasibility, raised interest, difficulties, and benefits of this kind of events,

https://doi.org/10.26376/GPR2019004

before possibly starting a full-scale dissemination project. The decision to organize the event in Portugal was due to the enthusiasm expressed by the local organiser and to the priority principle of disseminating information about GPR first in countries where this technology is rarely used (and particularly in the less research-intensive countries).

The programme of the workshop is reported in Table 1. As is well known, the penetration of English language is non-uniform across Europe and, even when the penetration of English is sufficient, lectures in native language help Attendees to concentrate on the presented topics, as they don't have to put efforts into decoding a foreign language. For this reason, we decided that most talks had to be given in native language. Nonetheless, lectures given by Action Members coming from abroad were included in the programme, too, to offer a European perspective to Attendees; those talks were of course given in English. Additionally, most slides were written in English to facilitate the foreigners in the comprehension of the presented topics.

In total, 104 persons attended the event, with a high prevalence of local Attendees, as expected (see Figure 2(a)). Figure 2(b) shows thenumber of Attendees from universities and research institutes, industry, and public agencies (we were pleased by the high number of participants from industry). Figure 2(c) shows gender distribution of Attendees. Based on questions asked by Attendees during the event, we observed that, beyond the civil engineering applications of GPR, there was a significant interest in the use of GPR in geology, water management, and sedimentology.

After the event, we sent an evaluation form to all Portuguese Attendees, via email; the form was sent only once, and we got answers from 48% of the recipients (the feedback was very strong). Questions and answers are reported in Table 2. Some participants asked us to organise further dissemination events in Portugal, and possibly a training course including practical sessions on data acquisition and processing. End-users with previous GPR experience expressed appreciation for the initiative and commented that these events can concretely foster a wider use of GPR, as well as help to demystify subjectivity in GPR data interpretation.

We were glad to learn that, after attending the Lisbon event and discovering the numerous applications and high potential of the GPR technique, a company without previous experience in GPR decided to extend their activities to this area. They tried and contacted various GPR

https://doi.org/10.26376/GPR2019004

manufacturers, proposing them to become their national representatives in Portugal, and nowadays they are Portuguese representatives of IDS Georadar srl. The company reported that during the first six months of activity they managed to sell two systems in Portugal and they also started demonstration and rental businesses.

Table 1: Programme of the dissemination event held in Lisbon (Portuguese edition of TU1208 GPR Roadshow).

Seminário Aplicações do Georadar (GPR) em Engenharia Civil (Seminar on Georadar Applications for Civil Engineering)	
Time	**Session**
09:00-09:30	*Receção dos participantes*
09:30-09:45	Sessão de abertura
09:45-10:00	"Princípios de funcionamento do Georadar e campos de aplicação," Doutora Simona Fontul – LNEC, PT
10:00-10:30	"Aplicação do Georadar na avaliação de infraestruturas ferroviárias," Doutor Eduardo Fortunato & Doutora Simona Fontul – LNEC, PT
10:30-11:00	*Intervalo*
11:00-11:30	"Avaliação da humidade e presença de fendas em misturas betuminosas," Prof. Jorge Pais & Prof. Francisco Fernandes – Univ. do Minho, PT
11:30-12:10	"Ground Penetrating Radar inspection of buildings: looking inside advantages and limitations," Prof. Vega Pérez-Gracia – Univ. Politécnica de Cataluña, ES
12:10-12:30	Debate
12:30-14:15	*Almoço (livre)*
14:15-14:35	"Aplicação do Georadar em geotecnia e estruturas," Doutora Maria João Coelho – LNEC, PT
14:35-15:00	"Introduction to the COST programme and to Action TU1208 "Civil engineering applications of Ground Penetrating Radar," Prof. Lara Pajewski – Universidade "Roma Tre", IT
15:00-15:20	"Ground Penetrating Radar for bridge inspection," Prof. Mercedes Solla – Universidade de Vigo, ES
15:20-15:50	*Intervalo para café*
15:50-16:15	"Aplicação do Georadar na avaliação de infraestruturas rodoviárias e aeroportuárias," Doutora Simona Fontul & Doutoranda Vânia Marecos – LNEC, PT
16:15-18:00	Painel: Experiências e desafios na aplicação do Georadar – Sessão de encerramento

https://doi.org/10.26376/GPR2019004

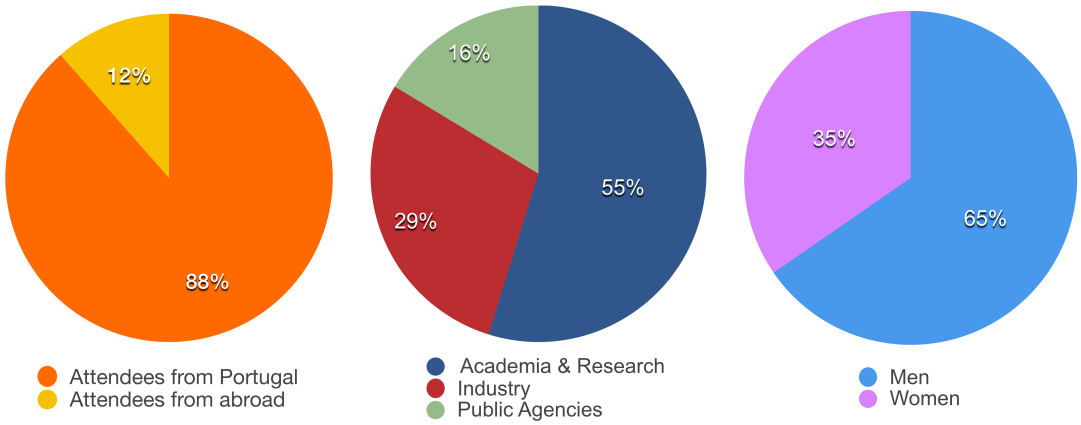

Figure 2: (a) Number of Attendees from Portugal and from other countries; **(b)** Number of Attendees from universities and research institutes, private companies, and public agencies; **(c)** Gender distribution of Attendees (Portuguese edition of TU1208 GPR Roadshow).

Table 2: Evaluation form sent to Attendees, with statistics on the received feedback (Portuguese edition of TU1208 GPR Roadshow)).

1 - Qual era o conhecimento que detinha sobre o Georadar antes do Seminário? 1 - What was your knowledge about GPR before attending the workshop?	*Nunca tinha ouvido* *Never heard about it*	*Já tinha ouvido* *Knew about its existance*	*Utilizei resultado* *Saw GPR results before*	*Sou utilizador* *GPR user*
	3%	56%	22%	19%
2 - Utilizava o equipamento Georadar para aplicações na sua área se tivesse a oportunidade? 2 - Will you use GPR in your area, if you will have the opportunity?	*Não*	*Talvez*	*Sim*	*Não se aplica*
	No	*Probably*	*Yes*	*Not applicable*
	6%	19%	72%	3%
3 - Considerou o Seminário útil para adquirir conhecimentos sobre o funcionamento e a utilização do Georadar? 3 - Do you think that the event was useful to acquire knowledge on GPR basic principles and applications?	*Nada*	*Pouco*	*Médio*	*Muito*
	Not at all	*A little*	*Fairly*	*A lot*
	0%	3%	34%	63%
4 - Tem sugestões para futuras participações/ colaborações de divulgação nesta área? Quais? 4 - Do you have suggestions for future cooperation / dissemination activities in this area? Which one?	*Não*	*Sim*		
	No	*Yes*		
	75%	25%		

https://doi.org/10.26376/GPR2019004

3 Roadshow in Italy

The Lisbon workshop revealed that communication initiatives towards non-scientific audiences were (and still are) strongly needed in the GPR field. Therefore, the Action decided to modify its Work & Budget Plan and organize further dissemination events to be held during the subsequent 15 months in different countries.

The second event was held in Rome on 29 April 2016 and was a great success. The main focus was again on the civil-engineering applications of GPR. The venue was the Department of Engineering of Roma Tre University and the local organiser was Dr Lara Pajewski. The flyer of the event, including the programme (in Italian), is in Figure 3.

The event was attended by 96 participants, with a high prevalence of local Attendees (Figure 4(a)); participants from other Countries were also present since the technical workshop was held right after the 2016 Working Group Progress Meeting of the Action. Most slides were written in English to help foreigners in the comprehension of exposed topics; however, all talks were given in Italian. Figure 4(b) shows the number of Attendees from universities and research institutes, public agencies, and industry. The number of participants from industry was especially high: some private companies attending the event were already working with GPR, other companies did not yet have experience with GPR and were interested in discovering more about this inspection technique; there were also representatives from a manufacturer of radar systems (not GPR) and two telephone companies. Concerning the participation of stakeholders, there were representatives from the Regional Agency for Environmental Protection, the Ministry of Telecommunications, and Carabinieri Corps. It has to be mentioned that this event was organised with short notice (for financial reasons), else attendance would have been stronger; this also explains the low participation of stakeholders, who usually need a longer notice than researchers and companies. Figure 4(c) shows gender distribution of Attendees, which is similar to the Lisbon one. As a general comment, we noticed that the participation of women was stronger at TU1208 dissemination events than at scientific events.

When the event was planned, COST key principles were faithfully followed and young researchers were invited to give most of the lectures, instead of experienced professors; this was also done to stress how, in Italy, young researchers suffer from a strongly hierarchical academic

https://doi.org/10.26376/GPR2019004

environment and struggle to have the opportunities and visibility they need and deserve. During some talks, scientific information was intercalated by interesting historical anecdotes. Attendees asked several questions and expressed appreciation for the professionalism and clarity of the Speakers, stating that lectures were one better than the other.

The workshop included a roundtable with companies offering GPR services. Before the event, TU1208 Members from Rome looked on the internet and found 27 Italian companies active in the GPR field: they all were invited to attend the workshop and join the roundtable. Several companies participated in the workshop, and three of them accepted the challenge of the roundtable: GeoLogica from Rome, Geo3D from Rieti, and GRS from Rome. These companies were asked to:

1) Introduce themselves and their activities;
2) Based on their experience, point out GPR strengths and limits;
3) Suggest topics that might be introduced in training programmes at university level, to bridge the gap between industry needs and higher education;
4) Tell about their past or ongoing collaborations with Universities and participation in research projects, if any;
5) Suggest ideas about how to achieve a stronger involvement of Italian industry in research.

The companies reported that they mainly use GPR in the civil engineering fields of application: assessment of airport runways and reinforced concrete infrastructures, support during construction and renovation works, structural investigations, detection and localization of cavities and utilities (optical fibres being the most frequently sought utilities, as they easily move from their initial position). Moreover, they are sometimes asked to carry out geophysical surveys; sporadically, they use GPR for forensics and archaeological investigations. When needed, GPR is combined with other non-destructive testing techniques to overcome its limits and/or increase the accuracy of results.

Difficulties encountered by the three companies reside more in the wrong reputation of GPR and/or weak awareness of customers about GPR capabilities, rather than in the intrinsic limits of the technique. Sometimes customers request surveys on soils with high conductivity, where good results cannot be obtained (such as clayey soils), or in scenarios where radargrams cannot be easily interpreted due to the presence of too many reflecting structures (such as the basement of a building), or else they wish to reach higher resolution and/or deeper

https://doi.org/10.26376/GPR2019004

Figure 3: Flyer of the technical workshop held in Rome (Italian edition of TU1208 GPR Roadshow).

https://doi.org/10.26376/GPR2019004

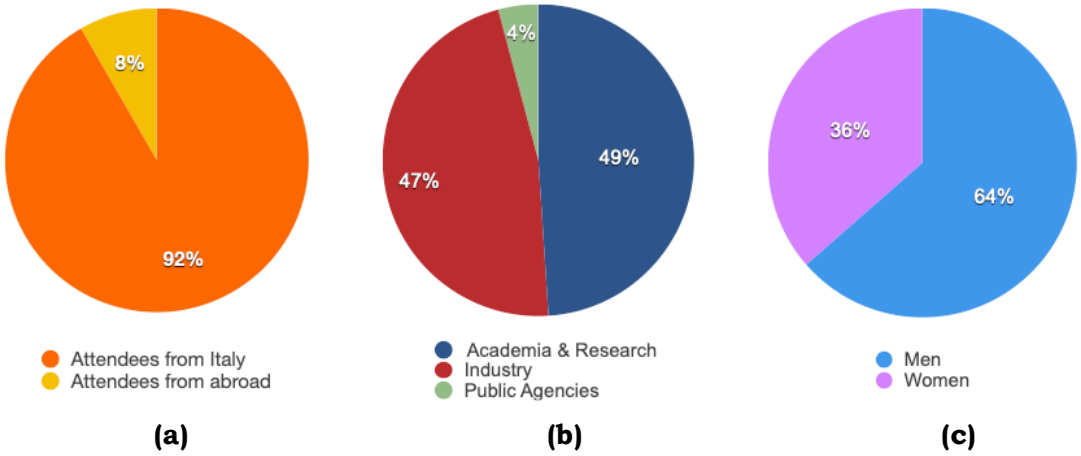

Figure 4: **(a)** Number of Attendees from Italy and from other countries; **(b)** Number of Attendees from universities and research institutes, private companies, and public agencies; **(c)** Gender distribution of Attendees (Italian edition of TU1208 GPR Roadshow).

penetration than possible. In such situations, companies try and explain that, although GPR has recently achieved some spectacular successes, there are environments where it cannot be used to image the subsurface with high resolution, moreover not every kind of target can be detected. Whenever possible, companies propose to customers the use of complementary non-destructive testing approaches in combination with GPR. However, sometimes customers think that companies are recommending to use other techniques to increase their profit and not because of actual necessity.

The companies participating in the Roadshow would gladly welcome the establishment of a license for GPR end-users in Italy and the introduction of national guidelines for the use of GPR in civil engineering and possibly also in other areas. Another issue raised by companies is the absence of GPR training opportunities in Italy: manufacturers organize short and expensive introductory courses, but end-users substantially have to learn how to use their GPR autonomously, and this strongly limits a wider diffusion of the technique. GPR technology and methodology have been evolving fast in the last decades, and nowadays an enormously wide range of applications exist; hence companies believe that it is high time for Italian universities and associations of engineers to start offering GPR courses.

 https://doi.org/10.26376/GPR2019004

All participating companies stated that they found the workshop very useful. They suggested repeating the experience regularly, for example every six months, to share expertise and foster stronger cooperation between academia and industry. Delegates from academia agreed that frequent meetings between scientists and private end-users are highly desirable; and they observed that such initiatives might be organised by companies, too, not necessarily by universities.

An article resuming this science communication day was published in "Strade & Autostrade," [11] ("Roads & Highways"), an Italian technical bimonthly journal dedicated to issues pertaining to the construction, maintenance, and management of transport networks in Italy.

Among the positive outcomes of the Italian Roadshow, shortly after the event the local organiser was contacted by the Special Operations Department of Carabinieri Corps, to establish a scientific cooperation on the use of GPR for forensic investigations and law enforcement.

4 Roadshow in Greece

The third edition of the Roadshow was held in Athens and spanned over two days (27 and 28 September 2016); the poster of the event is shown in Figure 5. The main focus was on the use of GPR for archaeological investigations and cultural-heritage management, these being the main areas where GPR can be employed in Greece. The local organiser institution was Geoservice, a Greek company funded in 1990 and providing state-of-the-art services, at European level, in the field of non-destructive geophysics. The event was also supported by the Hellenic Ministry of Culture, Education, and Sport, via its Directorate for Conservation of Ancient and Modern Monuments.

The event was attended by 76 participants; two Speakers came from abroad, all other Speakers and Attendees were Greek (Figure 6(a)). Figure 6(b) illustrates the number of participants from universities and research institutes, public agencies, and industry; the local organiser was able to attract the interest of many private companies and stakeholders. The attending companies declared that they did not have any previous experience with GPR. Stakeholders were from the Hellenic Ministry of Culture, Education and Sport, National Archaeological Museum of Athens, Corfu Archaeological Ephorate, Ephorate of Antiquities of West Attiki, Korinth Archaeological Ephorate, and Water Company of Athens. A few participants were unemployed conservators

https://doi.org/10.26376/GPR2019004

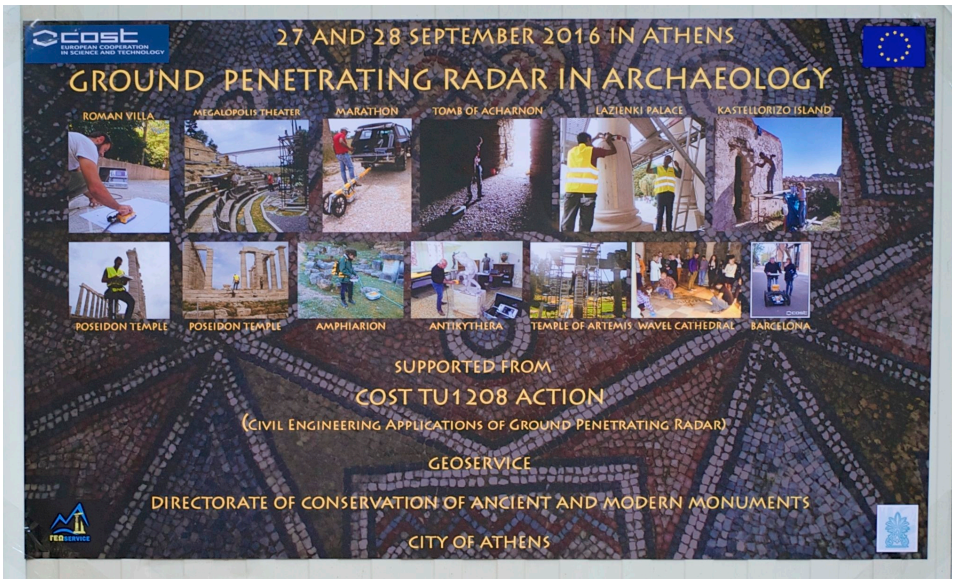

Figure 5: Flyer of the dissemination event held in Athens, hanging on a wall in the National Gardens of Athens (Greek edition of TU1208 GPR Roadshow).

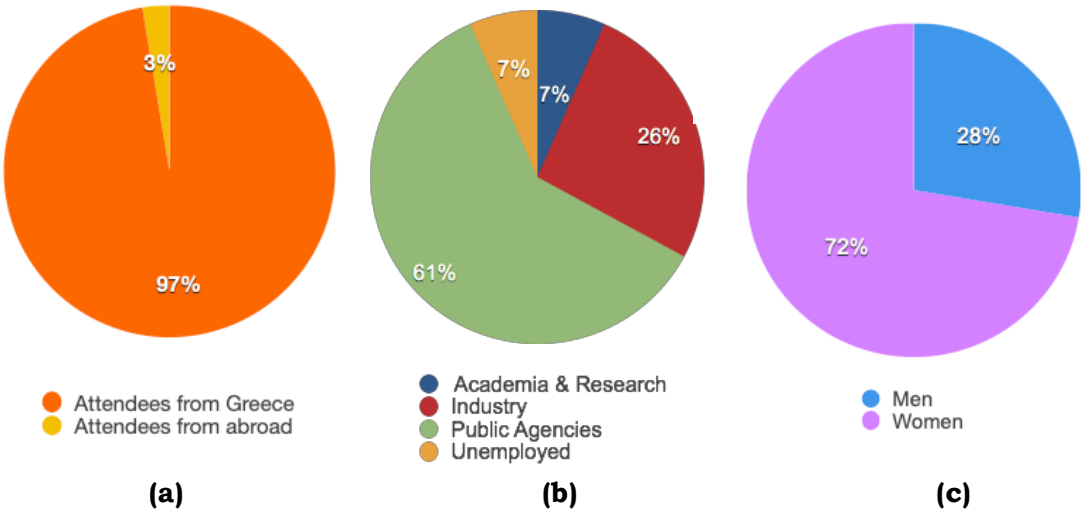

Figure 6: **(a)** Attendees from Greece and abroad; **(b)** Attendees from academia and research, industry, public agencies, and unemployed Attendees; **(c)** Gender distribution of Attendees (Greek edition of TU1208 GPR Roadshow).

and archaeologists. Figure 6(c) shows gender distribution of Attendees: the percentage of women was notably higher than in all other Roadshow editions; this is most probably due to the fact that more women work in the fields of archaeology and cultural-heritage than in civil engineering.

https://doi.org/10.26376/GPR2019004

During the first day, the GPR technique was explained to Attendees while performing practical demonstrations in the National Gardens of Athens, a public park in the centre of Athens where ancient ruins, tambourines, Corinthian capitals of columns, mosaics, and other archaeological artifacts, are present. In the morning, an area with mosaics was investigated (Figures 7 and 8(a)-(c). The measured data were plotted, printed, and then interpreted and discussed with Attendees. In the afternoon, we surveyed a 10 m × 10 m flat green area with buried archaeological ruins (Figure 8(d)). These activities required a preparatory work to choose suitable areas and inspect them in advance.

During the second day, a workshop was held in the City of Athens Cultural Centre (Antonis Tritsis Amphitheatre), including a series of technical talks and a final discussion. A photo taken during the workshop is shown in Figure 9; a translation in English of the workshop programme is in Table 3 (the original programme was written in Greek); almost all lectures were given in Greek and slides were in Greek, only the contributions of Dr Lara Pajewski and Dr Fabio Tosti were in English. During the final discussion, the Speakers tried and stimulated ideas in the audience for implementing non-destructive methodologies in the conservation of cultural heritage and starting new projects where GPR could be employed. Moreover, Speakers and audience reflected together about opportunities for the creation of new international synergies in the field of non-destructive assessment by using GPR.

Figure 7: Aerial photo of the mosaics in the National Gardens of Athens, surveyed with GPR during Day 1 (Greek edition of TU1208 GPR Roadshow).

https://doi.org/10.26376/GPR2019004

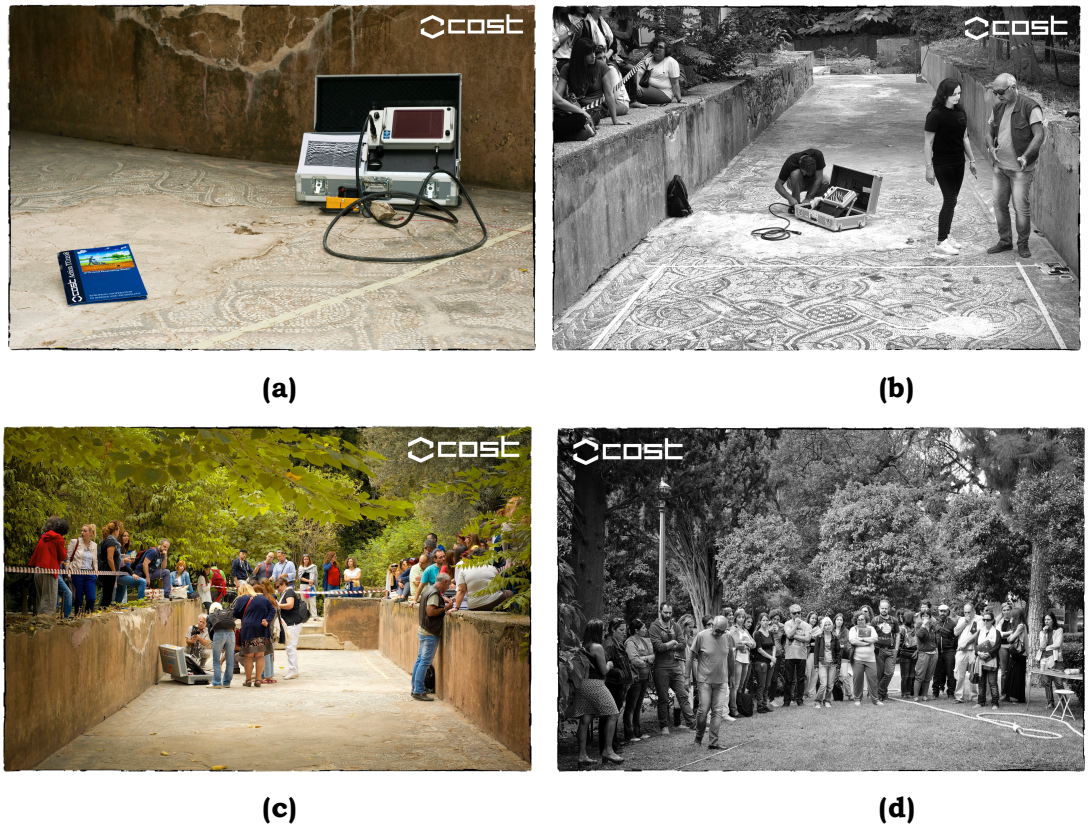

Figure 8: (a) GPR equipment used to inspect the mosaics of the National Gardens of Athens; **(b)** Morning demonstration on the mosaics; **(c)** Preparing the acquisition grid on the mosaics; **(d)** Afternoon demonstration over buried archaeological structures (Greek edition of TU1208 GPR Roadshow).

Figure 9: Attendees in the Antonis Tritsis Amphitheatre of the City of Athens Cultural Centre (TU1208 GPR Roadshow – Greek edition).

https://doi.org/10.26376/GPR2019004

Table 3: Programme of the workshop held in Athens (TU1208 GPR Roadshow).

Time	Speaker	Activity
10:30 - 10:45	Klisthenis Dimitriadis (President of GEOSERVICE, EL) & Maria Mertzani (Head of Directorate of Conservation of Ancient and Modern Monuments in Greece, Hellenic Ministry of Culture, Education and Sports, EL)	Welcome to participants and introduction to the workshop
10:45 - 11:30	Dr Lara Pajewski (Chair of COST Action TU1208, Roma Tre University, IT)	Introduction to the COST programme and to Action TU1208 "Civil engineering applications of Ground Penetrating Radar"
11:30 - 11:50	Dr Fabio Tosti (Research Fellow, University of West London, UK)	Use of Ground Penetrating Radar (GPR) in archaeological surveys
11:50 - 12:10	Prof. Andreas Loizos (Vice-Chair of COST Action TU1208, National Technical University of Athens, EL)	Overview of GPR applications in transport infrastructure
12:10 - 12:30	Klisthenis Dimitriadis (Geoservice, EL)	An example of non-destructive assessment using GPR, in the Mycenaean Tomb of Acharnon (work supported by COST Action TU1208 with a STSM Grant)
12:30 - 13:00		*Buffet at the foyer*
13:00 - 13:20	Dr Georgianna Moraitou (Head of Conservation, National Archaeological Museum of Athens, EL)	Non-destructive assessment using GPR, of the Antikythera sculptures
13:20 - 13:50	Maria Mertzani	Non-destructive methods for the conservation of cultural heritage
13:50 - 14:10	Dr Demosthenes Giraud (Emeritus Director, Directorate for Conservation of Ancient and Modern Monuments in Greece, Hellenic Ministry of Culture, Education and Sports, EL)	Non-destructive assessment with GPR in the ancient theater of Megalopolis, in the FP7 EU project STONECORE
14:10 - 15:30	All participants	Open discussion

https://doi.org/10.26376/GPR2019004

5 Roadshow in Croatia

The Croatian edition of GPR Roadshow consisted in a technical workshop held on 6 March 2017, prior to a three-day training school organized by COST Action TU1208, too. The event was hosted by the Faculty of Civil Engineering of the University of Osijek and the local organizer was Prof. Damir Varevac. The main focus of this edition was on the use of GPR in civil engineering and especially on the assessment of transport infrastructures. The programme is in Table 4; all talks were given in English, since the local organizer suggested that the level of English is very good in Croatia. Most Speakers were from academia, two were from industry (KB GPR Surveys, United Kingdom, and Murphy Surveys, Ireland). The participation of Speakers from industry is especially useful in GPR communication events, whenever one of the goals is to reach potential new end users.

The workshop was attended by 44 participants: 24 of them were Trainees of the subsequent training school (mostly, they were PhD Students from Inclusiveness Target Countries: the Czech Republic, Croatia, Hungary, Macedonia, Poland, Serbia, Turkey; and one Trainee was a PhD Student from the United Kingdom); the other Attendees were local scientists and students from both scientific and humanistic faculties; the Dean and Vice-Dean of the Faculty of Civil Engineering, Architecture and Geodesy of the University of Split attended the event, too.

The quality of the workshop was very good: Speakers gave excellent talks, interesting discussions took place, and the host institution provided amazing facilities as well as a financial contribution to partially cover the expenses. However, the event was mostly advertised in the academic environment; for that reason, there were no Attendees from public agencies and local private companies, whereas reaching those categories was the main objective of the initiative. The workshop substantially turned into an introductory day to the subsequent training school. The Croatian Roadshow case study highlights and confirms that, when embarking on the first organizational phases of a science communication event, it is crucial to design not only an effective programme of the activities but also an adequate information campaign towards the targeted audiences.

https://doi.org/10.26376/GPR2019004

Table 4: Programme of the workshop held in Osijek (Croatian edition of TU1208 GPR Roadshow).

Time	Speaker	Activity
08:30 - 09:00		Registration.
09:00 - 09:15	Local Authorities	Welcome to participants.
09:15 - 10:00	S. Fontul (LNEC, Portugal)	Ground Penetrating Radar (GPR) basic principles, capabilities and limits. Applications of GPR in civil engineering.
10:00 - 10:45	L. Pajewski (Chair of COST Action TU1208, Roma Tre University, Italy)	Introduction to the COST programme and to the Action TU1208 "Civil engineering applications of Ground Penetrating Radar."
10:45 - 11:00	D. Varevac (University of Osijek, Croatia)	GPR activities in the Osijek Faculty of Civil Engineering.
11:00 - 11:30		*Tea & Coffee Break*
11:30 - 12:30	C. Van Geem (Belgian Road Research Centre, Belgium)	GPR applied to roads and bridges.
12:30 - 13:00	S. Fontul	GPR applied to railways.
13:00 - 14:00		*Lunch*
14:00 - 14:45	C. Van Geem	Pavement management. Combined use of GPR with complementary non-destructive testing techniques.
14:50 - 15:35	M. Govedarica & A. Ristic (University of Novi Sad, Serbia)	GPR applied to detection and localisation of utilities in urban areas. Guidelines and good practice in Serbia.
15:35 - 16:00	K. Banks (KB GPR Surveys, United Kingdom)	The point of view of a private end-user: Overview on GPR services offered by KB GPR Surveys. Case studies.
16:00 - 16:30		*Tea & Coffee Break*
16:30 - 16:45	S. Fontul	GPR applied to airports.
16:45 - 17:10	S. Santos Assuncao (Murphy Surveys, Ireland)	The point of view of a private end-user: Overview on GPR services offered by Murphy Surveys. Case studies.
17:10 - 17:30	T. Rukavina (Zagreb University, Croatia)	GPR activities in Zagreb University.
17:30 - 18:00	All	Discussion.

https://doi.org/10.26376/GPR2019004

6 GPR Roadshow in Serbia

The fifth Roadshow event of COST Action TU1208 was held on 10 March 2017 at the Faculty of Technical Sciences of the University of Novi Sad, Serbia. The local organizer was the Geoinformatics Laboratory of the Computing and Control Department, coordinated by Prof. Miro Govedarica. The event consisted of a science communication workshop entitled 'GPR Workshop – European experiences, standards and recommendations on the application of Ground Penetrating Radar,' preceded by an exhibition and followed by a practical demonstration. The programme of the event is reported in Table 5, and the flyer is shown in Figure 10.

The targeted audience primarily included public agencies, private companies, and professionals active in the civil engineering field, not only in Serbia but also in Bosnia and Herzegovina, Montenegro, and Macedonia, in consideration of the fact that all these countries share the same language and a similar economic situation.

Lectures started at 10:30, to allow Attendees to reach Novi Sad in the morning (so that it was not necessary for them to spend money on overnight stays). The exhibition entertained those who arrived earlier: it included a showcase of GPR equipment and a poster session. Posters were prepared and presented by selected local students and by Trainees of the TU1208 Training School held in Osijek during the same week (see photos in Figure 11(a)-(b)).

Lectures covered the fundamentals of GPR technology, a general overview on its numerous applications, and then a series of lectures on the use of GPR for utility detection, road and bridge inspection, and railway assessment (see photos in Figure 11(c)-(d)). Various questions asked by the audience regarded the detection of utilities in specific (challenging) conditions; there also was a special interest in the combined use of GPR and complementary technologies.

Taking inspiration from the event held in Rome, a roundtable with companies offering GPR services was organized. Before the event, TU1208 Members from Novi Sad looked on the internet and found five Serbian companies offering GPR services, which were invited to participate in the workshop and in the roundtable. All companies accepted the invitation. They reported that they mainly use GPR for

https://doi.org/10.26376/GPR2019004

Table 5: Programme of TU1208 GPR Roadshow held in Novi Sad, Serbia.

Time	Speaker	Activity
9.15 – 10.15	–	*Registration & Breakfast.* Exhibition of GPR equipment. Poster session.
10:15 – 10:30	Local Authorities	*Welcome to participants. (in Serbian)*
10:30 – 10:50	Miro Govedarica (Faculty of Techn. Sciences of Novi Sad, RS)	Introduction to the dissemination day. Overview on research and teaching activities at the Faculty of Technical Sciences of Novi Sad. *(in Serbian)*
10:50 – 11:20	Miro Govedarica & Aleksandar Ristic (Faculty of Techn. Sciences of Novi Sad, RS)	Introduction to Ground Penetrating Radar (GPR): basic principles, capabilities, limits, applications. *(in Serbian)*
11:20 – 12:00	Simona Fontul (Laboratório Nacional de Engenharia Civil, PT)	GPR applied to roads. Examples. *(in English)*
12:00 – 12:20		*Tea & Coffee Break*
12:20 – 13:15	Aleksandar Ristic (")	GPR applied to utility detection. Examples. *(in Serbian)*
13:15 – 14:15		*Lunch*
14:15 – 14:45	Simona Fontul (")	GPR applied to railways. Examples. *(in English)*
14:45 – 15:00	Damir Varevac (Faculty of Civil Engineering of Osijek, HR)	GPR activities in the Faculty of Civil Engineering of Osijek (Croatia). (*in English*)
15:00 - 15:45	Lara Pajewski (Sapienza Univ. of Rome, IT, TU1208 Chair)	Introduction to the COST programme and to COST Action TU1208 "Civil engineering applications of Ground Penetrating Radar" *(in English)*
15:45 - 16:15	Coordinated by Miro Govedarica & Lara Pajewski	Roundtable with Stakeholders and private companies *(in Serbian and English)*
16:15 - 16:30		*Tea & Coffee Break*
16:30 - 17:30	Coordinated by Milan Vrtunski & Željko Bugarinović (Faculty of Techn. Sciences of Novi Sad, RS)	Practical demonstration of GPR technique (measurements in the vicinity of the meeting venue, with different kinds of equipment)

https://doi.org/10.26376/GPR2019004

Figure 10: Flyer of the science communication event held in Novi Sad (Serbian edition of TU1208 GPR Roadshow).

Figure 11: Serbian edition of TU1208 GPR Roadshow. **(a, b)**: Poster session before the workshop; **(c)** Prof. Dragan Šešlija, vice-dean of the Faculty of Technical Sciences, opening the event; **(d)** Attendees (this is only a half of a very long room!).

https://doi.org/10.26376/GPR2019004

utility detection and localization, other civil engineering works, and geophysical surveys. Sporadically, they had the opportunity to employ GPR in the framework of archaeological investigations. The participating companies also offer Geographic Information System (GIS) and geodetic surveying services. They rarely use GPR in combination with other non-destructive testing techniques.

Attendees were very positive in terms of discovering more about the guidelines for utility detection prepared by COST Action TU1208; they expressed a strong hope that those guidelines would be presented in detail in the future and be used as a basis for developing utility detection standards in Serbia. Indeed, when the guidelines will be finalized and published, we will organize a dedicated event in Novi Sad. Attendees also expressed appreciation about the poster session and were strongly impressed by the significant efforts made by the Faculty of Technical Sciences in educating students about GPR technology and its applications.

An outdoor practical session concluded the event, coordinated by young scientists from the Faculty of Technical Sciences. In the gardens of the University, Attendees were introduced to practical issues commonly faced when using GPR equipment, such as setting the acquisition parameters in different conditions, choosing the most appropriate antennas, and using other non-destructive testing instrumentation along with GPR.

Looking at the number of Attendees, the event was a huge success, with 105 participants (more than in all other Roadshow events). The majority of Attendees was from Serbia, 88 of them; 17 Attendees were from abroad (Figure 12(a)) – in particular, 9 Attendees were from the region of former Yugoslavia (Bosnia and Herzegovina, Croatia) and 8 were from other countries (Italy, Portugal, Turkey, Spain, and the Czech Republic). Figure 12(b) shows the percentages of Attendees from university and research institutes (including professors, researchers, and students), public agencies, and private companies; there was also an unemployed citizen; it is apparent that the local organizer was able to attract the interest of several companies and stakeholders. Concerning gender distribution of Attendees, 77% of them were men and 23% were women (Figure 12(c)); hence the participation of women was lower than in Rome and Athens.

Since the event mainly focused on utility detection and assessment of road and railway infrastructure, it is interesting to analyze in detail

 https://doi.org/10.26376/GPR2019004

the participation of public agency representatives: statistics are presented in Figure 12(d). Participants belonging to this group typically do not yet own GPR equipment but may be interested in purchasing it, or in ordering GPR scanning services for infrastructure maintenance and development, urban planning, and for the utility and real estate cadaster.

Let us now look more in detail into the participation of private companies (Figure 12(e)). Attendees from companies that work on the detection and mapping of underground utilities usually already have and use GPR equipment, but they are interested in upgrading, as well as in learning about applications in new areas. Attendees from other companies sometimes own GPR equipment, or else they offer different services and are interested in purchasing GPR instrumentation to widen their market.

After the event, a questionnaire was sent to all participants, via email, along with certificates of attendance. The asked questions and some statistics on the received feedback are presented in Table 6. Ideas for future cooperation (question 5) included:

- To organize another GPR communication day, or even better, a communication conference spanning over multiple days where each day would be dedicated to a different GPR application (similar to training schools, but for the public);
- To repeat GPR communication initiatives periodically;
- To establish a national scientific network of cooperation among the companies and researchers that participated in the Roadshow.

Additional comments (question 6) included:

- Strong appreciation for the workshop, compared to previously-attended short courses organised by, e.g., the Serbian Chamber of Engineers or by various associations;
- Participants were happy about the lectures because topics were presented not only theoretically but also professionally, reporting application tips and experiences from practice, and offering a perspective on future GPR applications;
- Participants stressed the need to develop standards and define a legal framework in Serbia for the use of GPR technology;
- Most of the comments were congratulations for the excellent organization and thank you messages.

https://doi.org/10.26376/GPR2019004

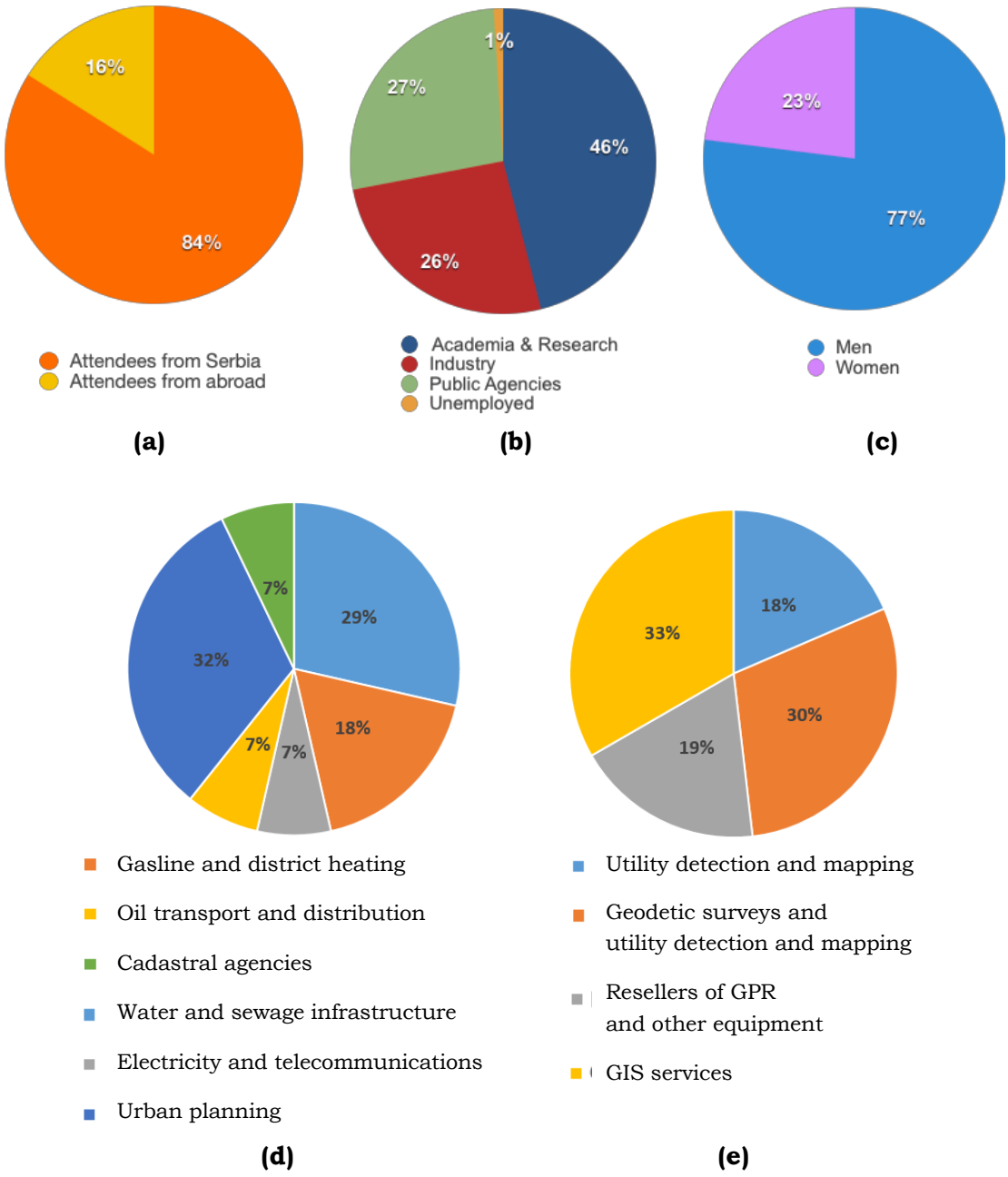

Figure 12: (a) Attendees from Serbia and from other countries; **(b)** Gender distribution of Attendees; **(c)** Attendees from academia and research, public agencies, and industry; **(d)** Representatives from public agencies; **(e)** Representatives from industry (TU1208 GPR Roadshow, Serbian edition).

 https://doi.org/10.26376/GPR2019004

Table 6: Questionnaire sent to participants of the Serbian GPR Roadshow and statistics on the received feedback.

1) Kakva su bila Vaša saznanja o COST pre učestvovanja na GPR Workshopu u Novom Sadu? 1) What was your knowledge about COST before attending the Road Show?	Nikad nisam čuo/la za COST	Upoznat/a sam ali nikad nisam učestvovao na COST događajima	Prisustvovao/la sam COST događajima ali nikad nisam učestvovao u COST akciji	Učestvovao/la sam u COST akciji / Učestvujem u COST akciji
	Never heard of it	Knew about its existence but never participated to COST events	I already attended a COST event but never participated to a COST Action	I already participated / I am participating to a COST Action
	30%	40%	8%	22%
2) Koliko ste bili upoznati sa tehnologijom skeniranja georadarom pre učešća na GPR Workshopu u Novom Sadu? 2) What was your knowledge about GPR before attending the Road Show?	Nisam bio/la upoznat	Čuo/la sam da navedena tehnologija postoji	Video/la sam primenu tehnologije, ali je nisam lično primenio	Korisnik sam ove tehnologije
	Never heard of it	Knew about its existence	I saw GPR results before, but never used it	I am a GPR user
	0%	15%	53%	32%
3) Da li planirate da koristite GPR tehnologiju u budućnosti? 3) Do you plan to start using GPR in the future?	Ne	Možda	Da	Korisnik sam
	No	Maybe	Yes	I already use it
	0%	43%	40%	27%
4) Da li smatrate da je GPR Workshop bio koristan u smislu informisanja o osnovnim principima, metodologiji i primeni GPR tehnologije? 4) Do you think that the Road Show was useful, to gain knowledge about GPR basic principles, methodology and applications?	Ni najmanje	Malo	Donekle	Prilično
	Not at all	A little	Fairly	A lot
	0%	0%	10%	90%
5) Da li imate ideje o realizaciji buduće saradnje sa članovima COST akcije TU1208, ili predloge za daljnju promociju aktivnosti u oblasti primene GPR tehnologije? 5) Do you have ideas for future cooperation with Members of COST Action TU1208 or suggestions for further dissemination activities in the GPR area?	Ne	Da		
	No	Yes		
	85%	15%		
6) Ako imate dodatne komentare u vezi GPR Workshopa, molimo Vas da ih specificirate 6) If you have further comments about the Road Show, please write them here.	Ne	Da		
	No	Yes		
	75%	25%		

7 GPR Roadshow in the Czech Republic

The sixth event of TU1208 GPR Roadshow was held in the Faculty of Transport Engineering of the University of Pardubice, in the Czech Republic, on 25 May 2017; Dr Vladislav Borecky coordinated the local organisation. The primary goal of this dissemination day was to introduce the GPR technique and its civil engineering applications to new potential private and public end-users. The intention was not only

 https://doi.org/10.26376/GPR2019004

to promote the GPR technology but also to point out the pitfalls and limitations of this technique in the various application fields.

The event further highlighted how international research projects, such as COST Action TU1208, can and shall play an important role in bringing private sector and academia together and in establishing an active link between researchers and stakeholders. GPR possibilities were presented to decision makers from regional and national authorities, which may result in support and funding for GPR related projects in the future; they were made aware not only of the cost-effective and time-saving nature of GPR investigations but also of the main outputs of recent and ongoing GPR-related scientific projects. During the lectures and roundtable, new ideas germinated for possible future studies and discussions took place among academicians about starting GPR-related University courses.

A dedicated website was created by the local organizers, prior to the event, with Czech and English versions, for the purposes of advertising the event (georadar.upce.cz). The University of Pardubice announced the event on its website (upce.cz/english/jptf/dts.html) and Facebook page (facebook.com/DFJP.KDS). After the event, a short article was published on the electronic journal of the University of Pardubice (zpravodaj.upce.cz/vzdelavani/2017/georadar-na-dopravni-fakulte/).

The local organizers built on the longstanding cooperation with the local road administrator SÚS Pardubického kraje, which offered financial support to partially cover the expenses.

The programme of the event included lecture sessions, a roundtable, and a practical demonstration (see Table 7 and Figure 13). Lectures were given in Czech and English; most speakers were TU1208 Members, some talks were given by experts not involved in the Action. During the practical demonstration, Attendees got acquainted with GPR systems belonging to the Department of Transport Structures and to the Transport Research Centre v.v.i. (manufactured by IDS Georadar and GSSI, Geophysical Survey Systems, Inc.).

Most participants were from the Czech Republic, there were also some Master and PhD students from abroad (Figure 14(a)). The event had 58 Attendees in total, from industry, academia and research centres, and public agencies; the proportion of these sectors was quite balanced (Figure 14(b)). Figure 14(c) shows the gender distribution of Attendees. Almost a half of Attendees had no knowledge or basic knowledge about GPR (Figure 14(d)).

https://doi.org/10.26376/GPR2019004

Table 7: Time schedule of the Roadshow edition held in Pardubice.

Time	**Speaker**	**Activity**
8:00 - 9:00		*Registration*
9:00 - 9:15	Local Authorities	Welcome to participants and presentation of the University of Pardubice (in Czech)
9:15 – 9:25	Özgur Yurdakul (Anadolu University, Turkey)	Introduction to the COST programme
9:25 – 9:55	Vladislav Borecký (University of Pardubice, Czech Republic)	GPR basic principles and applications
9:55 – 10:15	Pavel Lopour (University of Pardubice, Czech Republic)	Civil Engineering Applications of Ground Penetrating Radar: a European perspective. Activities carried out within COST Action TU1208.
10:15– 10:30	Vladislav Borecký (University of Pardubice, Czech Republic)	GPR activities at the Department of Transport Structures UPa (in Czech)
10:30 – 11:00		*Tea & Coffee Break*
11:00 – 11:40	Radek Matula, Michal Janků (Transport Research Centre, Czech Republic)	GPR applied to roads, bridges and tunnel (in Czech)
11:40 – 12:10	Salih Serkan Artagan (Anadolu University, Turkey)	GPR applied to railways
12:10 – 12:25	Rudolf Tengler (Georadar RTG – Tengler, , Czech Republic)	Presentation of the ROTEG GPR systém (in Czech)
12:25 – 13:25		*Lunch*
13:25 – 13:55	Jiří Nedvěd (SG Geotechnika a.s.)	GPR in geotechnics (in Czech)
13:55 – 14:25	Dušan Kocur (Technical university of Košice, Slovakia)	Person localization based on detection of their vital signs using Ground Penetrating Radar (in Czech)
14:25 – 15:00		Roundtable with stakeholders and private companies (in Czech & English)
– 15:30		*Tea & Coffee Break*
15:30 – 17:00		Laboratory tour and GPR practical demonstration in Educational and Research Centre in Transport

https://doi.org/10.26376/GPR2019004

Figure 13: Photos taken during the workshop, laboratory tour and GPR practical demonstration (TU1208 GPR Roadshow held in the Czech Republic).

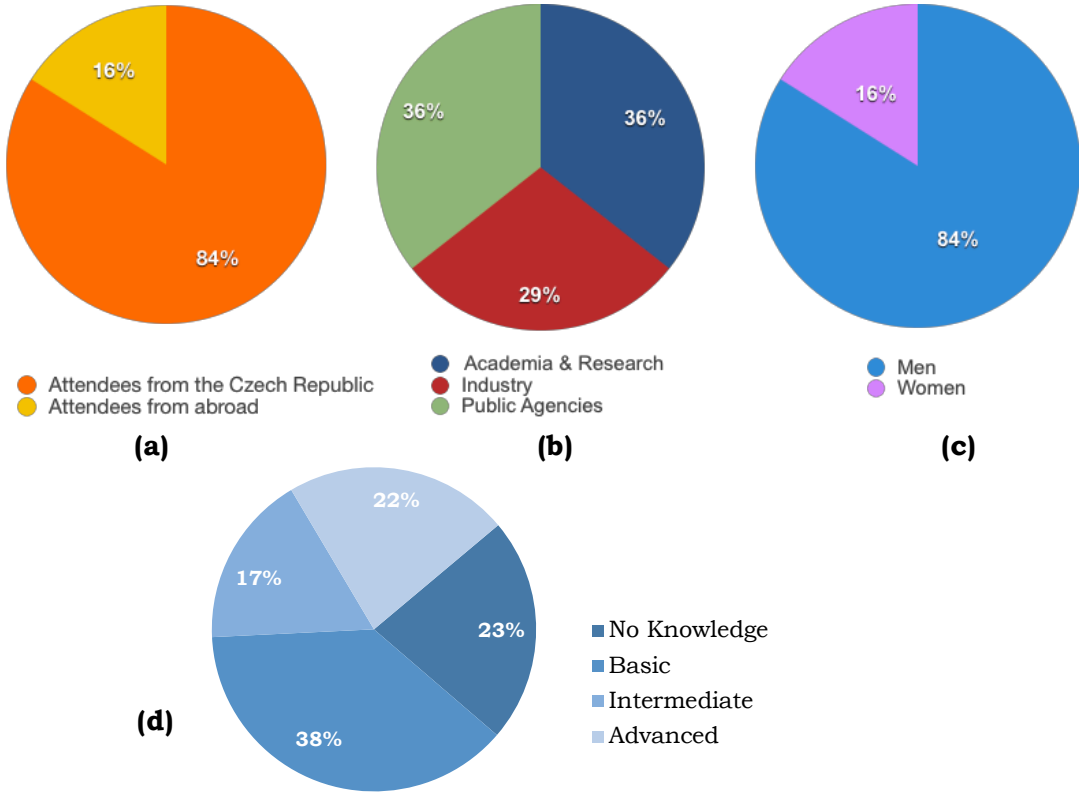

Figure 14: **(a)** Attendees from the Czech Republic and other Countries; **(b)** Attendees from academia and research centres, industry, and public agencies; **(c)** Gender distribution of Attendees; **(d)** Level of knowledge about GPR declared by Attendees (TU1208 GPR Roadshow held in the Czech Republic).

 https://doi.org/10.26376/GPR2019004

8 GPR Roadshow in Estonia

This section presents the successful and impactful science communication activities carried out in Estonia by a team of researchers from the Institute of Ecology of Tallinn University.

The Institute of Ecology is a small research unit at Tallinn University. The main research themes include wetland ecosystems – peat bogs, lakes, rivers, coasts, and shore processes. The Estonian coast is located in a region of tectonic uplift, making it possible to investigate the well-preserved ancient beach formations in a few-kilometre wide coastal zone; the ridge-swale complexes with peat bogs and lakes in between the ridges are valuable natural archives of palaeogeographical information. The GPR technique has been used in many occasions, by the researchers of the Institute of Ecology; actually, the GPR profiling is very helpful to detect storm layers in sandy beach formations, measure the thickness of organic layers in lakes and peat bogs, and more. A senior member of the research team started to use GPR already over 20 years ago. The older GPR devices owned by Tallinn University were rather heavy (had to be carried by car), limiting the use of them. A lightweight GPR system, SIR-3000 manufactured by GSSI, was bought in 2011: small size, light weight, and long-lasting batteries make it possible to use it everywhere.

The researchers noticed that several geology-related works carried out by public or private companies in Estonia were done by using destructive methods. It was apparent that most of the geological investigations (digging, drilling, etc.) could have been done by using GPR as a non-destructive, environment-friendly and less-expensive method. The researchers had a hope that they could increase the efficiency of the Estonian economy by educating various age and interest groups about the potential and capabilities of GPR. Therefore, they started devoting some time to dissemination and outreach activities among the ordinary people. As a result of their intensive and enthusiastic promotional work of the GPR technology, the researchers have recently carried out a number of applied projects for different enterprises and local authorities that helped them to include additional resources for their research. The promotional work and the applied projects have also improved their skills in the use of GPR in various geological conditions.

 https://doi.org/10.26376/GPR2019004

8.1 GPR lessons in secondary schools

Tallinn University is one of the leaders in the field of teacher education and training in Estonia. Many young teachers of geography, biology and natural sciences in schools have recently graduated from Tallinn University, and the researchers of the Institute of Ecology have kept contact with them. So, they offered the young teachers an opportunity to take GPR lessons for the pupils of their schools. The interest in the idea of providing such lessons was enormous. As the Estonian schools, in general, are lacking many needful devices for practical work, all initiatives that help to introduce new technologies and methods are usually very welcome. It was necessary to select a few schools from different regions of Estonia and plan the routes of the lectures, combining them with fieldworks after or before the lessons (in fact, most of the lectures were delivered in the vicinity of areas where the researchers were carrying out some scientific investigations). Lessons were given free of charge and schools were just asked to organize accommodation, if needed (for the most remote places). The researchers were able to visit over 15 schools all over Estonia. Mostly, pupils from grades 6 to 9 were expected to attend the lessons. However, some high schoolers attended the lessons, too. The groups usually consisted of 10 to 20 pupils.

The lessons were simple. During the first 15-20 minutes, there was a theoretical lecture where the basic principles of GPR were described, and some best examples of GPR pictures were illustrated (i.e., radargrams obtained over pipes, cables, caves, buried treasures and other objects). This short lecture helped the pupils to better understand GPR images during the subsequent practical work, which lasted about 30 minutes. The researchers and pupils walked around the school territory and searched for buried artificial objects by using GPR or mapped geologically interesting layers. The locations of heating pipes, power cables and other objects were marked on the ground by using wooden sticks on the grass or chalk on the asphalt. Finally, the pupils could draw the basic schemes of the utilities located on the school.

Once researchers and secondary school students visited a nearby lake, in winter; they measured the thickness of the organic layer on the bottom of the lake and verified the results by using drilling equipment brought by the researchers (Figure 15). Moreover, in one school the ruins of the old school house were found (nearly 100 years old). The

https://doi.org/10.26376/GPR2019004

most interesting finding was a cave described in an ancient legend: the researchers and pupils were the first ones who found it and can confirm that the old legend is actually a true story (Figure 16)!

It came out during the lessons that the younger the pupils were the more enthusiastically they took part in the GPR activities. Therefore, it was decided to organize one lesson also for the pupils of grades 1 and 2. It was decided to skip the lecture part with them and carry out the entire experience on the beach. A few “treasures” were buried in the sand to make the study more attractive. Moreover, several simple skills were needed to reach the final “treasure” (the initial finding was just the first clue to the real treasure), including the use of a compass, reading the distance from the measuring tape, etc (Figure 17). The lesson with such young pupils was a huge success. They were really enthusiastic and proud to find the “treasure” (candies, some lemonade and a book for the school library), and to hand over the book to the school library. The lesson needed a little more preparatory work, but the outcome was worth it. Moreover, the researchers were pleased to discover (from the feedback) that the parents of the pupils were very well informed by their children, after the lesson, on what GPR is and how it can be used in different tasks.

Figure 15: Educational event. GPR was used to detect the thickness of the organic layer on the bottom of a lake. Drilling was used to verify GPR results.

https://doi.org/10.26376/GPR2019004

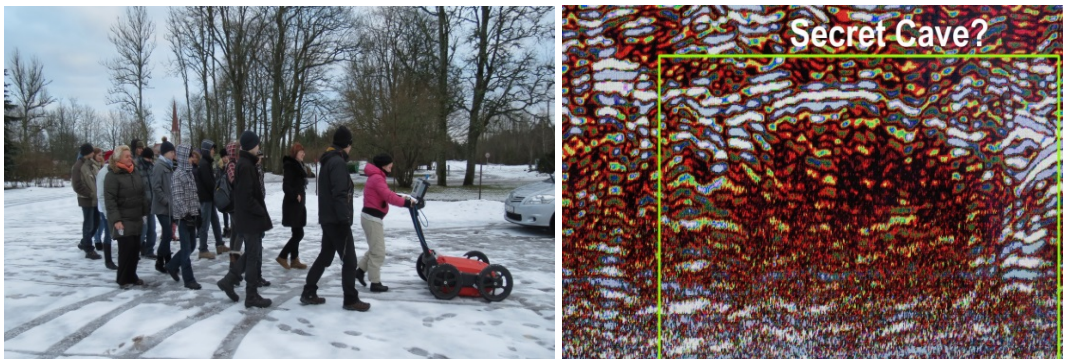

Figure 16: GPR lessons at school. The pupils were intensively working in the school's parking lot (left); An old legend describing secret caves from the local church to manor was confirmed (right)!?

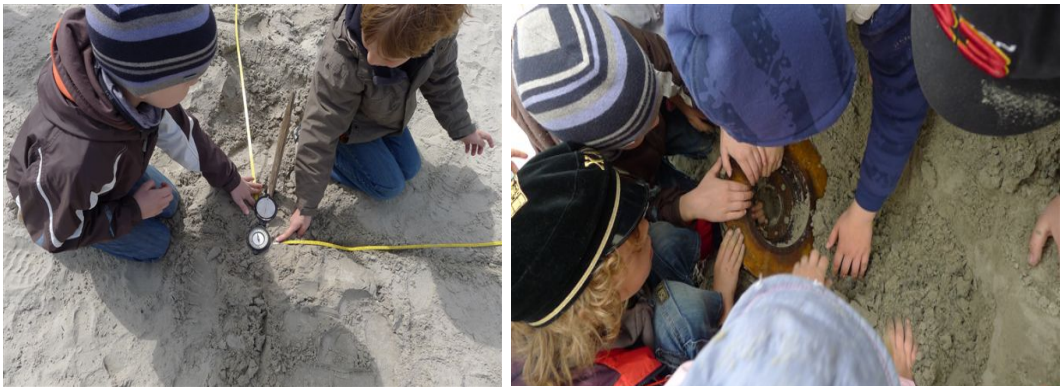

Figure 17: Second grade pupils in Tallinn during a lesson on the beach.

8.2 Investigations during the Researcher Night

The researchers from the Institute of Ecology of Tallinn University were discovered by several interest groups, as a result of their lessons in schools. They were invited to present their GPR equipment in the frames of the Estonian edition of the European Researchers' Nights for three consecutive years. The innovative and popular concept of the Researchers' Night was introduced several years ago in Estonia; during these open science events, science and the work of scientists are presented to non-scientific audiences all over Europe. Over the course of the day and throughout the night, children, adolescents, adults, older people, students, and entrepreneurs can get to know more about science through workshops, meetings with researchers, lectures and laboratory visits. In Estonia, the Researchers' Night is normally held in

https://doi.org/10.26376/GPR2019004

public spaces, in the city centre of Tallinn; numerous researchers introduce their studies, equipment and most recent findings to hundreds of interested people.

Tallinn city center is located just beside the medieval old town, and many archeologically significant features can be found below the contemporary ground surface. Therefore, the researchers from the Institute of Ecology of Tallinn University had the chance to organize very impactful GPR demonstrations, where GPR was used to show the presence of buried archeological objects to local people. The researchers got extremely positive feedback: the citizens understood the importance of non-destructive technologies and several new users of GPR services stemmed from those events. The audience attending GPR demonstrations during the Researchers' Nights was rather diverse – from kids to retired citizens (Figure 18).

8.3 Festivals with enterprises

Estonian universities have created a system called "Adapter." All services offered by the universities are registered there, and one can search the desired service by entering keywords. The GPR-services are also registered there. However, this is not all. In September 2016, an annual co-operation festival was held in the Estonian National Museum with the aim of bringing the entrepreneurs and researchers together. The researchers of the Institute of Ecology of Tallinn University were invited to introduce the GPR technology and its applications in civil

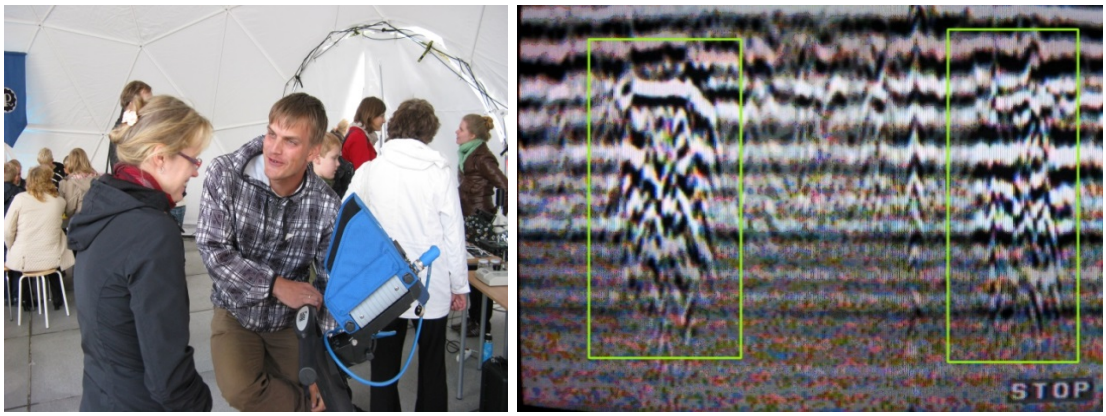

Figure 18: Researchers Night organized in the city centre of Tallinn. GPR was demonstrated and tested among other activities (left); the ruins of the buried medieval city walls were shown on the GPR screen (right).

 https://doi.org/10.26376/GPR2019004

engineering, archaeology and geological research. Each topic was presented in a 3- minute lecture. This presentation scheme is called “elevator pitch:” a brief, persuasive speech is given to spark interest in what an organization does, in a project, idea, or product – or in a person! A good elevator pitch should last no longer than an elevator ride, hence the name. As a result of the evaluation, the GPR service presented by Tallinn University was elected the most useful service of 2016. The best “elevator pitch” talk award was also received by Hannes Tonisson (www.youtube.com/watch?v=OzvKsmfE3yk).

8.4 Joint fieldworks with archaeologists and TV crew

The educational work presented in the previous subsections brought the researchers of the Institute of Ecology in contact with a lot of different interest groups, and several job offers arrived; the researchers also established new connections with other research teams.

A team of archaeologists had preliminary information about a buried Viking ship near Salme village, on Saaremaa Island. The site was investigated by using an older version of GPR, and the Viking ship was found (Figure 19). A pile of stones placed on top of the buried ship generated the strongest reflected signal and helped the researchers to locate the vessel. The archaeology students filmed the whole investigation process; an educational movie was realized, for future (archaeology) students.

8.5 Cooperation with Tallinn Harbor

As already mentioned, the voluntary promotional events led to several successful cooperation projects among the researchers of the Institute of Ecology and private enterprises, local authorities and state-financed companies. Another successful example is presented in this subsection.

Tallinn is known for its fully restored medieval Old Town (UNESCO World Heritage Site). Tallinn is also a seaside city where the signs of human activities date back to Stone Age when seal hunters and fishers were using the city center as their temporary camp [12]. Therefore, many archeologically essential findings can be found below the current surface (as stated in subsection 8.2), including old walls, water systems, tools, shipwrecks, etc. In cooperation with Tallinn City, the researchers of the Institute of Ecology have been investigating several sites where major buildings or new roads are planned. It must be highlighted that

https://doi.org/10.26376/GPR2019004

currently local authorities are recommending the developers to carry out GPR studies even before the planning phase, to avoid unwanted disruptions during the construction phase!

In this framework, the most successful cooperation took place with Tallinn Harbor, a state-owned company. The archaeologists of Tallinn suggested that there might be a major shipwreck in their territory, but the exact location, state (preserved or not) and size were unknown. They recommended carrying out a GPR survey. Hence, Tallinn Harbor ordered a GPR study from the Institute of Ecology. As a result of the investigation, an anomaly was found that might be the ship. The anomaly was over 50 m long, around 10 m wide and approximately 1 m below the current surface.

Figure 19: Searching for ancient Viking ship on Saaremaa Island. Search is in progress (top), ship was found (lower left) and archaeologists expose the ship remains (lower right). A special movie was realized for educational purposes.

https://doi.org/10.26376/GPR2019004

The archeologists carried out test excavations in a 2×1-m pit and confirmed that the finding was the historically valuable shipwreck (Figure 20). This information assisted Tallinn Harbor to change the development project in such a way that the ship area will be used as a parking lot and no buildings or utilities are any more planned there. The ship will be preserved for future generations and for archaeologists with more efficient excavation methods/technologies. So the state-owned company didn't suffer any losses, and the archaeologically valuable object was preserved.

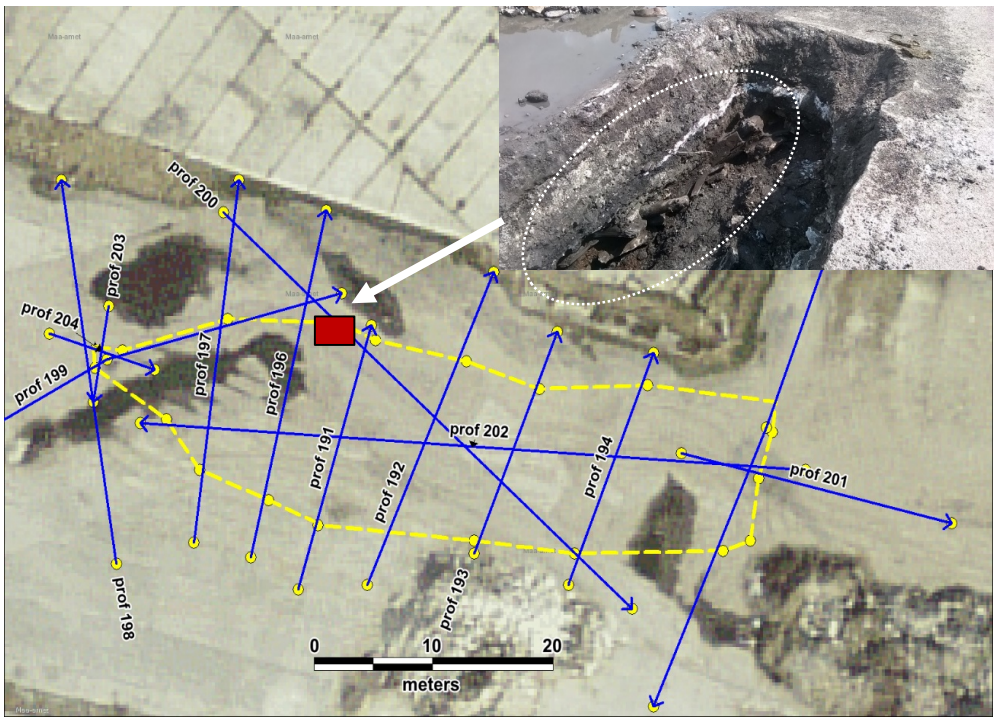

Figure 20: Blue arrows: locations of GPR profiles; yellow dashed contour: expected location of the shipwreck; red box: location and size of the excavation pit; top-right photo: excavation pit (a white-dashed oval indicates fragments of the shipwreck).

8.6 One-minute lecture on national TV channel

The final educational and also a little bit promotional product was a video lecture about GPR. Tallinn University was involved in a project called "one-minute lectures." These are short, easy to understand and high-quality lectures introducing scientific problems or new scientific

 https://doi.org/10.26376/GPR2019004

methods/equipment. The one-minute lecture about GPR, given by Dr Kaarel Orviku, was on air on the biggest national TV channel. A lecture with a longer introduction to GPR is still visible on the website of the national TV channel - Estonian TV; the one-minute lecture, instead, has been uploaded on the YouTube channel of Tallinn University and can be seen here: www.youtube.com/watch?v=vMCm0Qk8fUo

Finally, with this initiative the researchers managed to reach every Estonian's home!

9 Conclusions

Science communication is the public communication of science-related topics to non-experts. Science communication is increasingly essential in today's society, although its importance is often underestimated by researchers. In this paper, we have presented descriptions, principles, and results of a very successful series of science communication initiatives about the Ground Penetrating Radar (GPR) technique, recently carried out by Members of COST Action TU1208 "Civil engineering applications of Ground Penetrating Radar" and overall denominated "TU1208 GPR Roadshow."

Part of TU1208 GPR Roadshow consisted of a series of six non-scientific workshops and practical demonstrations held in Portugal (National Laboratory of Civil Engineering), Italy (Roma Tre University), Greece (Geoservice), Croatia (University of Osijek), Serbia (University of Novi Sad), and the Czech Republic (University of Pardubice), from March 2016 to May 2017. Audiences went well beyond the GPR scientific community and primarily included representatives from public agencies and private companies, as well as interested citizens. The workshops were attended by almost 500 participants in total and were a huge success; we were able to raise considerable interest in various countries and our events were catalysts for a series of new activities.

Another significant part of the Roadshow consisted of a series of promotional and educational initiatives carried out in Estonia. Before these initiatives, very few people in Estonia knew what GPR was and how it could be used in different application fields. The researchers from the Institute of Ecology of the University of Tallinn were able to spread the knowledge to a significant number of people without the need of a GPR-related project devoted explicitly to this (i.e., without dedicated funding). They delivered several lectures in schools, practical

 https://doi.org/10.26376/GPR2019004

workshops during the Researchers' Nights and during other large communication events, and even short lectures on TV. In this way, they have increased public awareness on the potential and capabilities of the GPR technique; Estonian companies have learnt about the possibility of using GPR to conduct more efficient business activities. The feedback was very positive and currently the Estonian researchers have a long pre-order list of schools who are expecting their visit!

As is shown by the map in Figure 21, our science communication project involved eighteen countries. In particular, the various initiatives took place in the seven countries coloured in yellow, while speakers, trainers, and attendees were from both the yellow and orange countries. The primary purpose of our project was to reach out to the public at local, regional, and national levels; however, the Roadshow had an international perspective and impact.

The authors of this paper hope to improve their science communication skills and continue with GPR communication, training, promotion, dissemination, and outreach initiatives in the future. We would like to put efforts into both "one-way" and "two-way" communication exchanges, where one-way exchanges may include preparing webpages with non-scientific explanation about GPR, brochures, posters, blog posts, and even videos, whereas two-way exchanges may include technical workshops of various kinds, exhibitions, visits of school pupils in research centres, lectures in schools, summer schools, and internet debates. There is a high potential in citizen science, too, i.e., public and societal engagement in research. For information about our future activities, please visit the dedicated webpage: gpradar.eu/events-dissemination/roadshow.html.

Acknowledgement

The authors acknowledge COST (European Cooperation in Science and Technology) Action TU1208 "Civil Engineering Application of Ground Penetrating Radar" for having encouraged and supported the activities presented in this paper. The authors would also like to thank the universities, research institutes, and schools that hosted the Roadshow and communicated about our events and activities. The Czech edition of the Roadshow was partially funded by the road administrator SÚS Pardubického kraje. Some lectures given to school pupils in Estonia were financially supported by the ESF grant 8549.

https://doi.org/10.26376/GPR2019004

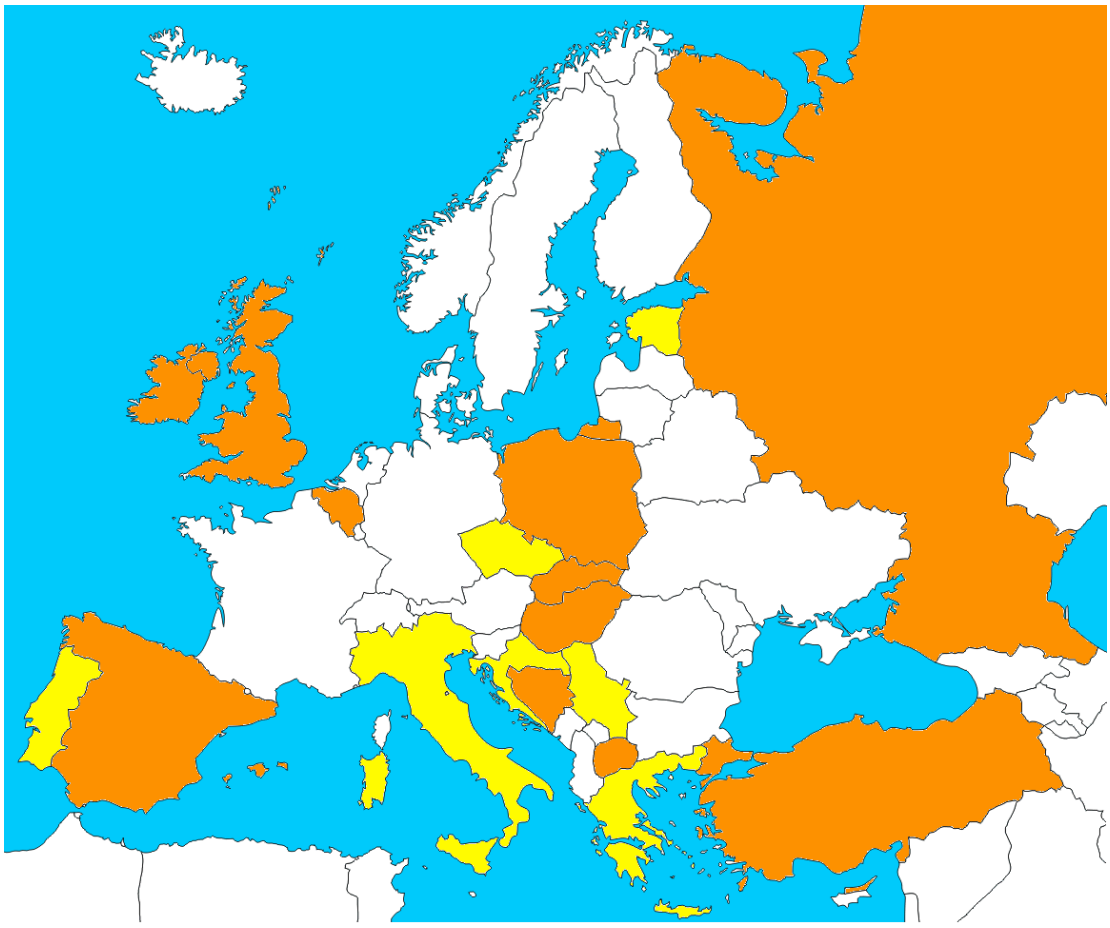

Figure 21: Countries involved in TU1208 GPR Roadshow. The initiatives took place in the yellow-coloured countries; participants were from both the yellow- and orange-coloured countries.

References

[1] T.W. Burns, D.J. O'Connor, and S.M. Stocklmayer, "Science Communication: A Contemporary Definition," *Public Understanding of Science*, vol. 12, pp. 183–202, April 2003, doi: 10.1177/09636625030122004.

[2] T. Bubela, M.C. Nisbet, R. Borchelt, F. Brunger, C. Critchley, E. Einsiedel, G. Geller, A. Gupta, J. Hampel, R. Hyde-Lay, E.W. Jandciu, S.A. Jones, P. Kolopack, S. Lane, T. Lougheed, B. Nerlich, U. Ogbogu, K. O'Riordan, C. Ouellette, M. Spear, S. Strauss, T. Thavaratnam, L. Willemse, and T. Caulfield, "Science

 https://doi.org/10.26376/GPR2019004

communication reconsidered," *Nature Biotechnology*, vol. 27, no. 6, pp. 514–518, June 2013, doi: 10.1038/nbt0609-514.

[3] *Communicating EU research and innovation guidance for project participants*, European Commission, Version 1.0, 25 September 2014, 14 pp.

[4] *H2020 Programme – Annotated Model Grant Agreement*, European Commission, Version 5.0, 3 July 2018, 810 pp.

[5] *H2020 Programme – Guidance – Social media guide for EU funded R&I projects*, European Commission, Version 1.0, 6 April 2018, 19 pp.

[6] *Making the Most of Your H2020 Project – Boosting the impact of your project through effective communication, dissemination and exploitation*, The European IPR HelpDesk, March 2018, 36 pp.

[7] *COST Vademecum*, available at www.cost.eu.

[8] P. Simeoni, L. Pajewski, and F. Frezza, "Strategies for Stakeholders involvement in COST Action TU1208," *Proceedings of the Third Action General Meeting;* Edited by: Lara Pajewski; Publishing House: Aracne; Rome, Italy, May 2015; ISBN 978-88-548-8486-1.

[9] S. Fontul, L. Pajewski, A. Ristic, and M. Vrtunski, "Road Shows as opportunities for dissemination and promotion of Ground Penetrating Radar use in Inclusiveness Target Countries - COST Action TU1208," *Geophysical Research Abstracts*, Vol. 20, 2018, Abstract ID: EGU2018-6957, European Geosciences Union General Assembly – Vienna, Austria, 8-13 April 2018, 1 p.

[10] M. Govedarica, A. Ristic, L. Pajewski, M. Vrtunski, and S. Fontul, "A series of educational and promotional activities within COST Action TU1208 - GPR Roadshow," *Geophysical Research Abstracts*, Vol. 21, 2019, Abstract ID: EGU2019-10619, European Geosciences Union General Assembly – Vienna, Austria, 7-12 April 2019, 1 p.

[11] "Il Notiziario LASSTRE – In questo numero del notiziario si illustrano le ultime attività condotte nell'ambito della COST Action TU1208 "Civil engineering applications of Ground Penetrating

https://doi.org/10.26376/GPR2019004

Radar" e in particolare la giornata divulgativa sul georadar in ingegneria civile svoltasi presso l'Università degli Studi Roma Tre." *Strade & Autostrade*, vol. 4, pp. 2-3, 2016.

[12] M. Muru, A. Rosentau, A. Kriiska, L. Lõugas, U. Kadakas, J. Vassiljev, L. Saarse, R. Aunap, L. Küttim, L. Puusepp, and K. Kihno, "Sea level changes and Neolithic hunter-fisher-gatherers in the centre of Tallinn, southern coast of the Gulf of Finland, Baltic Sea," *The Holocene*, vol. 27, no. 7, 2017, doi: 10.1177/0959683616678462.

Ground Penetrating Radar
Volume 2, Issue 1, March 2019
https://doi.org/10.26376/GPR2019RN1

RETRACTION NOTE: "ELECTRICAL RESISTIVITY TOMOGRAPHY INVESTIGATIONS IN MGARR (MALTA)"

The article entitled "Electrical Resistivity Tomography investigations in Mgarr (Malta)," authored by Raffaele Persico (National Research Council, Italy), Sebastiano D'Amico (The University of Malta, Malta), Enzo Rizzo (National Research Council, Italy), Luigi Capozzoli (National Research Council, Italy), and Aaron Micallef (The University of Malta, Malta), was published in January 2018 on Ground Penetrating Radar, Vol. 1(1), pp. 62-74, Article ID GPR-1-1-3, doi: 10.26376/GPR2018003.

This article is retracted by the Editorial Board. Luigi Capozzoli, Aaron Micallef, and Enzo Rizzo have recently reported to the journal that they did not agree with the publication of the article; by virtue of their copyright, and due to data ownership matters, these authors have asserted their right of retraction, which the other authors have accepted. The authors regret the confusion caused to the readers and editors of the journal. All of the authors have expressed consent to this wording of the retraction statement.

Ground Penetrating Radar
Volume 2, Issue 1, March 2019

TABLE OF CONTENTS

Ground Penetrating Radar
Volume 2, Issue 1, March 2019

NEWS & ANNOUNCEMENTS

Special Issue – Call for papers

2019 EGU GA Session GI4.1 "Ground Penetrating Radar: Technology, Methodology, Applications and Case Studies"

This *Ground Penetrating Radar* Special Issue will be a collection of extended papers resuming contributions presented during the scientific session GI4.1 "Ground Penetrating Radar: Technology, Methodology, Applications and Case Studies" successfully organized in the framework of the 2019 European Geosciences Union General Assembly (EGU GA), held in Vienna, Austria, on 7-12 April 2019 (https://meetingorganizer.copernicus.org/EGU2019/session/30181).

As is known, Ground Penetrating Radar (GPR) is a safe, advanced, non-destructive and non-invasive imaging technique that can be effectively used for inspecting the subsurface as well as natural and man-made structures. During GPR surveys, a source is used to send high-frequency electromagnetic waves into the ground or structure under test. At the boundaries where the electromagnetic properties of media change, the electromagnetic waves may undergo transmission, reflection, refraction and diffraction; the radar sensors measure the amplitudes and travel times of signals returning to the surface. Session GI4.1 aimed at bringing together scientists, engineers, industrial delegates and end-users working in all GPR areas, ranging from fundamental electromagnetics to the numerous fields of applications. The session provided a supportive framework for (1) the delivery of critical updates on the ongoing research activities, (2) fruitful discussions and development of new ideas, (3) community-building through the identification of skill sets and collaboration opportunities, (4) vital exposure of early-career scientists to the GPR research community.

The topics of interest for Session GI4.1, as well as for this Special Issue, are:

1. Ground Penetrating Radar instrumentation
- Innovative GPR equipment and antennas
- Equipment testing and calibration procedures

2. Ground Penetrating Radar methodology
- Survey planning and data acquisition strategies

- Methods and tools for data analysis and interpretation
- Data processing algorithms
- Electromagnetic modelling, imaging and inversion techniques
- Studying the relationship between GPR sensed quantities and physical properties of inspected subsurface/structures useful for application needs
- Advanced data visualization methods to clearly and efficiently communicate the significance of GPR data

3. Ground Penetrating Radar applications and case studies
- Earth sciences
- Civil engineering
- Environmental engineering
- Archaeology and cultural heritage
- Management of water resources
- Humanitarian mine clearance
- Vital signs detection of trapped people in natural and man-made disasters
- Planetary exploration

4. Contributions on the combined use of Ground Penetrating Radar and other geoscience instrumentation, in all applications fields

5. Communication and education initiatives and methods

Special Issue Editors:
– Dr Alessandro Fedeli (University of Genoa, Italy) – alessandro.fedeli@unige.it
– Prof Lara Pajewski (Sapienza University of Rome, Italy) – lara.pajewski@uniroma1.it
– Prof Aleksandar Ristic (University of Novi Sad, Serbia) – aristic@uns.ac.rs
– Dr Milan Vrtunski (University of Novi Sad, Serbia) – milanv@uns.ac.rs

Deadlines and Milestones:
– Submission deadline: 15 September 2019;
– Publication of accepted papers: 31 December 2019.

Notes:
Submissions are open to scientists and experts who participated in the session (Authors of Abstracts and Attendees). When you submit your paper, please specify in your 'Letter to the Editor' that you wish to have the paper included in this Special Issue.

IDS GeoRadar

First Class GPR Solutions

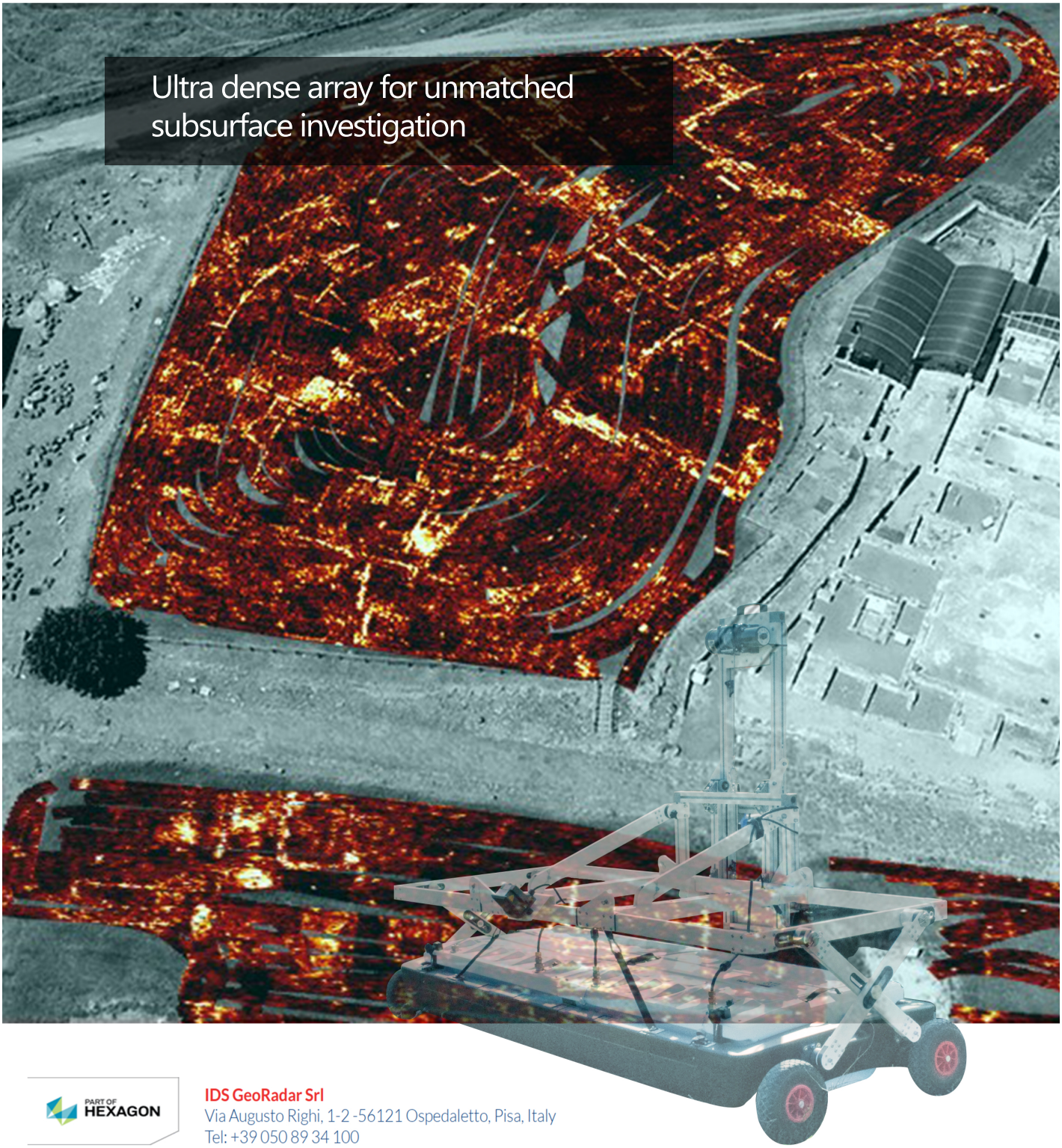

PART OF HEXAGON

IDS GeoRadar Srl
Via Augusto Righi, 1-2 -56121 Ospedaletto, Pisa, Italy
Tel: +39 050 89 34 100
www.idsgeoradar.com | info@idsgeoradar.com

Special Issue – Call for papers

New perspectives for the study and preservation of cultural heritage with the aid of noninvasive prospecting

Cultural heritage is a resource of maximum importance. Beyond its short- and medium-term economical value, it is the material testimony of our memory and roots. Preserving and valorizing it is a must for our future, in all the countries of the world. Ground Penetrating Radar (GPR) and other noninvasive diagnostic techniques can play a role for this, and the achievable results have been made progressively more refined over the years. Nowadays, it is possible to investigate floors and walls, but also columns, pillars, vaulted ceilings, arched historical bridges and even statues in order to acquire precious information regarding the monuments and works of art, related to their history, change of use and status of conservation. New techniques of visualization and enjoyment of the cultural heritage, both for specialists and for tourists, are nowadays possible, thanks to virtual reality and augmented reality, and the results of a GPR (and more in general geophysical) prospecting can be inserted and locally referenced to provide clear and suggestive (and at the same time scientifically rigorous) imaging results.

This Special Issue is mainly dedicated to publishing a selection of papers that provide a comprehensive and up-to-date overview of the state-of the art of research activities dealing with the combined used of GPR and complementary geophysical and/or remote sensing techniques, newest hardware devices devoted to this kind of applications, advanced data processing methods and skilled analyses for a correct interpretation of the data.

We invite you to submit a paper by November 30th, 2019. The publication of the Special Issue is scheduled as the first issue of the 2020 volume of the journal. Manuscripts can be submitted via the online submission form: www.gpradar.eu/journal/submission.html. Accepted papers are published in open access free of charge.

Sincerely,

The Editors
Raffaele Persico, Mercedes Solla, Xavier Dérobert

Ground Penetrating Radar, Issue 1, Volume 2 | March 2019
www.GPRadar.eu/journal, journal@GPRadar.eu

Published by TU1208 GPR Association, Rome, Italy